FACULDADE DE ENGENHARIA DA UNIVERSIDADE DO PORTO

Breast Modeling Towards an Educational Tool for Breast Cancer Surgeons

Daniela do Vale Afonso

Master in Electrical and Computer Engineering

Supervisor: Hélder Filipe Pinto de Oliveira, PhD

Co-Supervisor: Sílvia da Conceição Neto Bessa, MSc

April 11, 2019

Breast Modeling Towards an Educational Tool for Breast Cancer Surgeons

Daniela do Vale Afonso

Master in Electrical and Computer Engineering

April 11, 2019

Resumo

Deformações da mama que ocorram devido a possíveis complicações ou procedimentos da cirurgia de remoção de cancro da mama, podem ter impacto na aparência física e afectar negativamente o estado psicológico da pessoa em causa. Estes impactos psicológicos são mais frequentes nas mulheres, visto que as mamas são socialmente vistas como um ícone de feminidade e fertilidade. Quando diagnosticadas com cancro da mama, os tratamentos mais frequentes a que as doentes são sujeitas são radioterapia, quimioterapia e cirurgia. Dentro das cirurgias, a mastectomia é a que mais mulheres temem dado ser a mais radical e bastante invasiva pelo facto de ser removido todo o tecido que constitui a mama. Não obstante, hoje em dia já existem alternativas menos radicais como o tratamento conservador do cancro da mama, que é menos invasivo, pois só remove o tumor e algum tecido circundante. As técnicas mais recentes como Breast Conserving Surgery (BCS) têm como objectivo maior eficácia e a obtenção de um melhor resultado estético. Embora existam práticas de trabalho muito heterogéneas que levam a resultados estéticos diferentes.

Criar uma ferramenta educacional de treino para os novos cirurgiões para BCS revela-se bastante útil para cirurgiões recém-formados. A ferramenta ajudara-os a tornarem-se melhores profissionais antes de terem experiência, melhorando as suas habilidades profissionais, já que existe uma relação entre experiência e resultado estético de uma cirurgia. Estudos mostram que o resultado de uma cirurgia pode ser influenciado pela experiência do cirurgião ou seja, quanta mais experiência (número de cirurgias praticadas) este tiver, melhores serão os resultados obtidos.

Para poder criar uma ferramenta de treino foram usados modelos paramétricos 3D e sintéticos para simular a superfície da mama (com ou sem deformações), o seu interior e outras estruturas como tórax e o músculo do peitoral. O utilizador tem de introduzir certos dados como: volume, tipo de mama e projeção da mesma. A densidade mámaria é representada pelos quatro tipos em classificação Breast Imaging-Reporting and Data System (BI-RADS). Para representar o tumor no modelo é essencial: o quadrante onde se encontra na mama, estágio de desenvolvimento e a sua forma, redondo ou especulado. No total é possivel simular 43,200 modelos de mama diferente. A ferramenta educativa, disponibiliza de uma interface, previamente testada e validada pela sua usabilidade e eficacia por varias propostas de interface.

Dois inquéritos foram feitos para obter validação profissional acerca da naturalidade do modelo 3D da mama e sobre a usabilidade da interface. Os resultados obtidos foram satisfatórias, apesar das estruturas aparentarem ser artificiais, os médicos conseguiram criar vários modelos 3D da mama sem dificuldade, reconhecendo o potencial educativa da ferramenta.

Abstract

Breast deformities that occur due to possible complications or procedures of breast cancer removal surgery can have an impact on its physical appearance and adversely affect the psychological state of the person concerned. This psychological impacts happens particularly in women, since the breast is socially seen as an icon of femininity and fertility. When diagnosed with breast cancer, the most frequent treatments are radiation therapy, chemotherapy, and surgery. Within the surgeries, mastectomy is the one that most women fear since the intervention is more radical and quite invasive due to the fact that all the breast tissues are removed. Nonetheless, there are less radical alternatives such as the conservative treatment of breast cancer, which is less invasive and preserves more the breast aesthetics because it only removes the tumor and some surrounding tissues. The latest techniques such as Breast Conserving Surgery (BCS) aims to achieve greater efficiency and a better aesthetic result. Although there are very heterogeneous practices that lead to different aesthetic results.

Creating an educational training framework for conservative surgery will be very useful for newly trained surgeons. The framework will help them become better professionals before obtaining experience, improving their professional skills, since there is a relationship between experience and the outcome of a surgery. Studies show that the result of a surgery can be influenced by the experience of the surgeons, ie, the more experience (number of surgeries performed) the surgeon has, better are the results obtained.

In order to create a training framework, parametric and synthetic 3D models were used to simulate the surface of the breast (with or without deformities), its interior and other structures such as thorax and pectoral muscle. The inputs required to simulate the breast surface are volume, breast type and its projection. The breast density is represented by 4 types of Breast Imaging-Reporting and Data System (BI-RADS) classification. To represent the tumor in the model it is essential to know the quadrant in the breast, its stage of development and the tumor form, round or speculated. In total it is possible to simulate 43.200 different breast models. The educational tool has an interface, previously tested and validated for its usability and effectiveness.

Two surveys were made to obtain professional validation about the naturalness of the 3D breast model and the usability of the interface. The results obtained were satisfactory, although the structures appeared to be artificial, the doctors were able to create several 3D breast models without difficulty, recognizing the educational potential of the tool.

Acknowledgment

I would like to express my sincere gratitude to INESC-TEC, Hélder Oliveira and Sílvia Bessa for giving me the opportunity to explore this area and for all guidance through this work. I want to thank all the doctors who participated in this dissertation, for giving up a little of their time to help me improve this dissertation, by making suggestions and participating in the surveys.

First of all, I want to thank my parents for all the sacrifices that they made so I could achieve my goals. I know that it was not always easy for them to put a daughter studying away from home, with the minimum wage these days. Thank you, Mother, for making me a strong and independent woman, for the countless counsels you have given me. Thank you Dad for always getting a smile on my face even if the things were dark and for helping me rise up, fall after fall without letting me losing my sense of humor! Thank you Grandmother for all the prays you have done for me, although I am not as religious as you want me to be, I hope God will hear them. Thank you, Grandfather, for showing me that being childish never has an age. And we have come to thank the most boring and annoying person, who calls me a princess! Diogo, *maninho lindo*, thank you for supporting me. Complaining or not, you are always present, protecting me and illuminating my path. Could not ask for a better brother!

I want to thank my *palhonas*. What would I be without my cousins to hear my regrets when we all are tired of listening to them, for the soups, for the *eu so quero chão*, for every petit gateau and gin in the most depressing moments and for not only being my cousins but older sisters.

I thank my friends, Diogo Moreira, Filipa Pinheiro, Rita Carvalho, Vanessa Mofreita who accompanied these years. They are few but it is in fact the friends that I chose to be part of my "family". Rita Mendes, thank you to make my day to day a bit more random. A special thanks to Rita Carvalho, my traveling and ERASMUS companion. Who have indeed become an indispensable person for me. Thank you for celebrating with me all the successes and for never abandoning me in moments of failure. Thank you for letting me hit with my head a thousand times until I learn, without ever losing the patience, listening to my dramas even it is the version 303 of it. For participating in my most silly moments, for supporting me in times of madness.

Danke an meine lieben, Crisi, Tobi, Natalie for all the support in this path, it was a long and difficult journey, but I know that with you guys nothing bad can happen. My angel Christopher you are not present physically but you will always be with me, thank you for teaching me that muggles never should let me down.

Thank you to all the people who took part in this journey, sharing with me several steps to get here.

Daniela do Vale Afonso

*"The only way to achieve the impossible
is to believe it is possible"*

— Charles Kingsleigh in Alice in Wonderland

Contents

List of Figures

List of Tables

Abbreviations and Symbols

2D	Two dimensional
3D	Three dimensional
BCS	Breast Conserving Surgery
BI-RADS	Breast Imaging-Reporting and Data System
CAN	Complex Aureole Nipple
CT	Computed tomography
DCIS	Ductal carcinoma in situ
DNA	Deoxyribonucleic Acid
FE	Finite Element
FEM	Finite Element Method
FFD	Free Form Deformation
GUI	Graphical User Interfaces
MRI	Magnetic Resonance Imaging
PCA	Principal Component Analysis
QoL	Quality of Life
REM	Radical Elements Method
RBF	Radial Basis Functions
SVD	Singular Value Decomposition
TI	Transfinite interpolation
VB	Voxel-Based

Chapter 1

Introduction

Cancer is a common cause of death worldwide and the one that affects more Portuguese women, is breast cancer. It is estimated that 1 in 12 people may suffer from this type of cancer [1], and this number tends to increase [2]. In Portugal alone, every year 6000 new cases of breast cancer are diagnosed, 1500 from which end up with death.

Diagnosed with this disease, woman tend to face aggressive treatments like chemotherapy, radiation therapy, hormone treatment and surgery.

The fear of aesthetical deformations or loss of breastfeeding functionality which may be consequences of breast cancer removal surgery, exists in most women. These aftereffects can be disruptive and bring psychological damage like: lack of confidence, isolation, depression, loss of sexual libido, among others.

In a society where body image plays a big key role many attempts have been made to adapt the treatments not only to eliminate cancer but also to preserve the body image of the women involved. One of the reasons to preserve the feminine image is because there is a 90% of breast cancer survival, when it is diagnosed in early stage. It is necessary to prevent the patient from any trauma that they might suffer from marks or effects of the treatments. With the development of treatments in this area, the surgery is not seen as drastic as it was when it was necessary to remove the whole breast and surrounded tissues like the mastectomy. Nowadays, mastectomy continues to be performed but, new methods exist in which only the tumor and a small margin of healthy tissue are removed, this new method is called Breast Conserving Surgery (BCS).

Although this procedure is less invasive, several options for surgical procedures can be allied to heterogeneous procedures, that may contribute to different aesthetic results. The development of educational tools, to simulate the outcome for the various surgical options is beneficial to promote better results.

1.1 Motivation

The work to be developed can have a great impact on the lives of many women affected by breast cancer disease, by helping to improve the learning process of young professional surgeons linked to oncology and other related areas.

As usual when surgeons leave college, most of them do not have the experience that is needed to easily visualize the aesthetic outcome of surgeries. Therefore, the surgeons do not know how to choose the best methods for each case, and the practice to visualizing the final result.

By creating an educational tool that creates synthetic breasts joining breast deformations, based on breast characteristics, breast interior and the location of the tumor, would help the new surgeons to visualize and understand better the consequences of the surgery.

Besides the tool, it is also beneficial not only for the beginning of the professional life but it can be useful for surgeons during their professional life. Often, when faced with doubts about a specific case, they will be able to simulate the consequences of the surgery and see the final results from a 3D perspective and therefore to be able to choose the best method to apply. This work can also have a great influence in medical training of this specialty, creating a new generation of surgeons, richer in acknowledgement, since they come already with a certain ability in predicting results, even almost inexperienced.

In addition to provide better training in surgery room, this work can also have an impact in the creation of planning tools, which uses real data from patient to discuss the results of the several procedures. This helps women who are undergoing surgery to have a better acceptance of the results because they can contribute with their opinion and visualize the final outcome, which may help them to have a better perception of the final result.

Synthetic models of the breasts will also contribute to validate registration algorithms. The algorithms take into account various breast images perspectives, such as Magnetic resonance images, Computer tomography, Mammography, Radiological Exams and Ultrasound. Where several cloud points of various images are overlapped and joined to form one image. The formed image can be rotated and it can be observable the various breast aspects.

1.2 Objectives

The objective of this dissertation is to simulate synthetic breast models with adjustable parameters, incorporating it in an interface. The parameters that are going to be simulated are: volume, shape, profile, symmetry, ptosis, breast density, also the location, nature and size of the tumor.

1.3 Contributions

This dissertation main objective is to simulate 3D breast models that will be part of an educational tool for new surgeons train breast conservative surgery. The expected contributions are the development of 3D breast models including breast surface, breast interior and tumor. The accomplishment of the proposed objectives may also be an important improvement on the surgeons' professional life, contributing to their education about the effects of surgical cancer removal.

1.4 Structure

This report is organized in six chapters. This chapter presents the motivation for the research, its objectives, its main contributions and the structure of the document.

In Chapter 2 are presented fundamentals of the breast anatomy, statistics, cancer types, psychological impact in women and treatments. Being the focus in the treatments section: surgery and the learning curve of the surgeons.

In Chapter 3, the concept of 3D models and its various applications in diverse area, are presented. After introducing the concept of 3D modelling, the various breast's modelling categories are presented, being divided into two categories: Parametric and Biomechanical models. Along this chapter, studies of the various branches and subsections of each category are reviewed.

In Chapter 4 and 5 are shown the various methodologies used to obtain the several 3D breasts and its constituents. As the process to obtain the best interface and the results of the questionnaires.

Finally, the most relevant conclusions are shown in Chapter 6. Additionally some guidelines and recommendations for future developments.

Chapter 2

Breast Cancer

In 2012, 1.7 million cases of breast cancer were diagnosed worldwide, 12% of all new cancer cases. In the same year, 25% of all cancers diagnosed in women were breast cancer [3]. Thus, cancer is recognized as being the disease that marks the XXI century, early diagnosis is a great concern and innovative treatments are fundamental.

In this chapter, a brief introduction of breast cancer is provided, including some breast anatomy details, the main cancer symptoms, incidence rates and statistics. Additionally, a general overview of the existent treatments and some psychological impacts that cancer treatments can have on a women self-esteem are described.

2.1 Breast Anatomy

The breast, also know as mammary gland is located on front of the chest, the breast itself has no muscle although it is located on the top of the pectoral muscle. The breast is full of blood and lymphatic vessels being, the last one, located mainly in the underarm area.

The breast tissues are divided into two main types: adipose and fibroglandular tissue. Adipose tissues are composed by fat cells that give the breast their size and shape, while the fibroglandular tissues are composed by ducts, lobs (milk glands) and connective tissue. Each woman usually contains 15-20 lobs in each breast [4]. Each of the 15-20 lobs are formed by several smaller lobes, as shown in Figure 2.1. The ducts are responsible to transport milk, produced in the lobs to the nipple. In Zucca-Matheus *et. al* [5] the authors show that the mean value of directed connected lobs to the nipple is approximate 12. The size of each duct is variable with its depth, so the ducts that are closer to the nipple are bigger than ducts that are further away.

Breast can be categorized according to its density. The breast density is related to a ratio between two types of tissue, fibroglandular and adipose. This main breast characteristic can be determined in mammography. Breast Imaging-Reporting, Data System (BI-RADS), are standards proposed by the American College of Radiology (ACR) in order to normalize the breast density classification. Hence, the breast analysis can be communicated in a more clear and consistent way

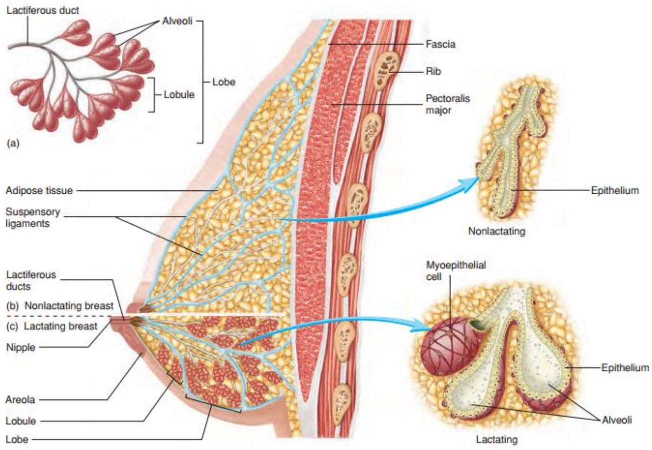

Figure 2.1: Anatomy of the breast [4].

by the medical personnel. BI-RADS classifies breast density into the following four types (Figure 2.2):

• Type I: mostly fat, the breast is mostly composed by fat tissue;

• Type II: scattered density, it has quite a bit of fat, but a few fibrous areas and glandular tissues;

• Type III: consistent breast density, it has many fibrous areas and glandular tissues;

• Type IV: extremely dense breast, the breast is almost made of fibrous and glandular tissues (Type IV).

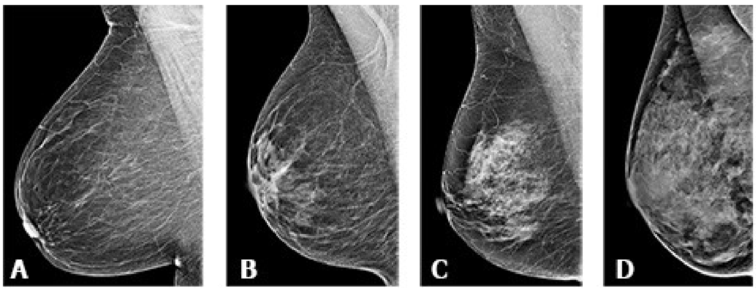

Figure 2.2: Breast density: A- mostly fatty breast B- scattered breast density C- consistent breast density D- extremely dense breast [6].

Among with other factors, breast density can be associated with the risk of developing breast cancer: women with a higher breast density are more likely to develop breast cancer [7], due to the different mechanical behaviours of the two tissues. Breast density is also often related to the outcomes of breast cancer surgery, along with other breast characteristics, such as size and volume. A woman with lower breast density may suffer more deformities because of the elastic property of the adipose tissue, so when the tumor is removed the adipose tissue tend to occupy the space that the tumor left in the breast, which results in a tissue displacement causing postoperative deformations in the breast shape.

2.1.1 Breast Shapes

Breasts can have many different shapes. Recently the company Thirdlove, a lingerie company, developed in their online shop a Breast Shape Dictionary, where many shapes of breast are exposed including the characteristics of each shape (Figure 2.3). The company goal is to make women understand better which bra is the ideal for their breast.

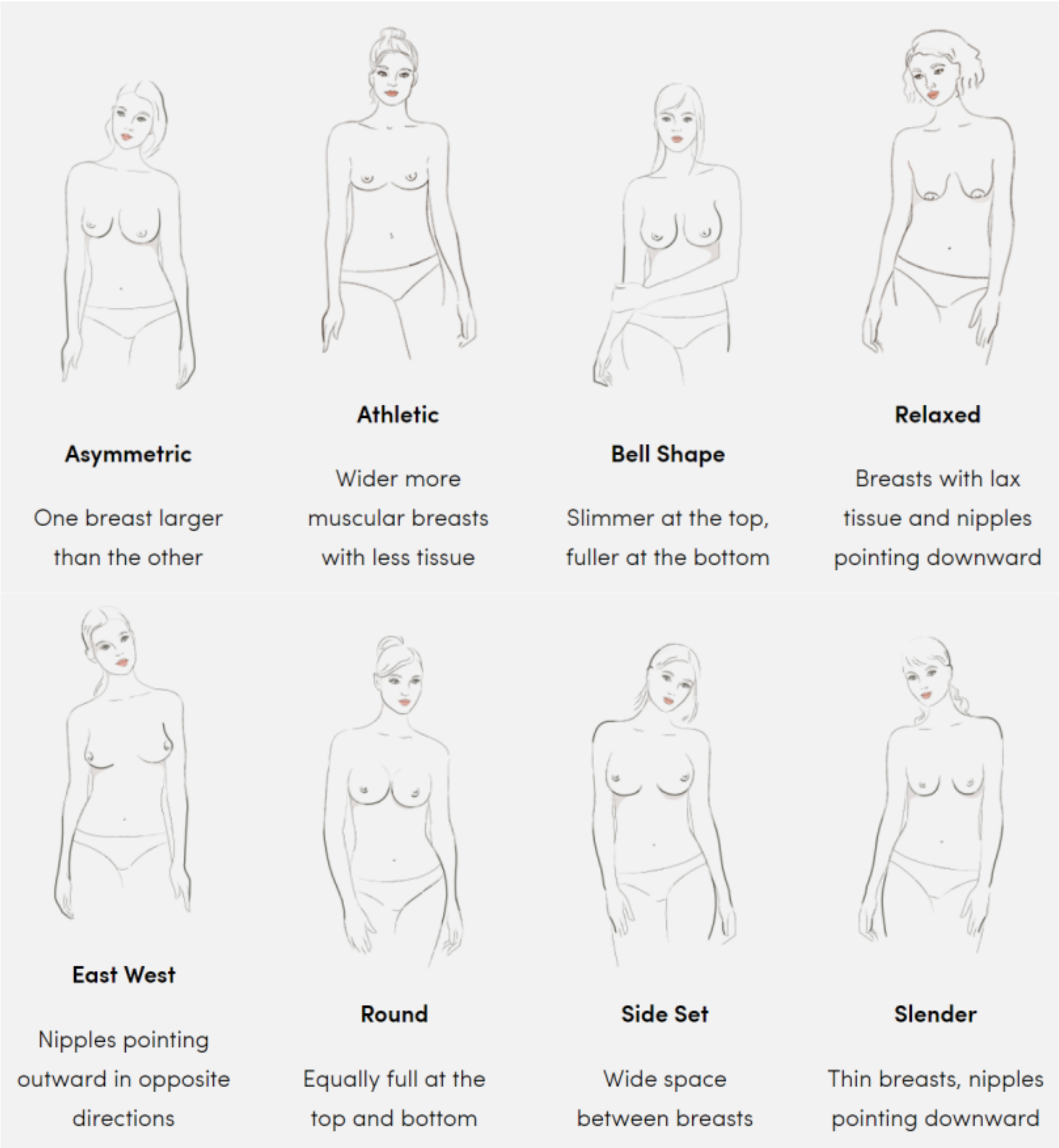

Figure 2.3: Breast Dictionary [8].

The breast measurements to classify breast shapes already motivated many scientific articles, where different investigators argued about the ideal breast measurements shape. In Swanson *et. al* [9], the author claims that only six dimensions are needed to provide an accurate representation of the breast shape, these dimensions are (Figure 2.4):

1. Breast projection;
2. Upper pole projection;
3. Lower pole projection;
4. Nipple level;
5. Lower pole length;
6. Lower pole width.

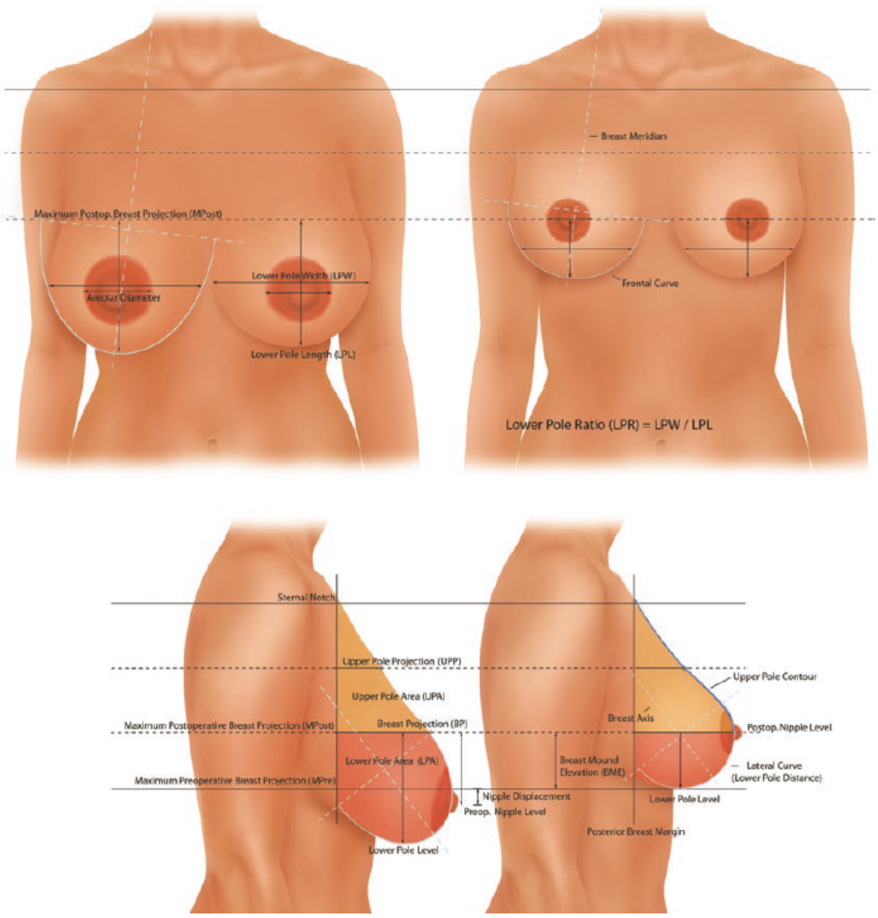

Figure 2.4: Breast measurements [9].

However, not all breasts are ideal and breasts may suffer transformation through aging. One of the most typical transformation associated with aging is known as Ptosis. Ptosis is the natural process of the breast sagging. The rate at which a woman's breasts drop and their Ptosis degree can be related to aging, gravity, massive weight loss, pregnancy or breastfeeding. The Ptosis classification is defined according to the nipple aureola complex as illustrated in Figure 2.5.

The Ptosis classification degrees are:

- **Degree 0**: the nipple and the parenchyma (glandular and adipose tissue) are above the crease underneath the breast or also called inframammary fold.

- **Degree 1**: This degree is called mild sagging and occurs when the nipple lies at the inframammary fold level and the parenchyma is below it.

- **Degree 2**: called moderate sagging where the nipple lies below the inframammary fold level but remains above the lowest hanging part of parenchyma.

- **Degree 3**: is a severe sagging in which the nipple lies below the inframammary fold and lies at the bottom of the breast, at the bottom of the breast.

- **Pseudoptosis**: is when the nipple lies above or at the level of the inframammary fold and the parenchyma has decended below the level of the fold.

- **Parenchyma maldistribution**: involves a lack of fullness in the lower portion of the breast, a high inframammary fold and a short distance from the nipple to the fold.

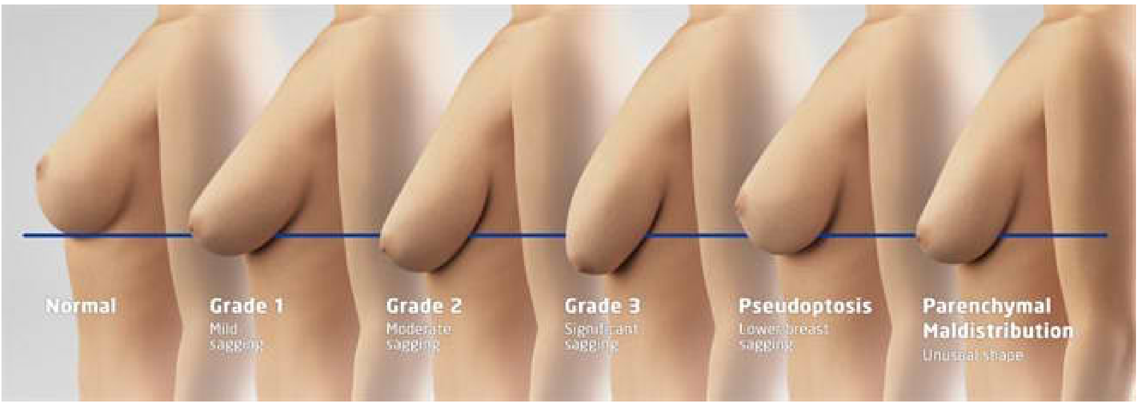

Figure 2.5: Degrees of breast ptosis [10].

The deformation which makes the nipple pointing to one side, is another quite frequent breast deformation. This deformity affects the symmetry of the breast because it occurs when the breast turns to the left or right sides, making the nipple pointing to the exterior side of the body symmetry line, which is illustrated in Figure 2.3 in the shape classified as *East west*.

2.2 Cancer

Cancer starts to be formed when cells in the body change their DNA and spread out without control. This mechanism of regeneration of cells is a natural control mechanism where cells under hormonal influence grow and divide themselves into new cells. The term regeneration implies a well-coordinated restoration of cells, tissues, and organs that have lost their physically or functionally behaviors. Cells die when they get older or are damaged, if this mechanism changes, neoplasia occurs. Typically, it happens when body's cells DNA is mutated and cells can no longer control their division process. Therefore, when cells loose control of their division they become cancerous cells. These cells begin to produce new unnecessary cells in an uncontrollable way [11].

Neoplasia can be divided in two categories: malignant and benign. Benign tumor is a tumor that grows slowly, self-limiting, which means it is unable to spread throughout the body and it is surrounded by a protective shell created by the immune system. The tumor is benign it does not mean it may not become malignant, reason why regular tests are recommended in these cases. Malignant tumor, known as cancer, occurs when the cells mechanism produces unnecessary cells. These new cells are very unstable and able to invade new tissues, traveling by the blood stream hosting in other organs or tissues that can be dangerous.

The malignant tumor developed from cells of the breast tissue is called breast cancer. The breast cancer diagnosis is confirmed by a biopsy of the nodule in question. Once the diagnosis is made, more tests are done to determine if cancer has spread beyond the breast and which kind of treatments can be applied. The three most common types of breast cancer in women are:

- Ductal carcinoma: originated from the cells of the ducts;
- Lobular carcinoma: carcinoma originated from lobular cells;
- Adipose carcinoma: originated in the adipose tissue.

Each of these classifications has several subcategories, such as *In Situ* or *Invasive*. These subcategories are related to the location of the tumor, varying if the tumor is in the structure where it began to grow or if it has already grown out of this structure respectively.

2.2.1 Statistics

Statistics show that breast cancer is one of the cancers that most affects women worldwide. Every year over 1.67 million breast cancer cases are discovered and about 522 000 women die [3]. The numbers are alarming, studies speculate that the tendency to suffer from cancer will increase over the next years. Although, over the years mortality rates have decreased, since the treatments have become increasingly efficient.

In 2018, GLOBOCAN [12] developed a study, analyzing the incidence and the mortality rate of breast cancer worldwide, generating the following values shown in the Figure 2.6.

Figure 2.6, shows two trends for developed and developing countries. Portugal follows the developed countries' trend with 4500 out of 5 million Portuguese women being diagnosed with breast cancer every year [2]. Calculations indicate that 11 new cases are detected and another 4 women die, every day.

2.2.2 Symptoms

The fight against breast cancer starts with being aware of its symptoms and an early diagnosis. In Portugal, the first mammography is recommend between 45 and 50 years. After the age of 49 years, doctors recommend to repeat the mammography every 2 years, although this interval varies

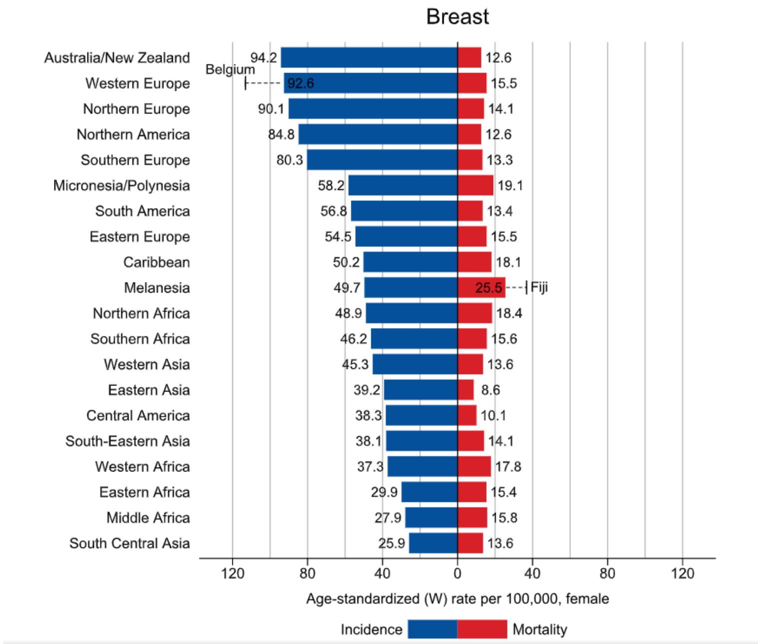

Figure 2.6: GLOBOCAN breast cancer statistics [12].

by country. *Liga Portuguesa Contra o Cancro*, one of the largest associations in Portugal, offers several support groups where psychological support is given to the patients and their families. One of the biggest achievements of this no lucrative organization is the free breast cancer screening. This was one of the actions implemented by the organization to help detect cancer in the early stages.

Among the risk factors for developing breast cancer are: age, obesity, lack of physical exercise, alcohol consumption, smoking, hormone replacement therapy during menopause, ionizing radiation B and about 5% and 10% of cases are caused by inherited genes [13]. Although there are risks that should be supervised with certain care such as having a family history of breast cancer. The first noticeable symptom of breast cancer is usually the appearance of a lump in the breast or in the lymphatic glands under the armpits. More than 80% of cases of breast cancer are discovered when a woman feels a lump during palpation. The other symptoms to keep in mind according to [14], are :

1. Modification of the breast size or shape;

2. Color change;

3. Breast or aureole skin sensitivity;

4. Retraction of the breast skin or nipple;

5. Nipple discharge;

6. Breast Enhancement;

7. Formation of crust or wounds in the breast or nipple;

8. Swelling, warmth or pain in the breast.

2.3 Treatments

Every second counts when the fight is against cancer, so it is necessary to act fast, since about 95% of the cancers in the initial state are healable. Many tests can be done to find out which is the type of cancer and its stage. The biopsy is one of the exams that may help to determine the tumor nature and whether it is benign or malignant. Figure 2.7 details the different stages in which the breast cancer can be identified:

- In Situ Ductal Carcinoma (DCIS, stage 0) or In Situ Lobular Carcionoma (LCIS,stage 0);
- Early breast cancer (stage 1 or 2);
- Locally advanced / inflammatory breast cancer (stage 2 or 3);
- Metastatic advanced breast cancer (stage 4).

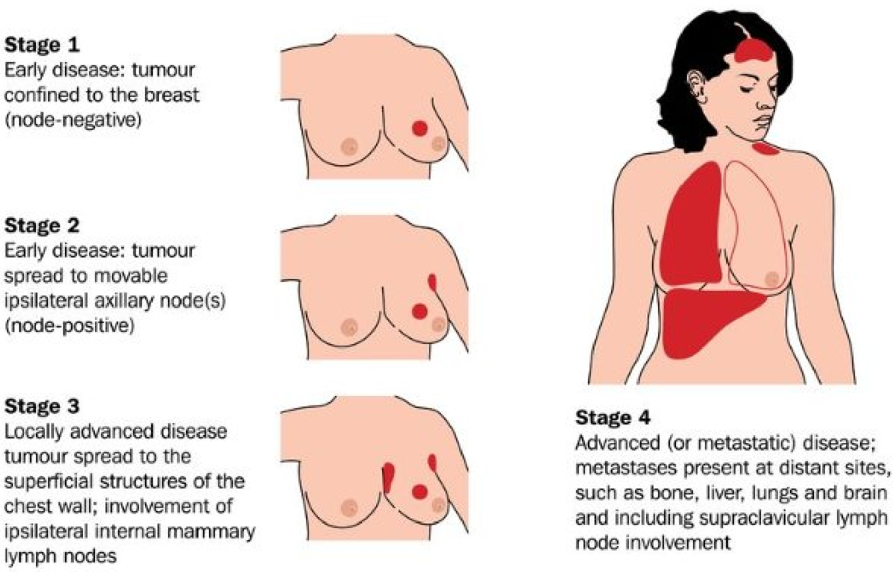

Figure 2.7: Stages of breast cancer [15].

The several stages of cancer are related to its development, which means the cancer stages depend on the breast cancer metastization. By definition, cancer can be invasive or non-invasive: in Situ or non-invasive breast cancer occurs when cells remain in the structure where they were formed. However, untreated cancer can evolve into invasive cancer which occurs when cells migrate and cause damage in the surrounding tissue. The treatment plans may depend on which stage the cancer is detected. The treatments are divided into two types:

- Local treatments: are treatments that do not affect the rest of the body like surgery and radiotherapy. These treatments remove or destroy cancer cells. These kinds of treatments are more likely to be used in early stage of cancer. The local therapy is used only to control the advancing of the cancer cells in the original tissue and not to combat the cancer metastases.
- Systemic treatments: chemotherapy, hormone therapy and targeted therapies are treatments that use the bloodstream as a mean to transport the medicament to the cancer cells all over the body. On this way, the medications can destroy or control the cancer cells. These kind of treatments are also used when the cancer has spread into other organs and tissues.

To decrease the size of the tumor before surgery or radiotherapy, some breast cancer patients receive systemic therapy so that the intervention is less extensive, being these treatments called neoadjuvant therapies. In other cases, the systemic therapy is used after surgery and/or radiotherapy to kill any cancer cells that remain, in order to reduce the risk of cancer return. These methods are known as adjuvant therapies.

Chemotherapy and radiotherapy in conjunction with surgery are the most common treatments for breast cancer. Radiotherapy is categorized in the local treatments, where high energy beams or radiation particles are used to kill cancer cells, killing good and bad tissues. In chemotherapy, one or several substances are administrated in the bloodstream to combat the cancer cells. These substances' kind and quantity depend on many factors like tumor size, estrogen presence or progesterone reception.

All of the treatments try to improve the patients' quality of life (QoL) and their chances of survival, without leaving great psychological and physical damage [16].

2.3.1 Surgery

Surgery can be done with several purposes such as: to remove the tumor and some healthy tissue to stop cancer cells from spread to other organs; to find out if cancer has spread to the lymph nodes; to reconstruct breast and assess the symptoms of advanced cancer. The most practiced surgeries in breast cancer removal, as illustrated in Figure 2.8, are:

- **Breast Conserving Surgery (BCS)**, also known as partial mastectomy or Lumpectomy, is the surgery that attempts to maintain the female body image and only the affected part of the breast is removed. The surgeon removes the cancer and a minimum small portion of the tissue that surrounds it. Usually, it is removed a smaller tissue's amount comparing with the mastectomy intervention. The breast's amount that will be removed will always depend on the tumor's size and other factors such as where the tumor is located.
- **Mastectomy**, this surgery is the intervention that women fear the most since the mammary tissues are completely removed. A few decades ago mastectomy was the standard procedure and it is still part of surgeons' daily routine. However, as this surgery is more radical, Mastectomy has the worst results regarding the patients' psychological damages when compared with less invasive treatments, like BCS.

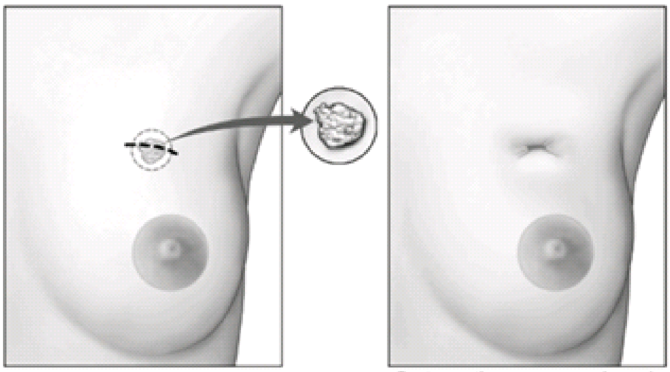

(a) Breast Conserving Surgery

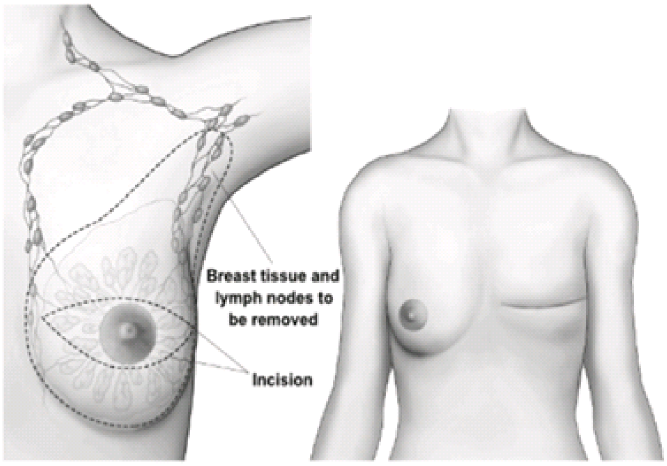

(b) Mastectomy

Figure 2.8: Types of breast Cancer surgery [17].

To understand better which treatments are used for each cancer stage, America Cancer Society has made a study in 2017 about Female Breast Cancer Treatments Patterns, whose results are summarized in the Figure 2.9. In these statistics, it is noticeable that surgery is one of the elementary therapies used for breast cancer in any type of stage [18].

2.3.1.1 Surgical Learning Curve

Since the surgery is a fairly common practice for breast cancer, the authors in [19] try to understand the learning curve concept and to address the common misnomer that steep learning curves are associated with difficult and complex procedures. Authors suggest methods by which surgical learning curves may be constructed and they describe their relevance to modern medical training, as Figure 2.10 presents.

In the graphic shown in Figure 2.10, it is observable that the curve is divided into four learning phases:

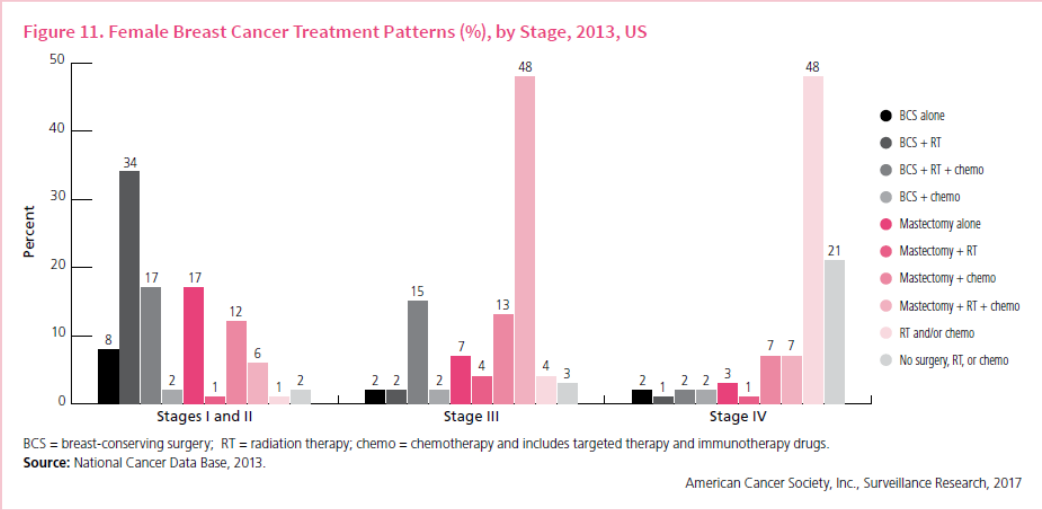

Figure 2.9: Breast Cancer Treatments for each stage [18].

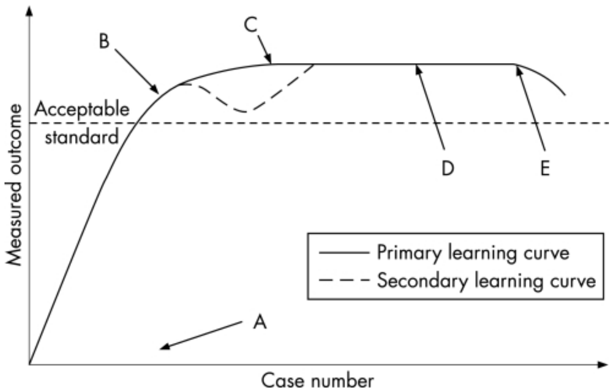

Figure 2.10: Learning Curve [19].

- **Phase A**: represents the beginning of the training. The gradient of this rise indicates how quickly individuals performance improves.

- **Phase B**: the curve can be a gradual ascent, as individuals learn and do the stages of a complex procedure. Improvements in performance tend to be faster at first and then to drop off when the improvement degree is achieved. Assuming adequate aptitude, a point is reached when the procedure can be performed independently and competently.

- **Phase C**: the additional experiment improves the results by small amounts until reaching a peak of the curve.

- **Phase D**:, peak of the curve.

- **Phase E**:, with advancing age, manual dexterity, vision, memory and cognition can deteriorate, overcoming any advantage derived from long experience, leading to a drop in performance level.

According to this study there is an increasing interest in the improvement of the training curve of new surgeons. An educational tool would help them to simulate parameters of real people and predict the final result. The goal of this dissertation is provide an educational tool to help to train surgeons, with an educational tool. The tool will aggregate factors known to affect the aesthetic outcomes of BCS, with newly breast characteristics. This will hopefully improve the understanding of the tumor and the breast attributes that most affects surgery outcomes, contributing so with a better training of surgeons.

2.4 Psychological Impact

Surviving breast cancer is a hard path which can leave physical and psychological marks on patients and their families. When diagnosed with breast cancer, most women feel that their female identity is being threatened [20]. That is one of the reasons that most women experience a sequence of negative emotions, both at the social level and in their love life.

Breast's deformations caused by surgery are one of the reasons why women may feel insecure. The main challenge though surgery is to predict how the breast will be post-surgery, because all surgeries are done in the supine position which the surgical outcome may vary if the patient is in the stand position. On the other hand, the lack of practice of each surgeon could be an issue. Besides depending on the surgery and the surgeon, the breast's deformation may depend on several other factors, such as breast density and breast shape. Women with lower breast density tend to suffer more deformation since adipose tissue tries to recover the lost mass of the breast tumor by shifting some fat tissue to the side, modifying the breast shape.

Like in any surgery, the big question apart from the therapeutic results is " What will be the outcome?", and in the surgery that removes tumor from the breast is no different."Will my breast be deformed?" and for some younger patients the question "Will I be able to breastfeed?". These are some of the more frequent questions in the doctor's office when the medical advice is that they should have a surgical treatment.

When deformations occur, women may experience feelings such as anger, anguish, sadness, frustration, fear of loss and mutilation, but also it can bring long-term consequences in their QoL. Studies show that women experience a sequence of negative emotions which can cause damage in their social and private life. The most common psychological problems associated with surgery breast deformation are: depression, anxiety, social isolation, insecurities and loss of sexual libido [20]. Family support and its environment are extremely relevant in helping to accept their condition and expressing their feelings [21]. Inclusively, there are also associations that offer assistance, in Portugal "Liga Portuguesa Contra o Cancro" that has a movement "Win and live" that promote psychological support, trying to increase the self-esteem's and shares or sells products such as hairpieces, adequate bras or scarfs.

Although there is an increasing care and innovation in the treatment's areas in order to preserve the physical aspect, which includes softwares where it is possible to predict surgical outcomes or plan surgery. Studies show that women undergoing mastectomy surgery experience more dissatisfaction with their physique and suffer more from social isolation, depression and lack of sexual libido, among others already mentioned, than women subjected to BCS. However, mastectomy is still a current practice to deal with breast cancer because the probability of metastasis or cancer recurrence decreases when the entire breast is removed.

2.5 Summary

Breast cancer is one of the diseases that characterizes the XXI century and the one that most affects women worldwide [3]. The treatments to fight against breast cancer have improved the survival rate and are increasingly concerned with the aesthetic results, like BCS. In surgery, factors such as the used technique, the placement of incisions, the volume of excised tissue, localization of the tumor or varying surgeon expertise lead to different types of results and breast shape deformations. Leaving patients who suffer or have suffered from breast cancer, experience some negative emotions, such as depression, anxiety, social isolation, low self-esteem, and sexual libido loss, which can also impair their QoL. Developing 3D breast models and incorporating then in an educational tool with the goal to improve the understanding of factors which affect the aesthetical outcomes of different surgeries. Hopefully, this will contribute to reduce the suffering of the patients. The next Chapter is about 3D Modelling and some of the existent techniques to simulate the breast shape.

Chapter 3

3D Modeling

3D modeling is a technology largely present in our daily life. Design, medicine, facial reconstruction and modeling of realistic human characters in games and animation are examples of areas where it is already applied [22, 23].

In the medicine scope, the 3D technology can have a huge importance on planning breast surgeries, since many surgeons are still learning with 2D images and breasts' drawings which gives them a quite limited perspective. Incorporating 3D models in an educational tool simulating synthetic breast, may help the day-to-day routine of surgery training and improve surgeons professional growth. Such framework will help them to visualize and simulate the breast with different characteristics, allowing, for example, to vary the volume, the shape, the tumor, and to determine the potential aesthetical outcomes of BCS.

In this chapter, the 3D modeling is presented with a brief explanation and several studies of 3D modeling in general, followed by specific 3D breast modeling examples.

3.1 Overview

3D is the representation of an object in a three-dimensional space, making it possible to simulate objects, scenarios or characters in animated scenes, which allows multiple perspectives of them.

Human body simulation has several applications in areas like medicine, movies animation, design, motion capture or games. The 3D human bodies representation helps to create more realistic games and animations, and, within the medicine area, it helps to understand and better study the human body and its movements.

A high-quality avatar was created in the work of Zollhöfer *et al.* [24] with a combination of colour images and depth. The algorithm combines robust non-rigid registration and a fitting of a morphable face model in order to reconstruct a high- quality facial geometry and texture. In 2012, Weiss *et al.* [25] create a new method to model human body shape by combined low-resolution image silhouettes with coarse range data. To obtain multiple angles of the human body, the authors capture several movements perspectives by changing the body pose. The project's main goal was to obtain a simple method to simulate body measurements through the SCAPE model

[26], which demonstrates the accuracy of their method and makes it competitive with commercial body screening. In Treleaven *et al.* [27], the authors simulate the body with the help of point-clouds, representing the body surface. The key of the work was to locate body landmarks, points, making it possible a reliable automated extraction of the body measurementsts (Figure 3.1).

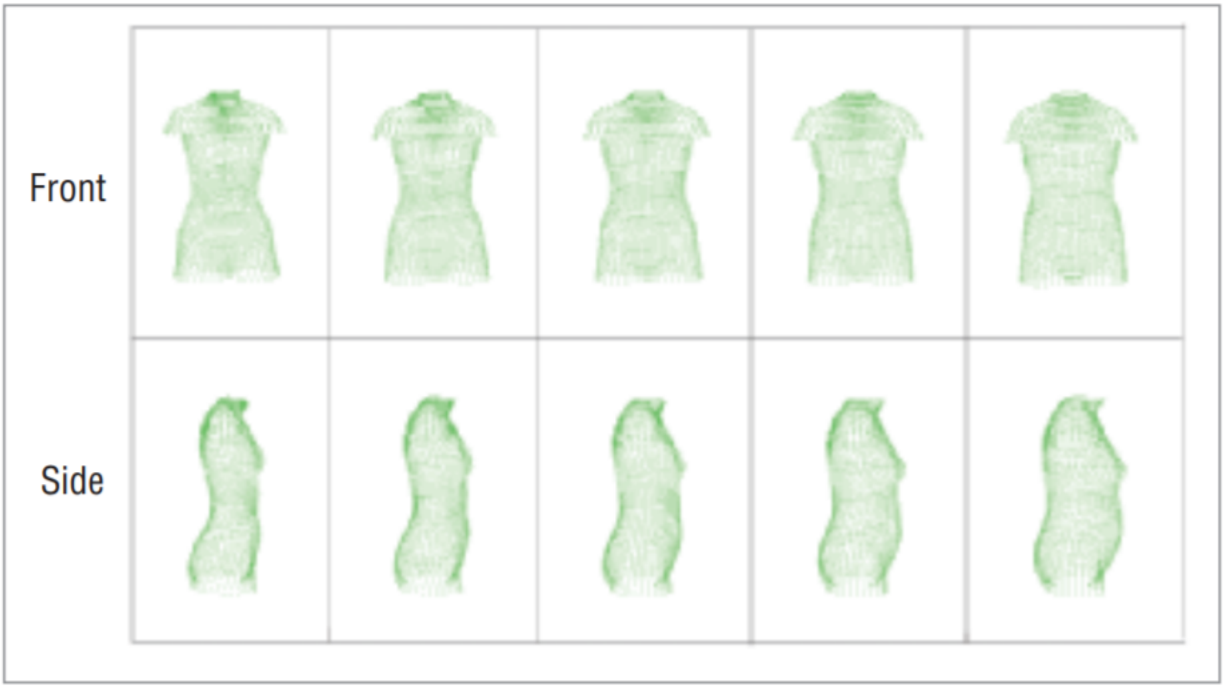

Figure 3.1: Body 3D modelling: Body size variation [27].

Although there are many studies that try to simulate the human body, there are still few trying to simulate individual organs. In 2013, Zhang *et al.* [28] used a database with 36 3D CINE MRI scans along with 2D delineation to study the heart, where all images were obtained at different times and so in several phases of the cardiac cycle (Figure 3.2). The 3D heart model was created in 3 steps: surface reconstruction, surface registration and statistical analysis. A triangular mesh approximation was calculated in order to reconstruct the surface and the heart shapes were extracted with the help of a Principal Component Analysis (PCA) algorithm. The most difficult part in the work of Zhang was to reconstruct the heart surface, considering the difficulty to obtain a quality 3D model since the heart is never still and so always bombing blood all over the body.

The difficulties felt in Zhang's heart reconstruction have similarities with the ones experienced in breast modeling. One of the biggest challenges felt in the breast modeling is associated with the breast volume, variability in the shapes, absence of anatomical landmarks and the noise associated with the breathing. There are already several frameworks that simulate plastic breast surgery, helping to select the implants from the major manufacturer, positioning the implant above or below the muscle, and adjusting the elasticity of the tissue with its behavior properties. However, few of those frameworks take into consideration the cancer factor such as the tumors' nature, its location and the breast density.

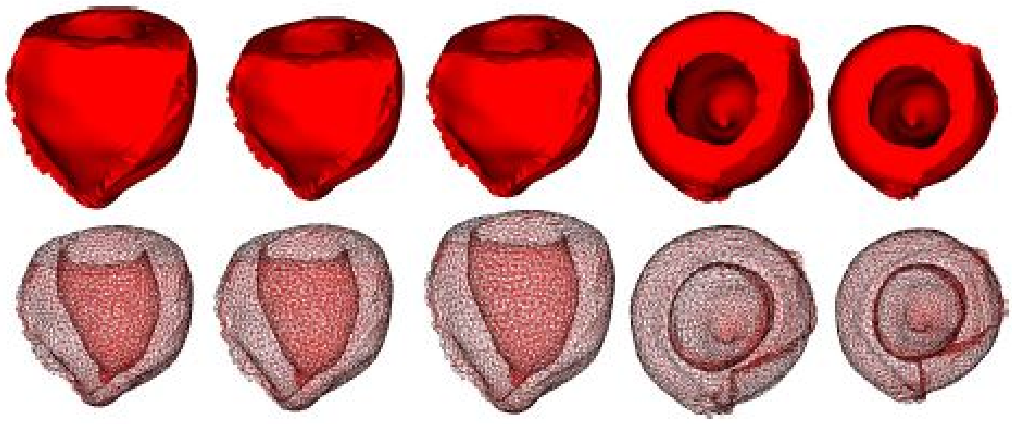

Figure 3.2: Samples of the decimated 3D mesh, from five different cardiac phases [28].

In Farinella *et al.* [29, 30] work, the authors used a commercial laser scanner to acquire the breasts' data. Volunteers sat in a chair with an inclination of 45 degrees and diverse perspectives of the volunteers breasts were acquired. It is required to identify seven landmarks to explore geometric primitives such as planes, lines and geodesics, creating so, the area of interest named box hull. These planes and points are used to obtaine distances, areas and curvatures. The tool automatically calculates and displays all the relevant planes as soon as all the required points are positioned. The final 3D model is represented by colours in a range from red to blue to green, that represent various types of curvatures such as convex, concave and flat, respectively (Figure 3.3). This analysis of the breast curvature helps to plan the surgery.

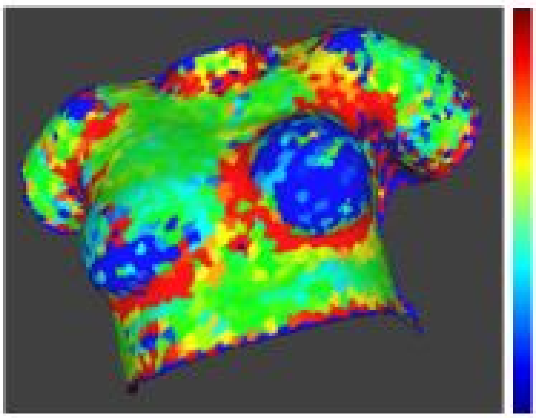

Figure 3.3: Farinella Curvature [29].

Seo *et. al* [31] created a breast model that takes into account parameters given by the user. The model is obtained with a set of 28 3D scans, which were mapped to a template mesh in a coarse-to-fine manner. The process to map the mesh to data has the following sequence:

1. template mesh prior to the pre-processing;

2. to target scanned mesh;
3. the lower level template mesh is deformed by relocation;
4. the feature points are defined;
5. the higher level mesh is obtained by subdividing each patch in the mesh;
6. deformation of the higher level mesh.

At the coarse level, a feature-based method is applied to combine the low level mesh, which connects landmarks points based on triangles, to the data mesh. The higher level mesh is obtained by dividing each triangle into a fixed number of finner triangles, see Figure 3.4. The adjustment is performed by non-rigid registration of the fine mesh to data scans, so that each data mesh has the same set of points and triangles that make up the shape vectors. The use of PCA algorithm to reduce the shape vector dimensionality and a linear model that relates intuitive user-supplied parameters of the breast shape was obtained. The RBF interpolation helps to map attributes supplied by the user to the shape vectors. In this way, the user creates the model according to the supplied parameters.

Figure 3.4: Template Mesh [31].

3.2 Breast Modelling

Most of the 3D models that simulate the breast are based on data withdrawn from Magnetic Resonance Imaging (MRI), Computed Tomography (CT), 3D surface images and attempted representation from 2D photographs. Therefore many investigators have studied several methodologies to recreate a woman's breast, making the area of breast modeling vast in methods with different approaches. The different breast modeling approaches could categorized according to Figure 3.5.

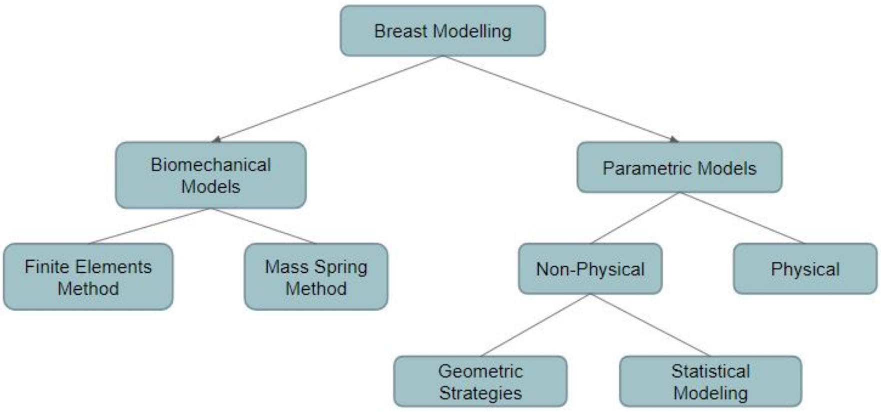

Figure 3.5: Breast Modelling categories

3.2.1 Biomechanical Models

Biomechanical models, shape the objects through equilibrium equations of forces that are applied in the object where the deformations are achieved with the following equilibrium Equation 3.1,

$$\Pi = \Lambda - W \tag{3.1}$$

where Λ is the object potential energy, Π is the energy stored by the undergoing a deformation and W is the work performed by external factors on the object such as gravity or pressure.

The equilibrium of the object is reached when the potential energy (Π) reaches a minimum value, in other words, the equilibrium is reached when the equation finds the zero derivative of Π with respect to the material displacement. This approach leads to a continuous differential equilibrium equation which can be solved for the material displacement.

In the following subsections, two biomechanical methods are presented, the Mass-Spring method and the Finite Elements method. The differences between these two biomechanical methods are the numerical methods used to solve the continuous differential. The Mass-Spring uses the discretization of the breast as a finite mesh point and Finite Elements divides the breast in elements and approximates the equilibrium equation over each element.

3.2.1.1 Finite Element Method

Finite Element Method or FEM has been commonly used in modeling tissues such as bone tissue [32, 33], myocardium [34] and brain deformation [35, 36].

The reliability of the Finite Element (FE) model consists in a reasonable FE geometry, to predict deformation and other parameters: using accurate elasticity parameters and boundary conditions. These biomechanical breast models have been evaluated based on the location of anatomical landmarks identified in breast images. The landmarks are acquired before and after in *ex vivo* compression by visual comparison of the simulated compressed breast image and the uncompressed breast. To use this method it is necessary to know the material properties of the tissues that involves the breast. The material parameters of these tissues are usually measured with *ex vivo*, uncoming Parameters from fibroglandular and fatty tissues are generally obtained from ex vivo indentation tests [37]. Most of the authors agree that the breast should be modelled with quasi-incompressible isotropic materials [38].The most common constitutive model to be used is the hyperelastic formulation with Neo-Hookean and Mooney-Rivlin models.

The performance of the biomechanical tissues can be influenced by many factors, several studies try to discover these factors by quantifying the impact of different factors on the models accuracy [39] or by comparing different materials [40]. Generally, hyper-elastic constitutive models tend to be superior than the linear models, having the boundary condition a big impact on the model performance. Palomar *et al.* [38] affirm that the complexity of the breast can be simplified by giving a average value of mechanical properties to fibroglandular and apipose tissue. While Ruiter *et al.* [41] concluded that the results do not vary within a significant range of stiffness ratios of gland and fat regarding the required simulation accuracy. The exponential and Neo–Hookean models can be used as approximations, where the linear elastic approaches performance is not so good. They argued that the simplest tissue model for breast simulation was the Neo–Hookean one, ignoring the differences between the material properties of gland and fat tissues. By comparing different biomechanical breast models Tanner *et al.* [39] found that, for a compression of 20%, the effect on accuracy caused by the modification of the material properties was less significant than the application of correct boundary conditions. With regard to the skin, Samami *et al.* [42] made the assumption that it can be considered as linear elastic and isotropic for strains lower than 50%. Reishner *et al.* [43] examined the two-dimensional mechanical behaviour of human skin, with samples obtained from different anatomical sites, concluding that the skin have varying degrees of anisotropy in different regions of the body.

Palomar *et al.* [38], establish a relation between spatial features of the breast between lying and standing position. The study is composed by two patients, A and B, with ages of 52 and 36 respectively. CT images were used to obtain the 3D model. Each breast tissue was reconstructed with triangles mesh, using the Marching Cube algorithm, and tetrahedral elements. The mechanical properties of the breast depend on the estimated property of each tissue that constitutes it. This estimation is based on the volume of each tissue measured in the segmentation procedure. The assembly of the involving tissues properties was performed from a finite element model developed from CT images, simulating first the breast in a supine position and then in standing position.

Samani *et al.* [42] in 2001 generate the FE mesh with two techniques. To model the adipose and fibroglandular tissue, the authors use an eight noded hexahedral elements with hyperelastic properites. For the skin, four noded hyperelastic membrane elements were used. The simulation of soft tissues were approached as incompressible hyperelastic materials based on experimental data. However, it does not take into account the viscoelastic response. The first technique is the voxel based (VB), that converts image voxels into hexahedral elements which is identical to edge detection. The second method is based on transfinite interpolation (TI) that uses standard thresholding based tools to segment the image so that various tissues can be separated. In the VB method, one FE is generated for to each voxel. The node that was generated is based on the pixel size. The node coordinates of the lattice are calculated and placed in the array. Tissue elements are generated in each slice starting from the left boundary point and only stops when it reaches the prior point to the right boundary, this iteration is made for each slice. The skin is generated with four quadrilateral membrane elements.

In the second technique (TI), each slice is divided into three segments, the breast area will be enclosed by the chest wall. The next step is to generate nodes by mapping them from the unit square grid to a set of nodes. The skin mesh is created by finding nodes connections of three of the unit square's circumferential. In the final, the VB method use less elements numbers to represent the breast surface. See Figure 3.6.

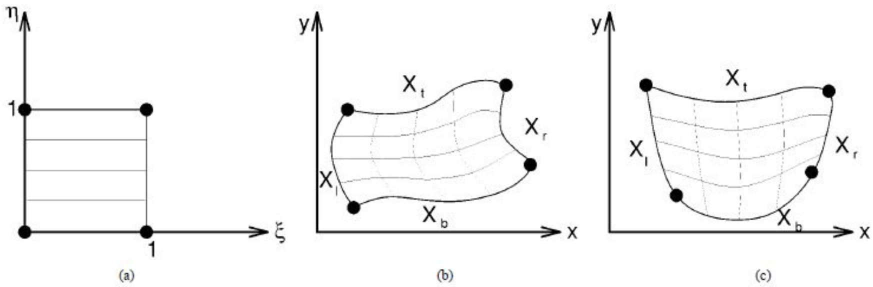

Figure 3.6: a) A unit square. (b) A physical space. (c) Breast boundaries in the TI meshing technique. [42].

3.2.1.2 Mass-Spring Method

Mass-spring method is widely used in face modeling in which three-layer mesh modeling are modeled: the dermis, a layer of subcutaneous adipose tissue and muscular layer. This method was adopted to the breast modelling. One of its applications areas is in the sport area, as the example of the creation of a dynamic breast model during exercise, comparing the displacement of the breast with and without sports bra.

Patete *et al.* [44] adopts this method to model breast deformation. The authors extract volumes from patients' MRI and tetrahedral meshes to represent skin, fat and mammary glands are created. The deformation is given by the Mass-spring method, by estimation of the length and stiffness of the spring rest. The obtained parameters are used to deform the uncompressed model (patient in prone position) to reach the real one (lateral breast compression).

In the work of Balaniuk *et al.* [45], the object surface is obtained using a triangular mesh that is connected by the ends. The deformation is obtained through Mass-Spring method in which the authors introduced a new method called the Radical Elements Method (REM). In each, it is discretized the volume of the object together with radical elements that radiate from the center of the object to the surface. The equilibrium forces and the deformations are simulated with the radical elements that were defined as the previously estimated parameters (length, rigidities, area of elasticity and rotation). The deformable object is simplified to a single point, which corresponds to the center of the radical mesh. The advantage of this procedure is that it is possible to simulate in real time. Despite its advantage, the method can not use REM for star objects.

3.2.2 Parametric Models

Parametric models are characterized by using a limited number of parameters to mold an object. Several studies used PCA modes learnt from a exemplar data set to represent breast shapes [46] and others simulate breast by applying user-intuitive parameters to obtain breast shape vectors [31]. Principal Component Analysis (PCA) is a machine learning tool that reduces vector dimensions and learns from a set of exemplar data (training set). PCA has gained more and more ground in this area. Fitting geometric entities to represent breast data is also part of the parametric models. Barr *et al.* [47] were the first to use the superquadric family, composed by superellipsoids, super-hyperboloids as well as supertoroids in their study. The advantages in using the superquadrics family are:

- their parameters have an intuitive meaning, making their handling straightforward;
- superquadrics parameters have a large expressiveness power for natural shapes with rounded edges and corners, such the case of the rounded shape of breasts;
- the fitting of superquadrics to 3D data is a problem thoroughly investigated, robust and fast methods have been developed for this purpose.

In the work of Bardinet *et al.*[48] the authors explain how to fit a parametric deformable heart model, where a coarse fitting of data was accomplished with superquardics. Chen *et al.* [49] developed the idea from Bardinet and adapted to fitting a superquadrics into a breast model. In 2014, Pernes *et al.* [50] updated Chen's work by improving the fitting process of the proposed parametric model of the breast.

Initial models in the works of [48] and [49] were obtained describing the fitting of surperquadrics to data, although they propose an extra step of fine adjusting to represent data with accuracy. Nevertheless, the two authors use different strategies. Bardinet *et al.* [48] propose a geometric strategy to fully adjust the model to deformable data. In Chen work [49] physical equations are used to approximate superquadrics to the real shape of the breast.

3.2.2.1 Physical Strategies

In the Physical Strategies the work which stands out is the work realized by Chen [49] that approaches the breast by superquadrics. The work assembles geometric models by reducing the geometric distance instead of using the minimum distance between data and model. This is accomplished by changing the least squares cost function. To solve the optimization problem, the downward gradient and a Gauss-Newton method are compared, being the Gauss-Newton method the faster.

In order to approximate the breast shape, the primitive superquadric shape suffers five physical deformations: ptosis, turn, top-shape, flatten side and turn-top. Ptosis, models the flaccidity that affects the breast over the years as it ages. The turn deformation is the deformation that happens when the breast points to one side, left or right depending on the breast. The top-shape deformation models the breast upper half concavity and/or convexity in profile. Deformation known as flatten modulates the transformation of the inner of the breast toward the middle of the trunk. Turn-top is the deformation that turns the top breast half towards the shoulder (Figure 3.7). There are 23 parameters that must be defined by the fitting procedure, for this reason, it emerged a problem that was solved in a physics-based framework by using langrarian mechanics so it converted the model into a Dynamics models.

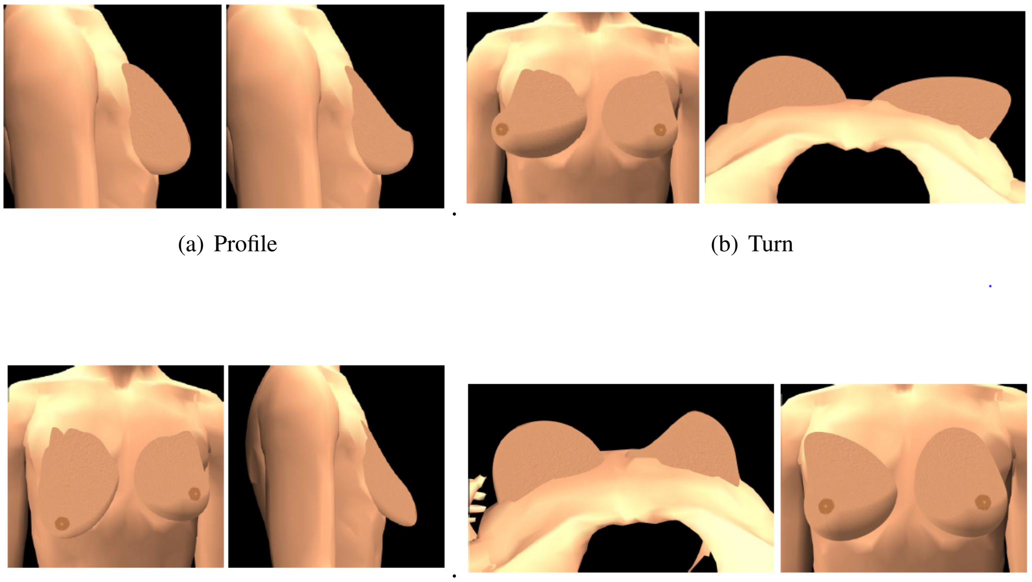

(a) Profile (b) Turn

(c) Ptosis (d) Flatten

Figure 3.7: Deformation from Chen's work.[49].

3.2.2.2 Non-Physical Strategies

The non-physical strategies are divided into: Geometric Strategies and Statistics Strategies.

3.2.2.3 Geometric Strategies

In Geometric Strategies, the object are made by curved lines. Control points are marked, to obtain the shapes of the objects. The form of the object is adjusted by moving the control points to the new positions, by deleting or adding control points or changing the control points weight. Common methods such as Bezier curves, B-splines or non-uniform rational B-splines (NURBS), specify curves with a small vector of control points, these approaches allow a representation of the object and support interactive modification, which even the simplest change may require adjustments of many control points [51]. Therefore Free form deformation (FFD) does not deform the object by adjusting individual control points. FFD adjust the space in which the object is embedded. All of this method is based on the assumption that the object is inserted in a parallelepipedic grid. The vertices of the object, are expressed in the coordinates of the grid frame, in order to deform the object. Pulling by a grid point, the parallelepipedic will deform and transmitted the deformation to the object using a re-expression of the coordinates [52]. The first step in getting a FFD is to create the grid space, defining X0 and frame vectors: $\overrightarrow{S}$, $\overrightarrow{T}$, $\overrightarrow{U}$. In which point X of the Object is expressed by:

$$X = X0 + s\overrightarrow{S} + t\overrightarrow{T} + u\overrightarrow{U} \tag{3.2}$$

$$s = \frac{\overrightarrow{S} \times (\overrightarrow{X} - \overrightarrow{X0})}{\overrightarrow{S} \times \overrightarrow{S}}; t = \frac{\overrightarrow{T} \times (\overrightarrow{X} - \overrightarrow{X0})}{\overrightarrow{T} \times \overrightarrow{T}}; u = \frac{\overrightarrow{U} \times (\overrightarrow{X} - \overrightarrow{X0})}{\overrightarrow{U} \times \overrightarrow{U}} \tag{3.3}$$

Each vertex of the resulting mesh is a control point, Pijk, and its location in the frame (X0; $\overrightarrow{S}$; $\overrightarrow{T}$; $\overrightarrow{U}$) given by:

$$P_{ijk} = x0 + \frac{i}{l}\overrightarrow{S} + \frac{j}{m}\overrightarrow{T} + \frac{k}{n}\overrightarrow{U}, with i \in [0...l], j \in [0...m], k \in [0...n]. \tag{3.4}$$

The Bernstein polynomial gives the relation between weight and the control points of each point of the object, X, being the equation that gives the deformation:

$$X = \sum_{i=0}^{l}\sum_{j=0}^{m}\sum_{k=0}^{n} C_i^l C_j^m C_k^n (1-s)^{l-1}(1-u)^{n-k} P_{ijk} \tag{3.5}$$

Bardinet *et al.* [53] worked with heart model strategy, using the FFD to deform the superelipsoid. After the coarse adjustment of a superquadratic to the data, the model is deformed. In detail, the grid of control points is initially defined by the dimensions and orientation of the previously superelipsoid. The axis sizes a1, a2 and a3 define the grid size and orientation. The axes are adjusted according to the rigid transformation coefficients ϕ, θ,ψ, tx, ty, tz. The origin of the frame, X0, is chosen to be (a1; -a2; a3), and the frame divided into (l + 1) (m + 1) (n + 1) control points. The new points can be described with the Equation 3.6,

$$X = BP \tag{3.6}$$

in which P is the matrix containing the coordinates of the contour points and B the deformation matrix. The deformation of the box is based on the displacement field between the model and data points. From the displacement field, a new set of control points is obtained, which multiplied by the deformation matrix origin the new model. The errors between the model and the data are verified by a threshold, marking the end of the iterative cycle.

3.2.2.4 Statistical Strategies

Statistics models have gained increasing importance in the simulation of synthetic breast models. These models come from a training set of images, annotation or landmarks. The fundamental idea is that any new form can be modeled as a linear combination from the data in the training set. To use this method it is necessary to identify the points that will by classifying landmarks, these points must be consistent located from one image to another. The position of these points forms the vector. Combining all the vectors of each image it is obtain the training set. In order to obtain better results, it must represent the vectors in the same frame coordinates. The training set must be configured to derive a parameterized model from the form and restrict the range of plausible forms.

The new data (X_{new}) can be obtained with a combination of n exemplar shapes like:

$$X_{new} = \sum_{i=1}^{n} \alpha_i X_i, with \sum_{i=1}^{n} \alpha_i = 1 \tag{3.7}$$

Principal Component Analysis (PCA) is a popular and valuable approach to reduce the high dimensionality of the dataset and remove just the most significant features to get few parameters, ie, it calculates the major variation axes in the data set. The first step to using PCA is:

• Compute the mean shape $\bar{X}$:

$$\bar{X} = \frac{1}{n} \sum_{i=1}^{n} X_i \tag{3.8}$$

• Compute the covariance of the shapes:

$$S = \frac{1}{n-1} \sum_{i=1}^{n} (X_i - \bar{X})(X_i - \bar{X})^T \tag{3.9}$$

• Compute the eigenvector, ϕ_i and corresponding eigenvalues λ_i of X (sorted in descendent order).

If Φ contains the t eigenvectors corresponding to the largest eigenvalues, the training set, X can be approximated using:

$$X \sim \bar{X} + \Phi b \tag{3.10}$$

where vector b defines a set of parameters of the model and is a t dimensional vector given by

$$b = \Phi^t (X - \bar{X}) \tag{3.11}$$

the vector b define a set of parameters of a deformable model. As consequence, the Equation 3.7 can be simplified to:

$$X_{new} = \bar{X} + \sum_{i=1}^{n-1} \alpha_i x_i \tag{3.12}$$

By applying limits of $3\sqrt{\lambda}$ to the parameter, B_j, ensure that the shape generated is similar to those in the original training set.

Seo *et al.* [31] created a breast model that takes into account the parameters provided by the user. The model is obtained with a set of 28 3D scans, which were mapped to a template mesh in a coarse-to-fine manner. At the coarse level, a feature-based method is applied to combine the low level mesh, which connects landmarks points based on triangles, to the data mesh. The higher level mesh is obtained by dividing each triangle into a fixed number of finner triangles. The adjustment is performed by non-rigid registration of the fine mesh for data scans so that each data mesh has the same set of points and triangles to make up the shape vectors. The use of PCA algorithm to reduce the shape vector dimensionality and a linear model that relates intuitive user-supplied parameters of the breast shape was obtained. The RBF interpolation helps to map attributes supplied by the user to the shape vectors. In this way, the user create the model according to the supplied parameters.

Statistical models can also be combined with other deformation models such as FE. A 3D statistical deformation model of the breast is shaped from biomechanical simulations. The displacement fields from FEMs were mapped to a common space and normalized by breast size. Variability is modelled based on the principal components of the FEM displacements between all examples and the common space. Two statistical models were built. The first model captures the motion between compressed and uncompressed breasts, and the second defines the difference due to variations in patient positioning and compression magnitude.

The works from Gallo *et al.* [46] had a 3D dataset that is composed by 40 Nuclear Magnetic Resonances of breasts where they applied PCA to the dataset. The results are manipulated to generate new breast models. Although a precise mapping between the proposed modes and common properties like volume, roundness or concavity is not possible some clinical correlation was made. Gallo concluded that the first 6 eigenvalues are sufficient to produce a fairly good approximation to the real data, even in the case of extremely deformed shapes.

Kim *et al.* [54] developed a 3D virtual simulator for breast plastic surgery using image-based modelling and an example-based approach to obtain the breast shape. First, the 3D torso data were obtained from 2D orthogonal photographs of patients. Several feature points are marked in the images, which are used to deform the 3D model template. To fit the breast: an affine transformation matrix was obtained with Singular Value Decomposition (SVD) to match the template model feature points to the feature points calculated from the 2D images. Local deformation of the model is further accomplished by interpolating the remaining vertices of the template mesh with RBF. The surgery outcome is simulated based that each subject can be expressed as a linear combination of the exemplar data. With a weighing matrix of the feature points applied to the displacement vector between exemplar data points before and after surgery it is possible to obtain pre-operative data.

3.3 Summary

Resuming, a 3D breast model can be obtained through several methodologies as seen in Section 3.2. In this chapter, 3D breast models were reviewed in order to understand better the difference between the several breast modelling division. The large division is between biomechanical models and parametric model. The former were widely used to model breast deformities, resulted from radiological procedures, in order to estimate the breast shape under gravity loads and even to simulate surgical results. However, such models generally require large computing times and adjusting the materials properties to suitably breast shapes, in a patient-specific manner, is still incompatible with the clinical set. Parametric models represent the breast with few parameters, which can be easily manipulated using physical equations, geometric modifications or statistical knowledge. Some examples are explained in order to understand the methods, proposed by the authors, to model the breast.

Although 3D breast models have been used in many applications such as surgical planning, post-operative changes, volumetric measurements and breast shape, there are few applications using 3D models incorporated in an educational tool.

Chapter 4

Synthetic Breast Models

In order to create a reliable and practical educational framework for surgeons, it is crucial to reflect on the newly graduate surgeons, since they do not have the experience and the accessibility to medical exams like MRI and mammographies examples. In this wise, creating a tool able to simulate synthetic breast models, using parametric equations, where new surgeons can learn, explore and manipulate different parameters such as breast form, symmetry and sagging, or the tumors location and nature, becomes meaningful.

The surgeries success and outcomes may be increased by the exploration of this modelling interface, with which the new surgeons may learn and have a better understanding of the BCS surgery procedure and its consequences. The necessary inputs values to simulate a synthetic 3D breast model are volume, type of shape, breast projection, the ptosis degree, breast symmetry, BI-RADS and for the tumor, its location, type, shape, and radius. To specify if the simulated breast should be the left or the right breast is also required.

The procedures and methodologies that have been used to create these models will be detailed in this chapter.

4.1 Breast Surface

The breast surface contains the elements that are directly visible to the human eye, like the breast shape, projection, symmetry, ptosis and the nipple aureole complex (CAN).

A torso from Mathworks, created by Walterio Mayol-Cuevas [55], was adapted for this dissertation with the purpose of obtaining only the torso. This torso was a suggestion from a doctor in order to give the user a referential in the breast simulation, see Figure 4.1. The torso was then modified to obtain real body measurements.

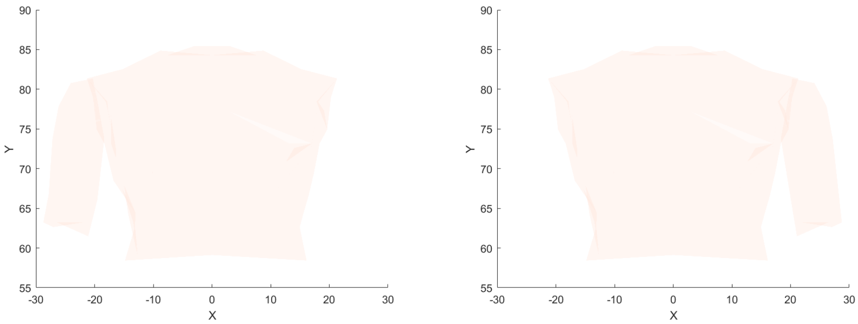

(a) Torso for right breast (b) Torso for left breast

Figure 4.1: Body torso adapted from [55].

The breast shape is simulated at first with the help of the superquadric family, more specific a superellipsoid, with the parametric equation, Equation 4.1.

$$\begin{bmatrix} H \times sin(\omega) \times cos(\phi) \\ W \times sin(\omega) \times cos(\phi) \\ CNL \times cos(\omega) \end{bmatrix} \tag{4.1}$$

The variable H is defined with the help of the torso, where H is half of the width of the torso. W depends on each breast shape and if it is the upper breast half or the lower breast half. Chest nipple length (CNL) value is the length between the chest to the nipple calculated based on the volume introduced (Figure 4.2).

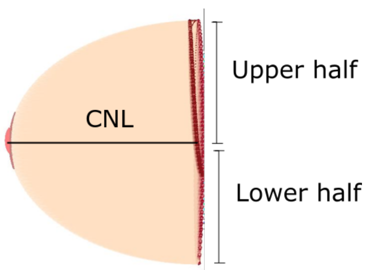

Figure 4.2: Chest Nipple Length.

The coordinates system associated to the breast model is (Figure 4.3):

• X axis : from the right to the left;

• Y axis : from the bottom (feet) up top (head);

• Z axis : from the chest wall outward thought the nipple.

4.1.1 Breast Shapes

Breasts can have many different appearances, in which, for example, the lower pole of the breast can be bigger or smaller when compared to the upper pole, and vice-versa. In such manner, six

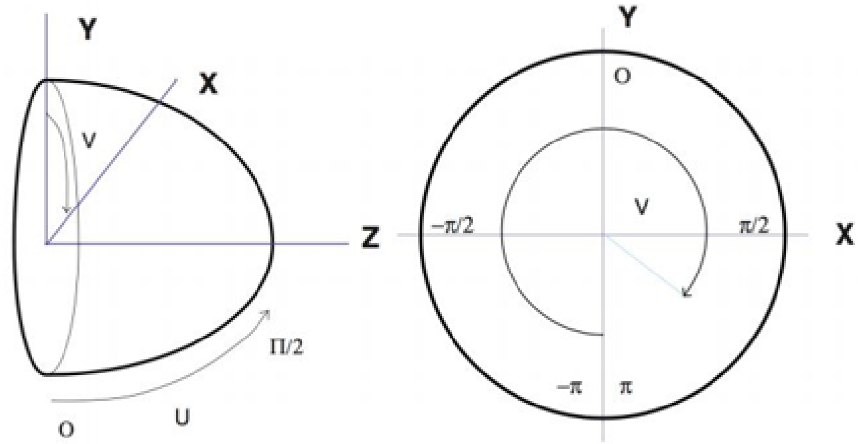

Figure 4.3: Coordinate system of synthetic breasts Side and Front View [49]

breast shapes were patterned: ideal, unappealing, oval, shaped-round, classic and round, depending on the upper (U), lower (L) half ratio of the breast.

Mallucci *et. al* [56] work was based on several anthropometric breast measurements to relate the upper pole of the breast with the lower pole, where the division between the two half's was the nipple line, creating a ratio.

In this dissertation, the results of Malluci *et. al* [56] were adopted such as the ideal and unappeling ratio while the shaped breast ratio were extracted from more common types of breast implants. All of the breast shapes were adapted to depend on the human torso. The height (H) of the breast relates the height of lower breast half (L) with the height of upper breast half (U) and u is the ratio of the upper half. All of the six breast shapes were simulated with convex lower poles. L and U are then calculated as function of H, see Equation 4.2.

$$\begin{aligned} H &= U + L \\ U &= u \times H \\ L &= (1-u) \times H \end{aligned} \tag{4.2}$$

For these breast characteristics only the Y axis is affected. In the Table 4.1 are presented the various rations adopted to each breast shape. From Figure 4.4 to Figure 4.9 the results of the different breast shapes generated with a volume of 300 cc are shown.

Breast shapes are simulated having into account a volume and the type of shape selected by the user. Since the U and L value are fixed by the torso and the shape type, the CNL will vary in order to the obtain the introduced volume input.

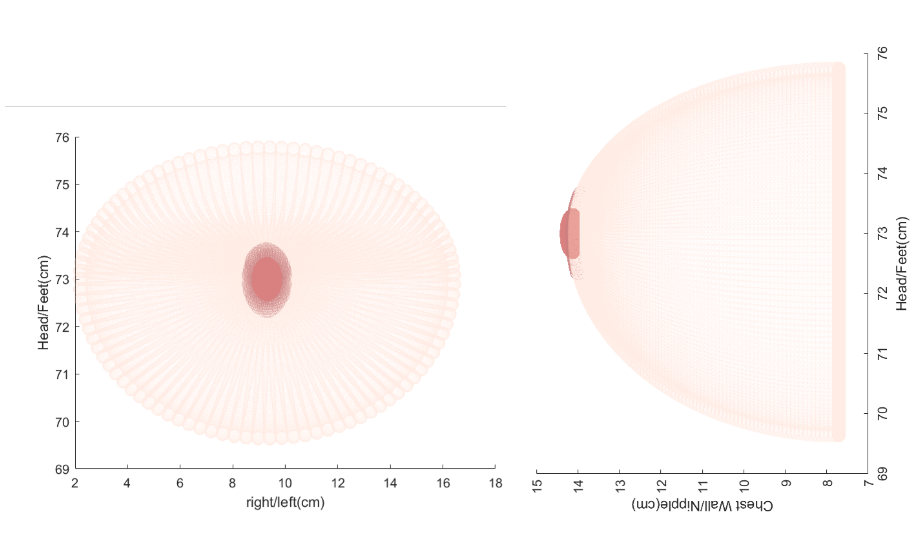

Figure 4.4: Ideal Breast.

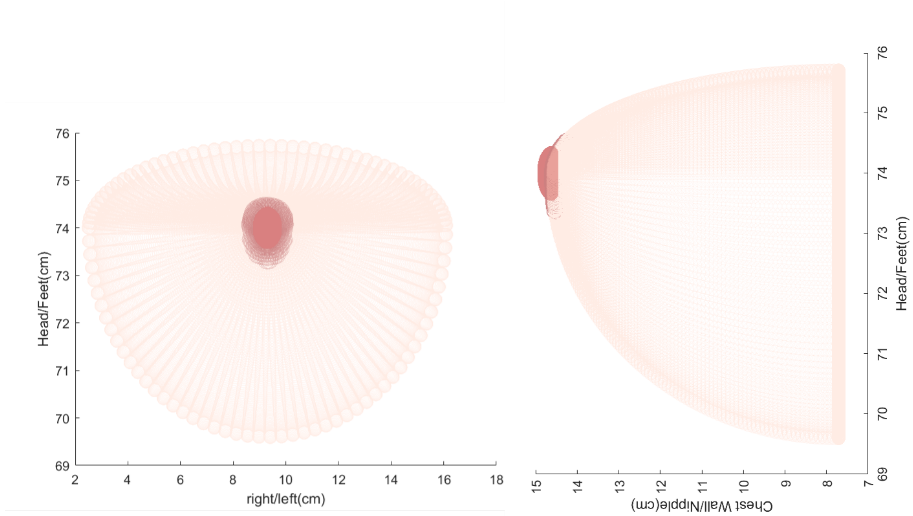

Figure 4.5: Unappealing Breast.

Type of breast	Upper and Lower
Unappeling	25:75
Ideal	45:55
Shaped-Round	60:40
Oval	69:31
Classic	73:27
Round	50:50

Table 4.1: Types of breasts and their associated upper/lower rations.

4.1.1.1 Breast Projection

Breast projection or profile is the perspective of the breast on the side view, where the top of breast can have many forms to decay towards the nipple. The breast profile simulated in this dissertation has been adopted by the work of Chen *et. al* [49], where the author describes it as a breast deformation, top-shape. The parameters used in [49] are s_0, s_1, t_0 and t_1 where s parameters are slopes, and t parameters define curvatures. The s_0 and t_0 are parameters that change the profile near the chest wall, while s_1 and t_1 indicate changes near the nipple, see Table 4.2.

With the defined parameters, the Y coordinates above the nipple will be scaled by a polynomial equation (Equation 4.3).

$$\begin{aligned}
A &= -0.5 \times t_0 - 3 \times s_0 - 3 \times s_1 + 0.5 \times t_1 \\
B &= 1.5 \times t_0 + 8s_0 + 7 \times s_1 - 0.5 \times t_1 \\
C &= -1.5 \times t_0 - 6 \times s_0 - 4 \times s_1 + 0.5 \times t_1 \\
D &= 0.5 \times t_0 \\
E &= s_0 \\
F &= 1
\end{aligned} \tag{4.3}$$

In this thesis, five types of profiles can be simulated, which are listed in Table 4.2, with the respective parameters. The results are demonstrated in Figure 4.10.

The user will select the breast profile where the upper half of the previously created breast will suffer the projection transformation with the right parameters of the top-shape used in [49].

Breast profile	$S_0 Value$	$T_0 Values$	$S_1 Value$	$T_1 values$
Linear	-1	0	1	0
Concave	-1.6	1.5	1	2
Convex	0	15	0.25	-5
Round	0	0	0	0
Ogge	0.6	-15	0.8	-5

Table 4.2: Type of breast profiles and top-shape parameters.

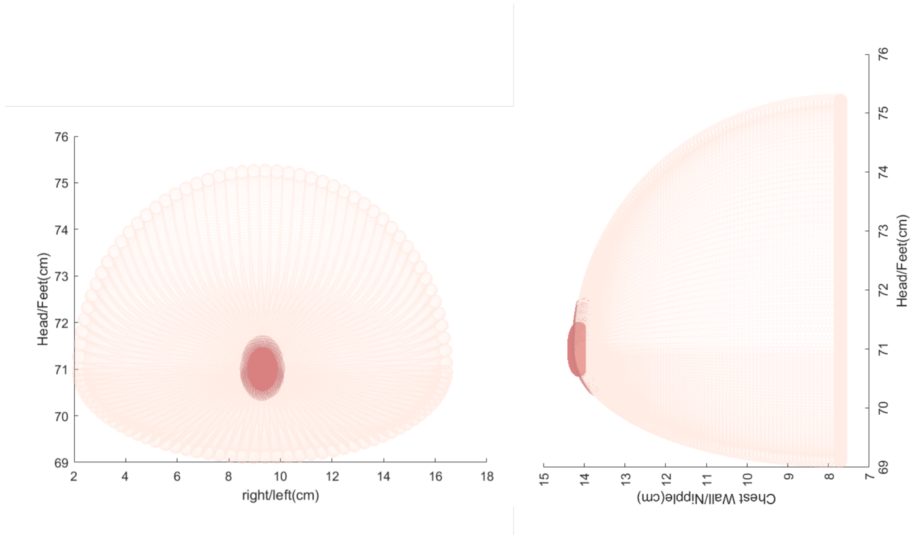

Figure 4.6: Classic Breast.

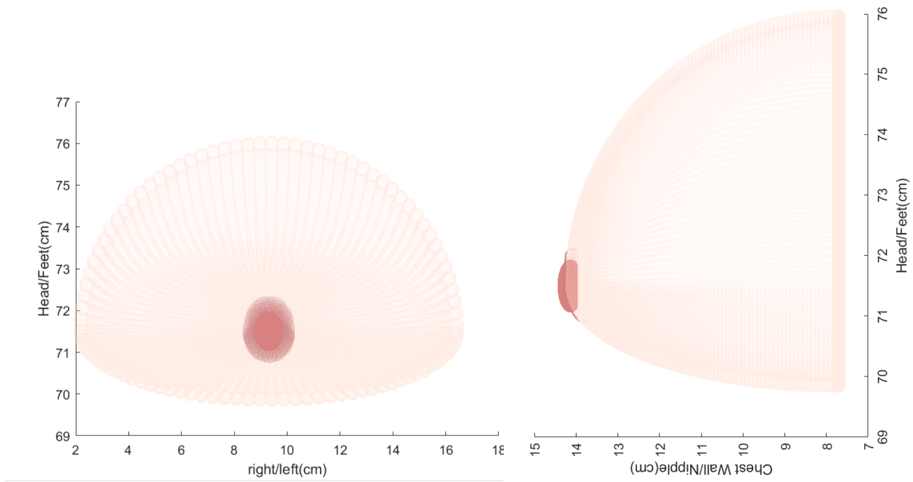

Figure 4.7: Oval Breast.

4.1.2 Breast Deformities

So far, the user can select the volume, shape and it is possible to model the upper pole projection of the breast. However, this initial shape is very symmetric, and all shapes share a convex unmutated pole. Like in real life, breasts are not always ideal and perfect, they can suffer deformation along time. Therefore, in this work, two breast deformations were modeled: ptosis and turn, based on Chen *et. al* [49]. The framework provided, allows the breast simulation with or without deformities, so it can be possible to simulate breast without ptosis or symmetry.

Ptosis is the natural process of breast sagging. The rate at which a woman's breasts drop is classified by its ptosis degree. This classification of the ptosis degrees depends if the complex nipple-areola is below or if it is above the infra-mammary fold and above or below the contour of

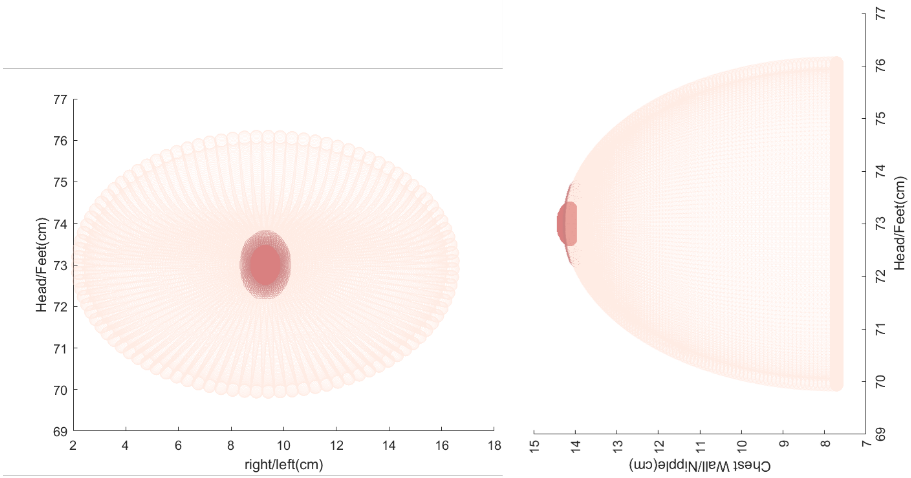

Figure 4.8: Round Breast.

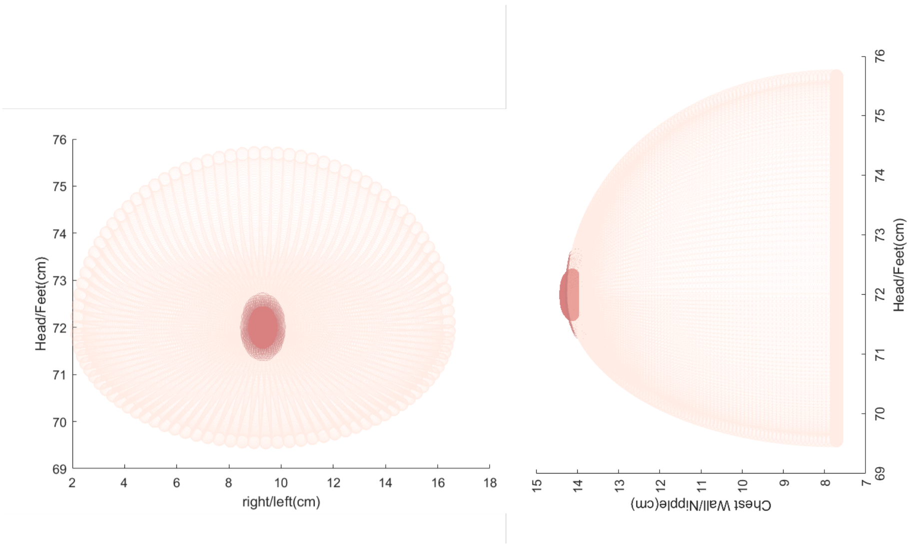

Figure 4.9: Shaped-Round Breast.

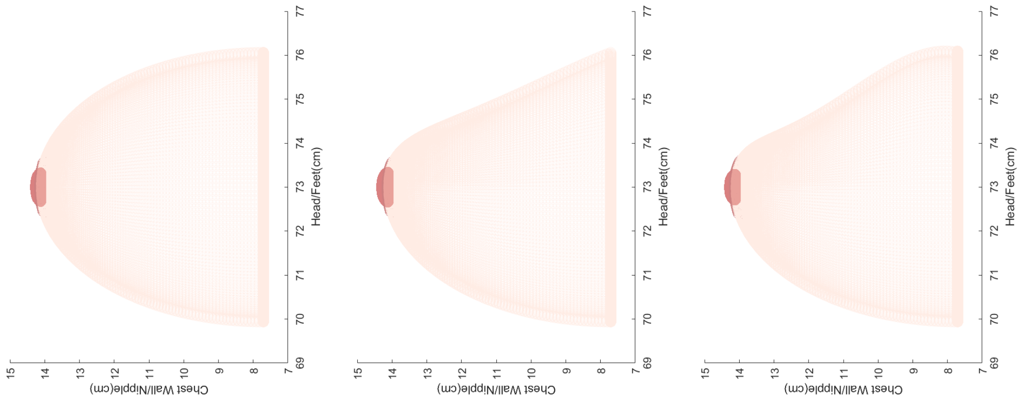

(a) Round (b) Linear (c) Ogge

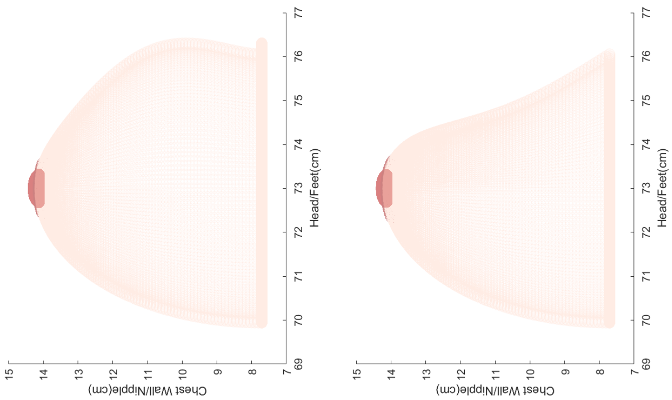

(d) Convex (e) Concave

Figure 4.10: Breast Profile results.

the breast, see Figure 2.5. There are 6 degrees of ptosis:

1. None;
2. Ptosis degree 1 - Areola below the infra-mammary fold and above the breast;
3. Ptosis degree 2 - Areola below the infra-mammary fold and above the breast contour;
4. Ptosis degree 3 - Areola below the infra-mammary fold and the contour of the breast;
5. Pseudoptosis - Areola above the mammary fold, losse, hyperpoplastic skin;
6. Parenchymal Maldistrubuiton.

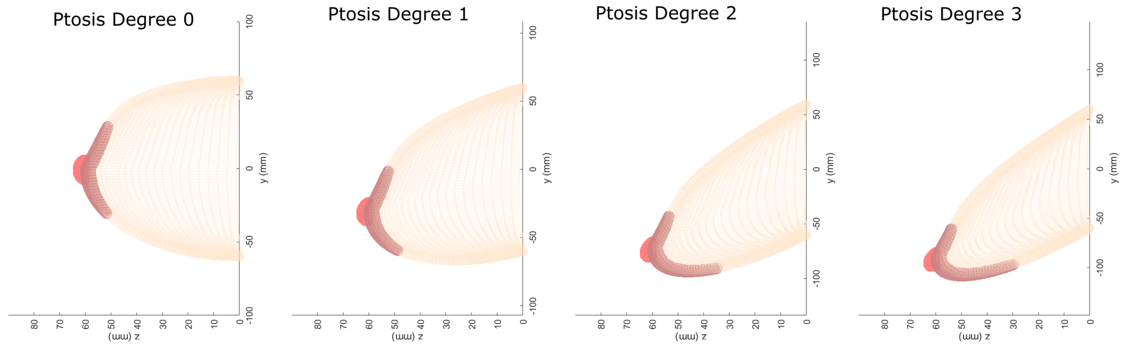

Figure 4.11: Breast Ptosis Degree adapted by Chen [49].

Nevertheless, in this dissertation only the first four degrees are modeled. To be able to recreate a realistic outcome of breast sagging and so the degrees of the ptosis, values were tested to approximate the ptosis values in order to obtain the Complex Aureole Nipple (CAN) above or below the infra-mammary fold which is the natural boundary of a breast and the chest from below.

In Chen [49], the author tries to recreate the sagging of the breast by updating y-coordinates with a quadratic function of z-coordinates with parameters (b_0, b_1, Equation 4.4). Similarly to the projection of the breast, both parameters were fixed to obtain four degrees of ptosis, as listed in Table 4.3.

$$\begin{aligned} Tlpd &= -(b_0 \times Z + b_1 \times Z^2) \\ Y &= Y + Tlpd; \end{aligned} \tag{4.4}$$

Ptosis Degree	b_0 values	b_1 values
None	0	0
Degree 0	0.5	0
Degree 1	1	0
Degree 2	1.5	0
Degree 3	1.7	0

Table 4.3: Adopted b_0 and b_1 values for ptosis degrees.

Figure 4.11 shows the visual results of applying such values.

It is notable that the ptosis simulation is not very realistic because in real life the breast sagging occurs near the body. In other words, the breast hangs on top of the body and not in front, and in comparison with Figure 2.5, the lower breast part is more convex than the ptosis simulated by [49]. So it was important to modify the approach of Chen, to approximate it to real ptosis degree without losing volume.

Therefore, the different degrees of ptosis are simulated combining the original ptosis equation proposed in [49] with a new deformation bottom-shape. The bottom-shape deforms the lower breast part of the breast in the same way of the top-shape deformation proposed by the same

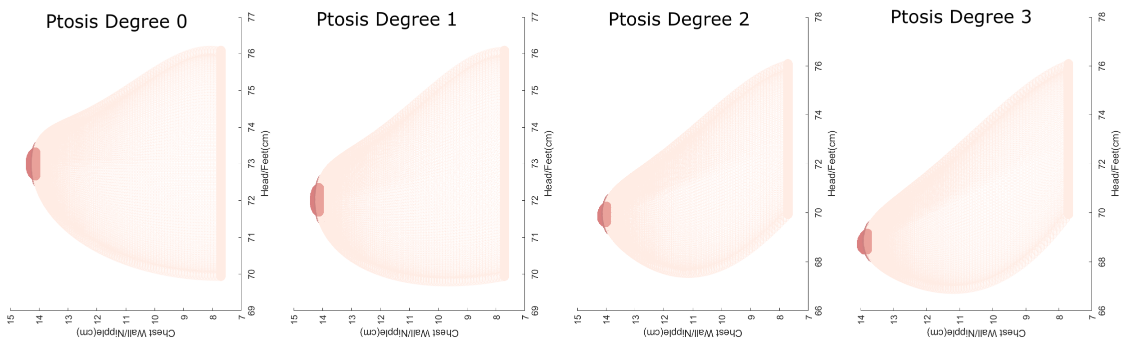

Figure 4.12: Breast Ptosis Degree.

author. The several ptosis degrees are done by creating a new Y point that defines were the maximum Y values will be in the new breast. The lower breast are recreated by using Chen's top-shape deformities [49], and inverted to modify the lower part with the parameters of a convex profile, named bottom-shape. Resuming, bottom shapes use the same equations like the ones to simulate the profile, the only difference is that it is applied in the lower half of the breast using convex values.

In order to be able to recreate a realistic model, an iterative process was created. At first, for each ptosis degree the Y coordinate correspondent to the maximum Z coordinate are adapted in order to respect the requisites of the degree, if the CAN is below or above the inframmamary fold, with the values shown in Table 4.3.

There, the iterative process follows, to find the right bottom-shape parameters. It only stops if the volume of the deformed breast is between certain values of an interval (70% and 120%) of the origin breast volume.

Breast ptosis with degree 2 and 3 suffer a change in their CNL value. Like in real cases breast with ptosis degree 2 and 3 lose some length due to the fact of the decay. The framework will slightly decrease the CNL value in order to achieve this outcome.

Concluding, the breast points will adjust towards the negative side of the Y axis. This change is conditioned, by their Z position, meaning that points near the chest will be less deformed than its opposite side. The nipple will be dislocated with the deformity, so it is necessary to adjust the nipple too, towards the negative side of the Y axis.

In real life breast are not always symmetric, sometimes happens that breast dislocates its mass into one side, which causes the nipples to point to a different direction. The presence of this kind of deformation is designated as breast symmetry or turn deformation and it consists in the dislocation of the breast mass to the opposite side of the body line.

Chen *et. al* [49] simulated the deformation with a parameter, c_0, and the equation demonstrated in Equation 4.5. Since this deformation will turn the breast to the opposite side of the body line it is necessary to know from the user the wished breast, if it is the right or left breast. This input is necessary in order to adjust the turn value to dislocate the breast to the opposite side of the body middle line. Therefore to achieve this characteristic of dislocation, it was necessary to adapt the c_0

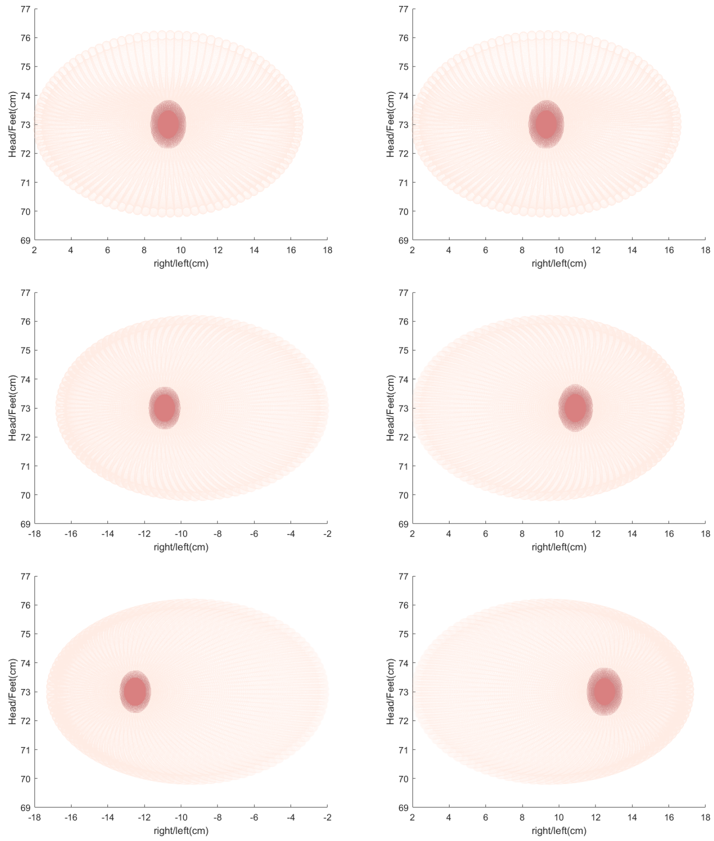

Figure 4.13: Results: Left and right breast with turn values 0, 0.5, 1, respectively.

value. If the wished breast is the left breast then the c_0 value will be positive generation the breast to dislocate to the left side of the body line. While if the wished breast is the right breast the c_0 value is negative provoking the breast dislocate its mass to the right side of the body line.

By changing the c_0 value the breast points will displacement along the X axis. In this dissertation the turn value is limited between 0 and 1. Where 1 is the maximum of displacement that the user can add to the previously created breast model and 0 is the breast without any displacement.

$$\begin{aligned} Thdd &= -(c_0 \times Z + c_1 \times Z^2) \\ X &= X + Thdd \end{aligned} \tag{4.5}$$

4.1.3 Nipple and Aureole

The created breast does not look like a realistic breast without the nipple aureole complex. In [57], the authors determine that the nipple measurements have a diameter between 0.7 - 1.9 cm, and 0.3 - 0.7 cm height. The nipple radius and its projection are given by a linear regression that

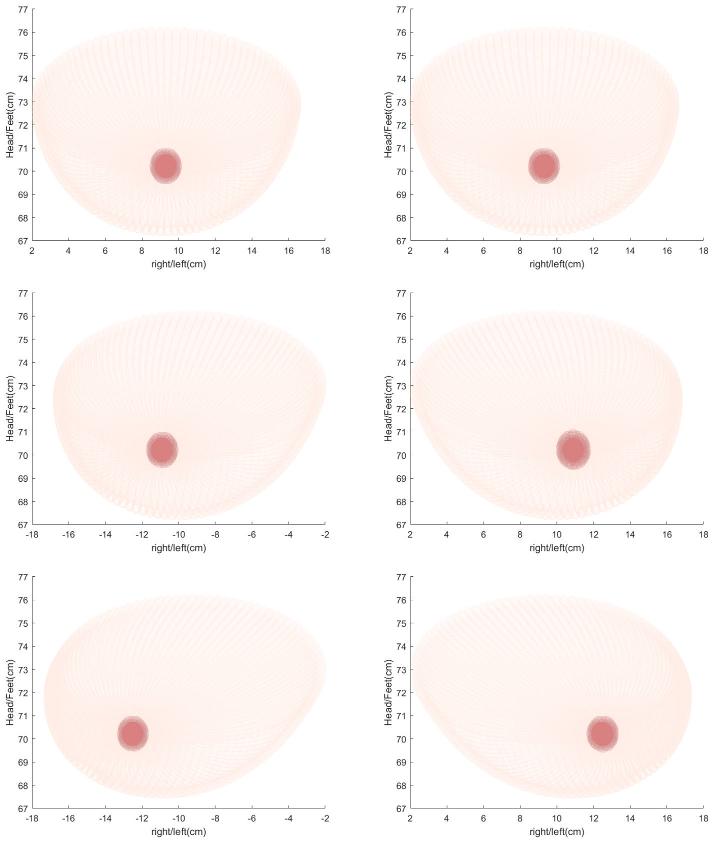

Figure 4.14: Results: Left and right breast with ptosis degree 2 and turn values 0, 0.5, 1, respectively.

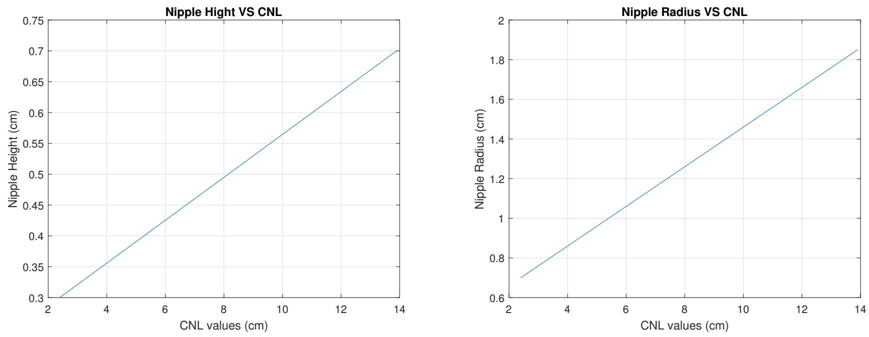

(a) Nipple Height (b) Nipple Radius

Figure 4.15: Nipple Dimensions VS CNL.

depends on the breast volume, shown in Figure 4.15. As in nature nothing is linear, nor in nipples a Random Gaussian Distribution was created, to achieve variance in nipple measurements between breast with the same breast volume.

The nipple is normally a oval form and situated on the maximum projection value. The methodology adopted was to approximate the nipple with a ellipsoid and to search for the maximum Z coordinate. This search is made before deformation (symmetry and ptosis), by tagging the index of the corresponding 3D coordinates, making it conceivable to follow the nipple point towards deformation.

Since the nipple is not a very symmetrical structure, the nipple will suffer the same changes of breast deformities introduced by the user. In order to adapt the nipple for the symmetry deformation it was necessary to find the tag of the 3D nipple point. The nipple will suffer the same transformation as the breast with the same turn value (c_0) and equations (Equation 4.5). Making it possible that the nipple appoints to the same direction as the breast. The results are visible in Figure 4.16 and Figure 4.17.

In the ptosis deformities, the nipple is normally pointing in the direction of the feet. In order to adapt the nipple for this kind of deformation it is necessary to find the tag of the 3D nipple point. To obtain the pretended nipple transformation corresponded to a ptosis degree, the same equation and values (b_0 and b_1) that deform the breast are used. So, it is guaranteed that the nipple

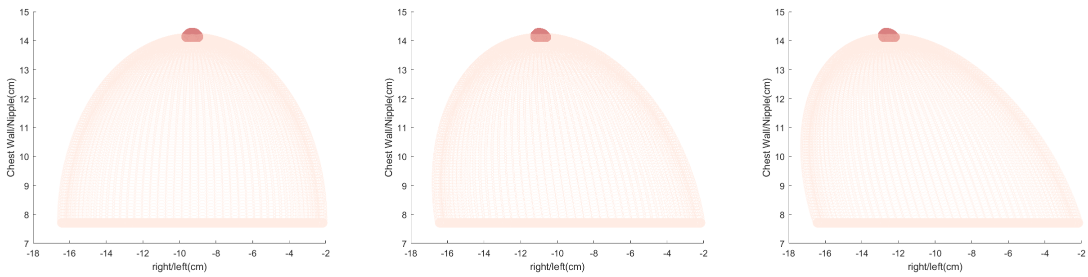

Figure 4.16: Nipple in right breast with turn values 0,0.5,1, respectively.

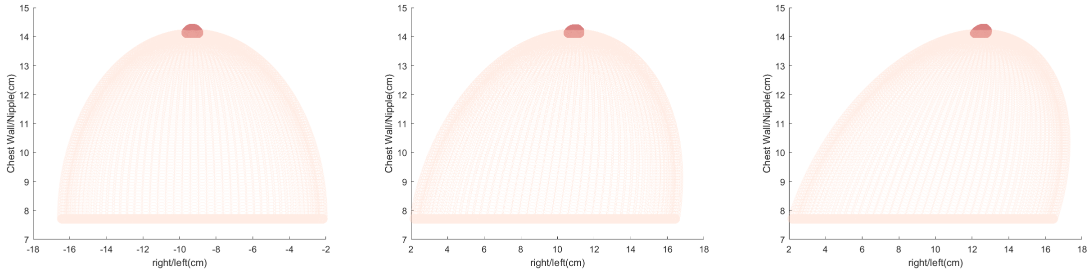

Figure 4.17: Nipple in left breast with turn values 0,0.5,1, respectively.

suffers the same deformation as the breast, pointing to the same direction. Figure 4.18 the nipple transformation for each ptosis degree are shown.

Aureole is the skin around the nipple which shape approaches a circular structure that normally has a different colour than the skin colour of the breast. The aureole diameter is between 3 cm to 6 cm [5]. Adding this structure to the breast model, it was necessary to identify the location of the nipple. The aureole radius was approximated to a linear regression depending on the breast volume, shown in Figure 4.19. The radius suffers a Random Gaussian Distribution to obtain variance between breast with the same breast volume. An euclidean search was made to obtain the distance between the nipple point and all the breast points and so, the breast points that are less or equal to the radius given by the Gaussian Distribution, were colored, with the colour that gives origin to the aureole.

4.2 Breast Interior

As described in the section above, the user can simulate different shapes of the breast with deformities, all these characteristics are visible for human eyes. In this section, a brief description of the methodologies used to create the pectoral muscle, thorax and the simulation of different breast density will be explained.

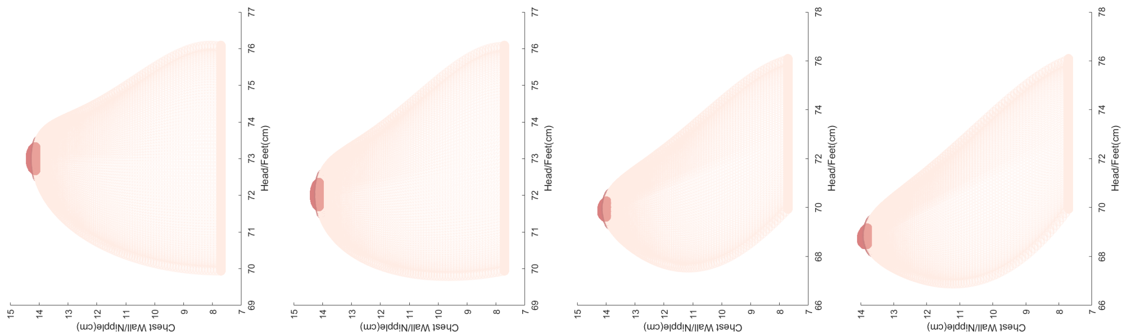

Figure 4.18: Nipple transformation for Ptosis degree 0 1 2 3, respectably.

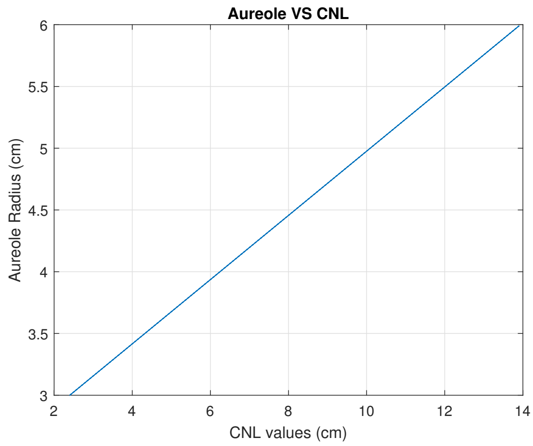

Figure 4.19: Aureole Radius VS CNL.

4.2.1 BI-RADS

Breast are mainly composed by two tissue: fibroglandular tissues, composed by ducts and lobs; and adipose tissue composed by fat cells. The ratio between the two tissue volumes gives the rate of breast density.

To normalize the density values, a standard was created, the international standard BI-RADS, an acronym for Breast Imaging-Reporting and Data System. BI-RADS refers to the mammography assessment categories. These are standardized numerical intervals typically assigned by a radiologist after interpreting a mammography. This standard allows a concise and unambiguous understanding of patient records between multiple doctors and medical facilities. BI-RADS is based on the relationship between the total breast tissues and the volume that the fibroglandular tissue occupies in it. This ratio is accomplished by dividing the fibroglandular tissue volume by the total breast tissue volume (Equation 4.6). With this value, it is possible to classify the breast in the different density categories. If the resulting value is low then it means that the breast has a low breast density. In fact, a breast with low breast density has more probability of being deformed in a surgery, due to the behavior of the adipose tissue to occupy the space left by the tumor.

$$BI-RADS = \frac{Volume of the fibrogranular}{Total Volume of the breast} \times 100\% \tag{4.6}$$

BI-RADS standards creators, from the American College of Radiology, classified breast density into four different categories. The values purposed for each category are presented in the Table 4.4.

BI-RADS Type	Interval of BI-RADS
Type I	0%-25%
Type II	25% - 50%
Type III	50%-75%
Type IV	75%-100%

Table 4.4: BI-RADS types and values.

For the purpose of simulating the internal part of the breast, some adjustments were made for the intervals seen in Table 4.4, in order to obtain better breast density outcomes. In the Type I, the minimum value is 10%, since woman breast has always fibroglandular tissue; and in Type IV the maximum value of the interval is 95%, by the reason of does not exist breast only with fibroglandular tissue. For each density type a random value is chosen between the interval of the correspondent BI-RADS category. The fibroglandular tissue is constituted by lobs and ducts, each breast can have 15 to 20 lobs, independently of the breast density [5]. A linear regression was created to obtain the corresponding lobs for the BI-RADS value. The linear regression functionality is to correspond the minimum rate of the BI-RADS interval to 15 lobs and the maximum value of the BI-RADS interval to 20 lobs. The lobs are approximated with an ellipsoid parametric equation (Equation 4.7), as a result of a woman's lobs have an oval shape and given the flexibility to change its parameters and so simulate lobs of different sizes. The lobs are connected by ducts which in this dissertation were simulated by a cylinder since the ducts have approximately a cylinder shape, Equation 4.8.

$$\begin{bmatrix} Lobradius \times sin(\omega) \times cos(\phi) \\ Lobradius \times sin(\omega) \times sin(\phi) \\ (Lobradius + Lobradius * 0.4) \times cos(\omega) \end{bmatrix} \tag{4.7}$$

$$\begin{bmatrix} Ductradius \times cos(\phi) \\ Ductradius \times sin(\omega) \\ distance \end{bmatrix} \tag{4.8}$$

These are the fundamentals of the three strategies developed for this dissertation. In the following subsection a brief explanation of the three strategies will be made.

1st Strategy

The first algorithm is based on a binary tree and a random distribution of points. A structure with the properties of coordinates, parents, node number, child1, child2, depth and radius was created. The depth on the breast density depends on the breast density type that the user introduces. For each density type the interval of the layers is calculated. When the breast type index is high, the density structures will fill the breast from its top until the top of the pectoral muscle. For the lower index it will only fill until the middle of the breast. An initial radius of each lob is given with the help of the CNL and the breast density type. The nipple is the first node to be initialized with the coordinates of the nipple center.

An iterative process is started in order to obtain the coordinates of the several nodes. The node Z coordinate is selected by the random function, where it is limited by the layer interval values. The next step is to find the equivalent X interval corresponding to the selected Z coordinate, extract so the maximum and minimum X points. However, selecting a random value within this limit creates the possibility of the point being on the opposite side of the breast. In order to avoid this situation, it was introduced a radius (depending on the CNL) in relation to the node parent in which the node could be created. Figure 4.20 shows a diagram that may be helpful for a better understanding of the process.

To be sure that the created node does not go out of the breast boundary, it is verified if the maximum of the interval is bigger than the maximum of the breast limit. If it is true the breast's limit is used to create the interval where the node will be hosted. The same process is repeated to search for the corresponding Y value.

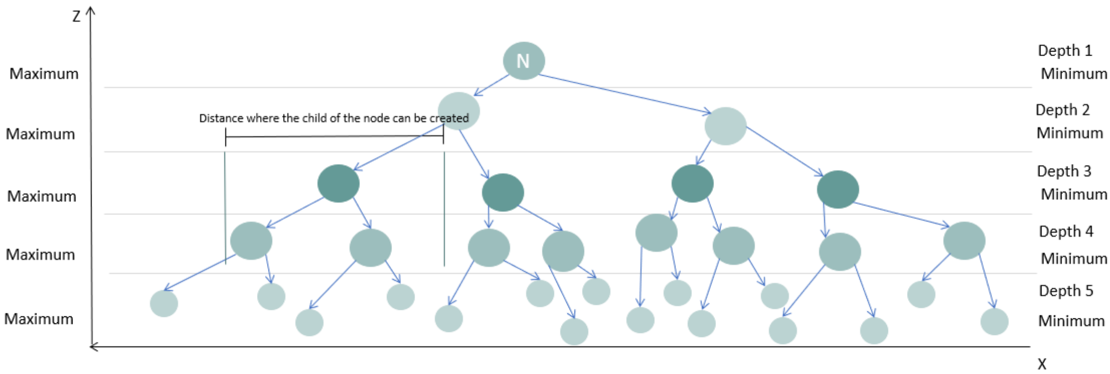

Figure 4.20: Diagram of the first algorithm.

To change the layer, the number of created children in the layer must be equal to 2^n , where n is the number of the layer and two is the number of children for each node. When the number of children is achieved, the radius of the ducts decrease by 10%. The iterative process stops when the depth value from the density type is achieved.

The fibroglandular volume is reached by a function where the ducts radius are increased or decreased until the volume is within acceptable values of the BI-RADS. After reached the duct volume, the lobs are placed in a random order in the ducts ending, as there are more ducts ending than lob, there will be many ducts without lob.

When analyzing the algorithm result, it was verified that there were many endless ducts, in other words, ducts that did not have correspondent lobs, a phenomenon that does not happen in the reality, because in reality all ducts have a corresponding lob in the end.

2nd Strategy

The second algorithm is an update from the first. The update is based on the need to create more children, improving the condition of gaps where children can be created and to provide a lob for each duct. For the second algorithm, two more children were added, in total one node has four children. The limits are influenced by the quadrant and by the coordinate of its ancestors. To know if the interval values of the lob are near the breast boundary, four auxiliary variables were used to save the breast boundary limit for each node. Figure 4.23 helps on the understanding of the description that follows.

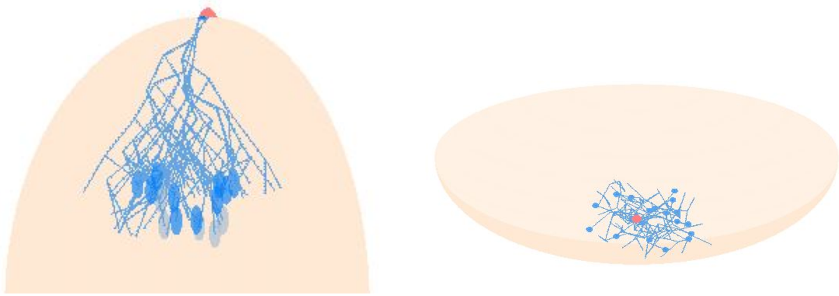

(a) Result: profile view (b) Result: profile view

Figure 4.21: Results of the first breast density algorithm.

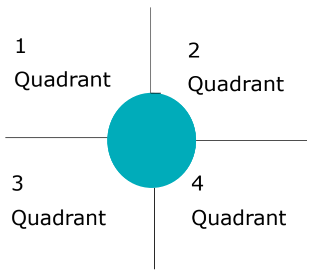

Figure 4.22: Coordinate system of the nodes structure.

The breast is divided in many layers, depending on the type of breast density selected. All lobs have the same radius that depends on the CNL value and the breast density type.

The first node is initialized in the nipple with the nipple center coordinates. Its first child will be in the first quadrant using the node as referential origin, second child in the second quadrant, third child in the third quadrant and the fourth child in the forth quadrant, see Figure 4.22.

The first node child must have the Z coordinate between the ranges of the first layer in question. The Z coordinate is selected by a random function. The next step is to search for its equivalent interval of X values. Like seen previously, the X values will be influenced by the quadrant where the child should be created. The Xs' limit is verified in order to know if the node is near to the breast surface or not. If the node is near the breast surface, then the maximum of the interval is given by the maximum of the breast boundary and the inferior limit is given by the X coordinates of the parent, else, the limit is given by the superior limit of the parent and inferior limit of X coordinate of the parent. Calculated the X coordinate, the same process is repeated to search for the corresponding Y value coordinate. For the rest of the children the process is similar. The difference is that each children is placed in each quadrant.

To change the layer, the number of created children must be equal to 4^n , where n is the number

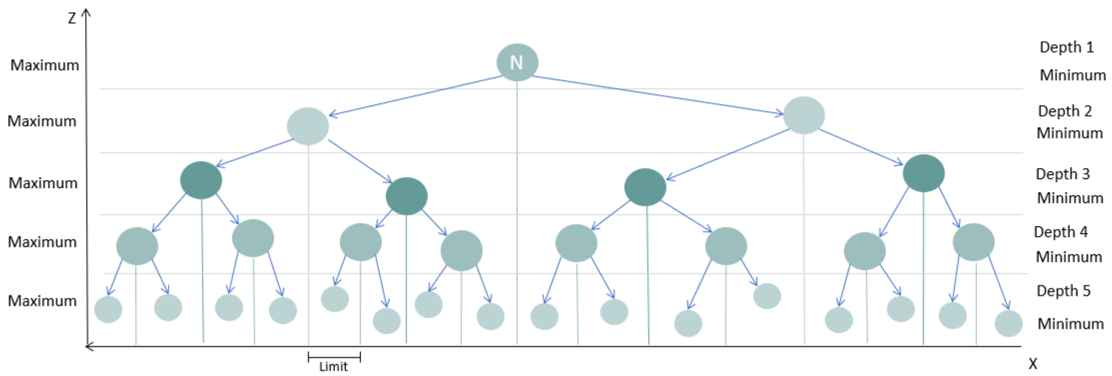

Figure 4.23: Diagram of the second algorithm.

of the layer and 4 the number of children that each node produce. When the number of children is achieved, the lob radius decrease by 10%. The iterative process stops when the number of children in the layer is equal to the number of lobs.

The ducts are created with a certain radius that afterwards, increases or decreases, depending if the volume is below or above the intended duct volume. The children of each node are connected to the parent and so on until the nipple. In the end the lobs are placed on each duct ending, updating the first algorithm.

Results are shown in Figure 4.24. In the end, it was verified that breasts with lower densities have structures that go down until the pectoral muscle and that the ducts are not as symmetrical as simulated with this algorithm.

3rd Strategy

After a deep analysis to the second algorithm, it was observable that this algorithm returned a very symmetrical structure in the X and Y views (Figure 4.24). For this reason was created another algorithm.

In this third algorithm, a new breast form is created from the other breast by copying the X, Y and Z values of the origin breast and multiplying the values by a constant (constant < 1). This guarantees that the new breast form has the same characteristics than the original breast, created by the user. This operation is essential in order to simulate the adipose tissue below the skin layer. For breast density with a lower index the constant will be near to 0.6 and so the adipose tissue below the skin will be bigger. For breast density with higher index the constant will be near to 1 and so the adipose tissue will be smaller below the skin. In this case, the values chosen are visible in Table 4.5. This new breast form will not only serve to recreate the skin layer but it will also host the density structures such as lobs and ducts.

The initial step is the user to selected between the four types of breast density, in order to calculate the ratio of the breast density. For each type of breast density, an interval is stipulated (Table 4.4) and a random number is picked of the interval. The lobs are given by a linear regression

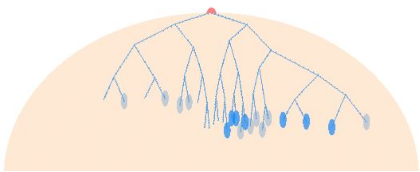

(a) Result: X Y view

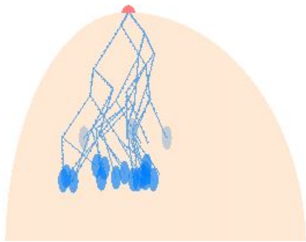

(b) Result: profile view

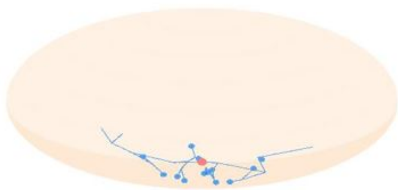

(c) Result: front view

Figure 4.24: Results of the second density algorithm.

BI-RADS Type	values for the new breast
Type I	0.7
Type II	0.75
Type III	0.8
Type IV	0.9

Table 4.5: Values to multiply to obtain the new breast.

where the minimum value of the interval corresponds to 15 lobs and the maximum value of the interval corresponds to 20 lobs.

In the breast anatomy, it is observable that the lobs are not all in the same line and they are distributed around the nipple. To achieve this characteristic, it was decided to divide the new breast into layers. Breasts with higher breast density are divided into 3 layers and breast with lower density into 2 layers, giving the breast density the perspective of depth. The number of layers will influence the number of lobs in each one of them. For higher breast densities the lobs in the first layer are about 20% of all lobs, in the second layer it will be 30% and in the last 50% of all lobs. In the case of low density rate, the lobs number in each layer is approximately 50% .

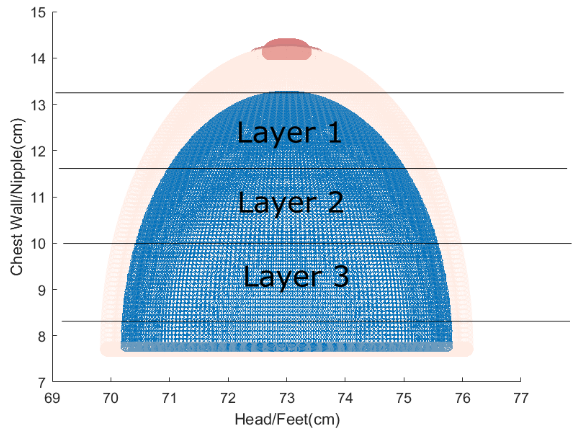

Figure 4.25: Layers of high breast density index.

The breast volume was previously calculated in the breast deformities: will be multiplied by the ratio of the breast type obtaining the volume to achieve of fibroglandular tissue. Fibroglandular volume is composed by duct and lobs, where the lobs occupy a big part of it. Since the tissue volume in question is mostly given by the lob volume, it has been decided that the lobs volume will be 85% of the total tissue volume being only 15% left for the ducts volume.

The equation of the lobs (Equation 4.7) makes it possible to determine the mean radius for each lob. Although, in real breast not all lobs have the same dimensions, a Gaussian Distribution is generated to obtain slight changes for each lob radius. To be sure that the slight changes of the radius does not affect the goal of the lob volume, an iterative process is created which calculates the volume with the given radius and verifies if the volume is within the acceptable interval.

Like seen in the breast anatomy section of Chapter 2, the ducts who are directly connected to the nipple, are only 12, so these occupy 80% of the 15% of the total ducts volume.

The lobs Z coordinate will be limited by the layers, in total the lobs must be between the maximum of the new breast and the maximum of the pectoral muscle. This distance is divided by the number of layers (see Figure 4.25).

To place the lobs in the new generated breast, the first step is to determine the lob position in the Z axes. The Z coordinate must be between the maximum and minimum of the layer in question a random value is chosen between the interval. From there, searches are done to obtain the maximum and minimum values corresponding to the given lobs coordinates, first for the X value and then for the Y value. In the case of Y value search, the X and Z coordinates of the new lob are used. Creating the lobs coordinates in this dissertation refers to chose random values within a certain interval. With this is possible that the function returns a very near point and by adding the radius it can overlap. The solution of this problem is to calculate the distance between the new created lob point to all existing lobs. The minimum value of the distance (so the nearest lob) should be greater than twice the lob radius, in order to prevent overlapping.

To switch density layers, a variable is created that counts the lobs created. If the number of lobs is equal to the number of lobs established for each layer, the layer changes. After all the lobes are created it is time to connect them by using a cylindrical structure (Equation 4.8) in order to simulate the ducts.

In [57] it can be read that not all lobs are directly connected to the nipple: a estimation is done where the study in [57] demonstrates that approximately 12 connection are done directly from the lob to the nipple. So, to recreate this propriety, the 12 nearest lobs are selected to make a direct connection with the nipple. The rest of the lobs connected to the nearest direct lob nipple connection. To be able to recreate the duct radius, a 3D distance is calculated, obtaining the length of cylinder (distance). With the help of the previously calculated duct volume and its length, the radius can be determined.

The results are visible in the Figure 4.26 to Figure 4.30, where the density is colored in purple and not blue, because blue is seen in the anatomy as venomous blood.

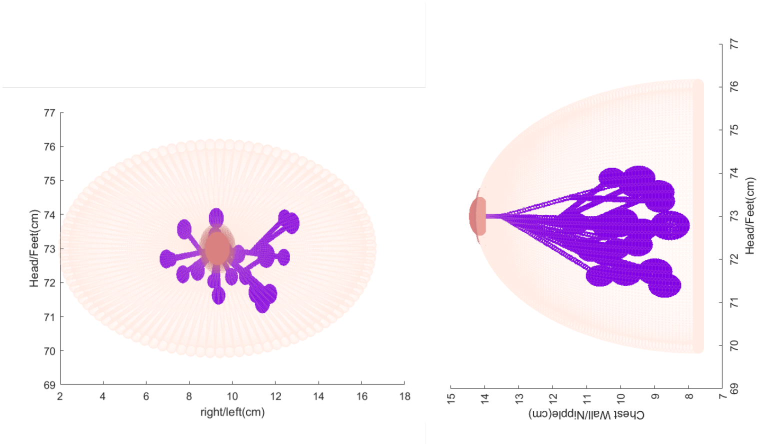

Figure 4.26: Breast density Type I.

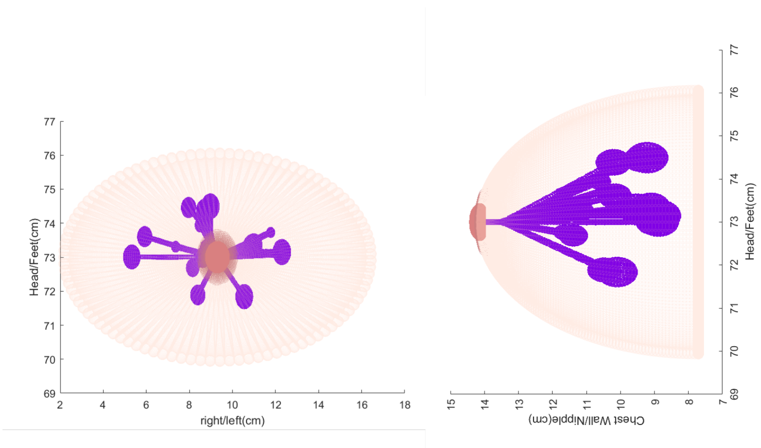

Figure 4.27: Breast density Type II.

In conclusion, a first algorithm was made based on a binary tree and the new node was restricted by a radius to the node parent but many of the duct were endless, without a lob. For this reason, a second version of this algorithm was performed where this did not happen and restricted

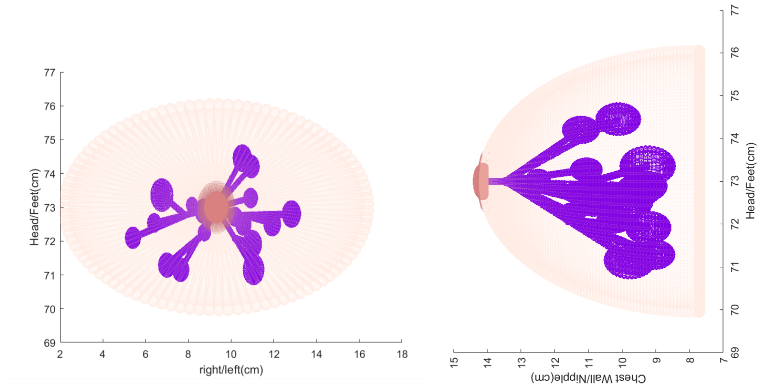

Figure 4.28: Breast density Type III.

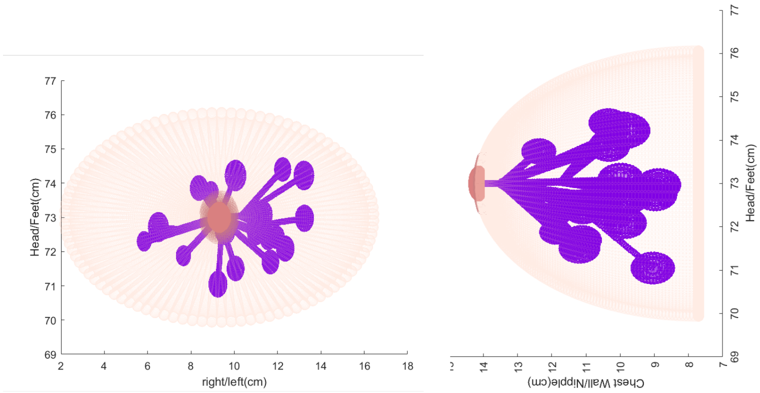

Figure 4.29: Breast density Type IV

.

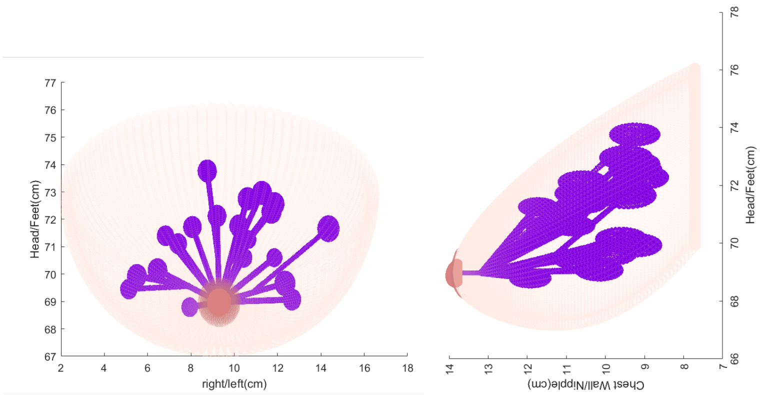

Figure 4.30: Breast density type III with ptosis degree 2.

not by radius but by limits. However, this second version was more symmetrical than reality and by analyzing several breast density images was notable that the fibroglandular structures go until the pectoral muscle independently of the breast density type. For this reason, the third algorithm was implemented as an improvement of all the disadvantages from the other algorithms used. In the third algorithm, the lobs are distributed randomly in the entire breast, only then the ducts are connected. In this way, it was possible to achieve the proprieties: only 12 lobs are connected directly; and as the distribution is random, it is possible to bypass symmetry and the lobs are distributed in the entire breast.

4.2.2 Thorax

The thorax is localized between the neck and the abdomen. It includes the thoracic cavity and the thoracic wall, protecting organs, such as heart, lungs and thymus glands, it supports all the entire breast and its constituents. In other words, the thorax is the border between interior and exterior of the body that is covered by the pectoral muscle.

The methodology adapted to simulate the thorax, was to create a cylinder with the parametric equation (Equation 4.9). The cylinder was chosen to simulate the thorax due to its slight curvature, in order to be able to simulate the curvature of the thorax.

$$\begin{vmatrix} a \times cos(\omega) \\ b \times n \\ c \times sin(\omega) \end{vmatrix} \tag{4.9}$$

With this parameter it is obtained the pretended slight curvature, where a and c are depending on the H value (Table 4.1), and b depends on the CNL value, which influence the cylinder radius giving the thorax its curvature.

With these parameters, the cylinder grows out of the breast limits so it is essential to fit the thorax in the breast limits, by cutting the excess of the cylinder. The cylinder and the breast were divided in four quadrants. A cycle was created to go through all breast points: for each breast point, another cycle was made to go trough all thorax points and subtracting the Z values from the breast and from the thorax. If the value of the subtraction was less than one, that means that the Z coordinates were coincidence, then the values of X and Y were compared. By using the euclidean distance the minimum distance is picked to be certain that the points are coincidence. In the end the X and Y were compared and, depending of each quadrant restriction and only the X and Y coordinates were saved that are localized in the breast interior.

For aesthetic reasons, the colored below the thorax were painted in the same color as the thorax, giving the illusion of the continuity of it. The results of the breast model with the thorax are visible in the Figure 4.31.

4.2.3 Pectoral muscle

The pectoral muscle is a thick, fan-shaped muscle, situated at the chest of the human body. It makes up the bulk of the chest muscles and lies under the breast [58].

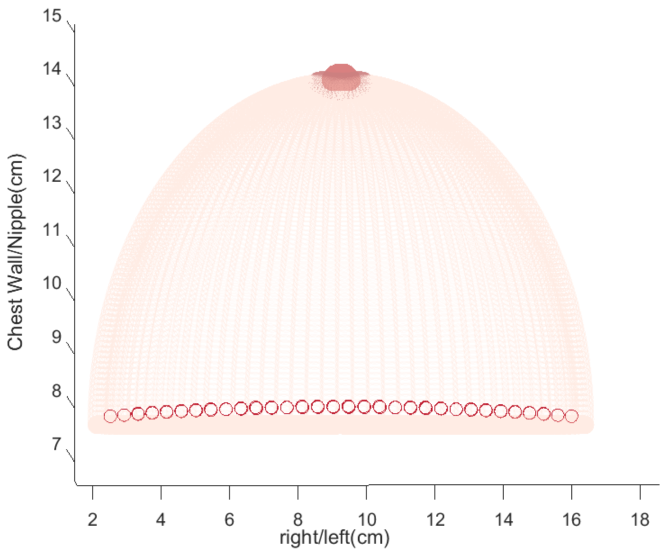

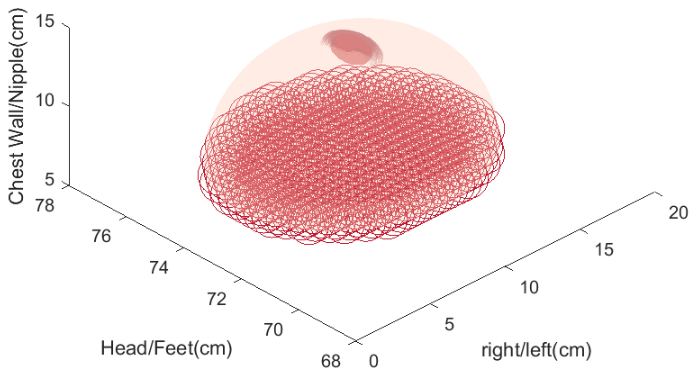

Figure 4.31: Results of the thorax.

In the BioDigital Human [59] website, it is noticeable that the muscle occupies only a certain part of the breast. The muscle goes a little bit below the nipple and it is observable that the muscle of one side is greater than the other and decrease with a slight curvature until the other side.

In [60] the author represented the pectoral muscle by an elliptical cone with the tip of the cone level in the same level of the nipple's position, Figure 4.32.

Based on this method, an elliptical cone was adopted to recreate the pectoral muscle, but soon it was possible to observe that the pectoral muscle does not fulfill the goals of simulating realistic 3D breast models, see Figure 4.33, as it does not resemble the pectoral muscle seen in BioHuman, due in [60] the pectoral muscle is to project the MLO view of a mammography.

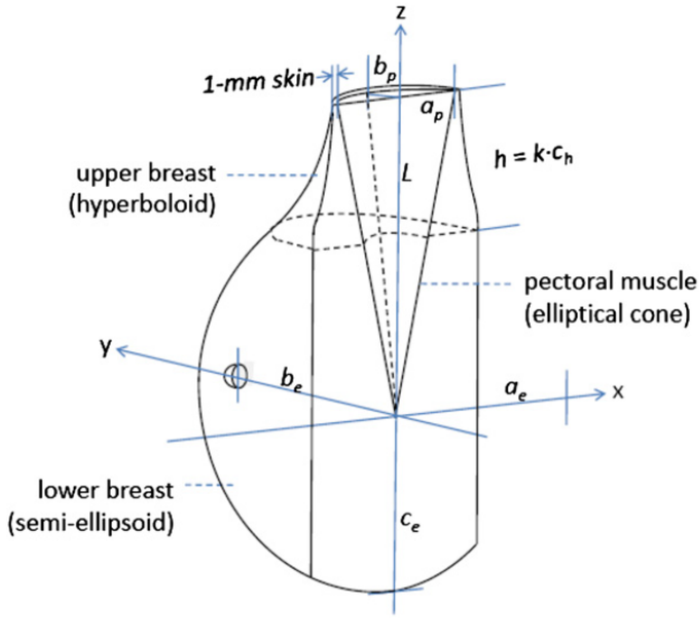

Figure 4.32: Elliptical cone pectoral muscle.

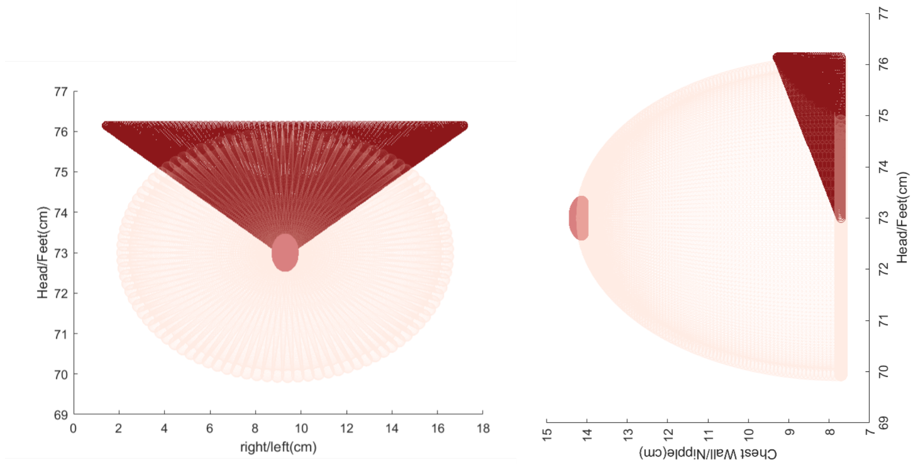

Figure 4.33: Results of The elliptical cone.

$$\begin{bmatrix} Radius \times cos(\omega) \\ Radius \\ Radius \times sen(\omega) \end{bmatrix} \tag{4.10}$$

So the idea in [60] of an elliptical cone was abandoned but, analyzing many images of the pectoral muscle, the idea that the muscle goes below the nipple and that the pectoral upper part is thicker then the lower seen in the work of [60] seams to be right. Other characteristics investigated by analyzing images was that the left pectoral muscle is a mirror-inverted of the right pectoral muscle and vice-versa and that the pectoral muscle is thinner in the opposite of the body line. To be able to fulfill all of the pectoral characteristics the adapted geometric form was a quarter of a super-ellipsoid. The advantage by using a quarter of a superelipsoid is it has a fan-shaped form and the parameters are controllable, so it is possible to recreate the different thickness of the pectoral muscle.

The parameters to create the structure depend on the H and W (see Equation 4.1) of the breast, the parametric equation are the same for a super-ellipsoid only interval of the ω and ϕ are adapted to obtain a quarter of the ellipsoid.

An additional variable was defined to record the user option for left or right breast side. This variable allows to obtain a mirror-inverted characteristic represented in the model by multiplying the X-axis by - 1. Afterwards the pectoral muscle is translated to the top of the breast (maximum of the Y coordinates) and to the top of the thorax. To place the muscle only into the breast without going out, it was necessary to divide the breast and the muscle into 4 quadrants. For each quadrant a loop is created to compare the Z values from the breast and from the muscle, calculating for each pectoral muscle point, the closed breast point. This is done with an euclidean distance by finding the minimum distance, making sure that the points are coincident. The last step was to compare if the Z values of the pectoral were smaller or equal than the Z value of the breast.

For aesthetic reasons, it was decided to colored between the thorax and the pectoral muscle, giving thus a realistic illusion of the pectoral muscle. The results obtained for the pectoral muscle can be observed in Figure 4.34.

4.3 Tumor

Tumor is originated when cells growth in an uncontrolled and disproportionate measure. This unconstrained grown is a consequence of a DNA mutation, that can cause the cells to migrate and host in other healthy tissue.

4.3.1 Tumor Type

The nature of the tumors can be invasive or *in situ*. An *in situ* tumor is when the tumor is completely emerged in a structure. An invasive tumor is when the tumor has already grown out of the structure and grown into surrounded tissues. The tool developed in this work allows the simulation of the following tumors' kinds:

1. Lobular In Situ;
2. Lobular Invasive;
3. Ductal In Situ;
4. Ductal Invasive;

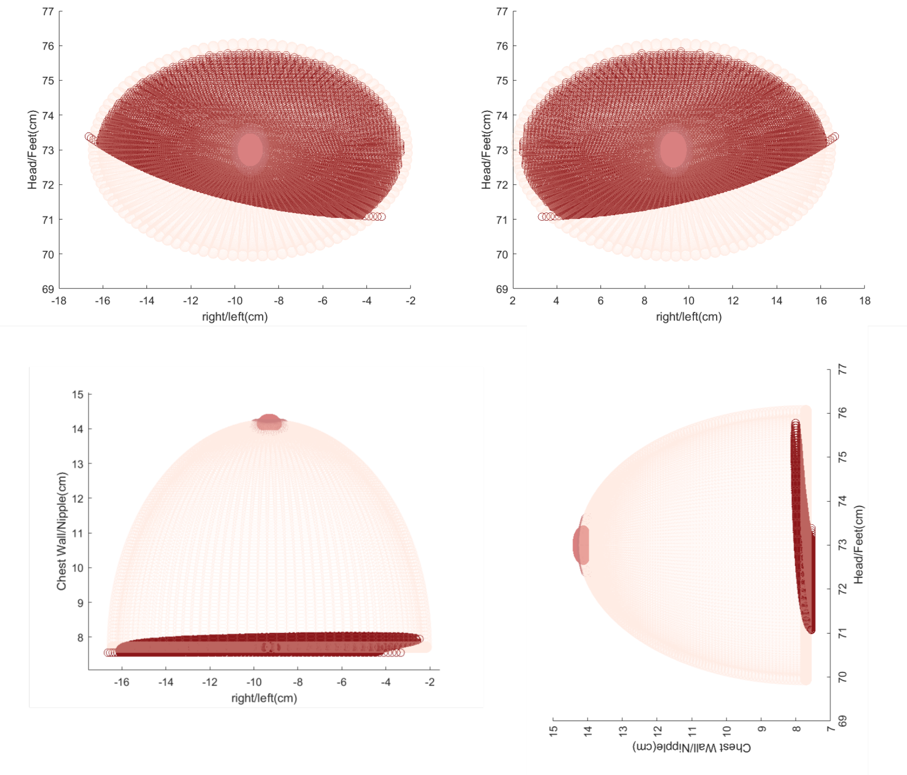

Figure 4.34: Results of the pectoral breast.

5. Adipose tissue.

To be able to simulate the tumor in the breast it is necessary to know which quadrant. The Figure 4.35 helps to identify each quadrant for each breast.

- Upper Exterior;
- Upper Interior;
- Lower Exterior;
- Lower Interior;
- Center;
- Transition Upper;
- Transition Lower;
- Transition Interior;
- Transition Exterior.

the nomenclature is the same used by the surgeons.

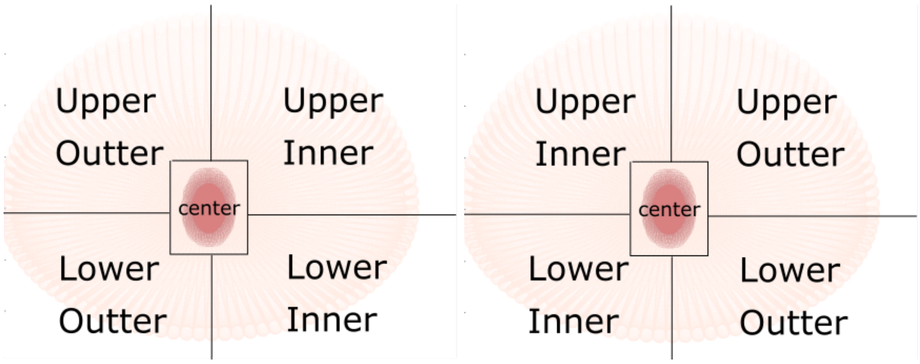

(a) Right breast quadrant (b) Left breast quadrant

Figure 4.35: Breast quadrants to simulate tumor location.

The user of the framework must introduce the input of the tumors nature, location and its shape. The importance of knowing the tumors' location, is to incorporate the article of Zolfagharnasab [61], which simulate the healing process of the breast after BCS. This process requires the location in quadrant of the tumor, because the location of the tumor may influence the surgical outcome and know how to begin the procedure.

A super-ellipsoid was used to approximate the tumor (Equation 4.7), where the tumors parameters depend on the radius the user introduced in the interface.

4.3.1.1 In situ

The method adopted was to simulate the *in situ* tumor in ductal vessels and in lobs.

Ductal In Situ One of the most common tumors is the ductal *in situ*, where the tumor is in an initial stage and for this reason, the tumor's radius is smaller than the radius of the ductal that hosts it. In order to create the tumor *in situ* in the ductal vessels, this algorithm search for all the lobs in the selected quadrant and returns them. The selection of one and one lob is done randomly. It is also necessary to know the ductal's radius that was assigned to the corresponded lob. The tumor is put in the middle of the duct, as illustrated in the Figure 4.36.

Lobular In Situ The *in situ* lobular methodology is very similar to the ductal. All lobs are verify, and are checked for the quadrant condition. The lob selected to host the tumor is chosen randomly. As it is *in situ* the radius of the tumor is the same radius of the lob. The result is shown in Figure 4.37.

4.3.1.2 Invasive

Invasive means that the tumor has grown out its original tissue or structure and already invaded the surrounded tissue. In this dissertation, the adopted method was to simulate the invasive tumor in

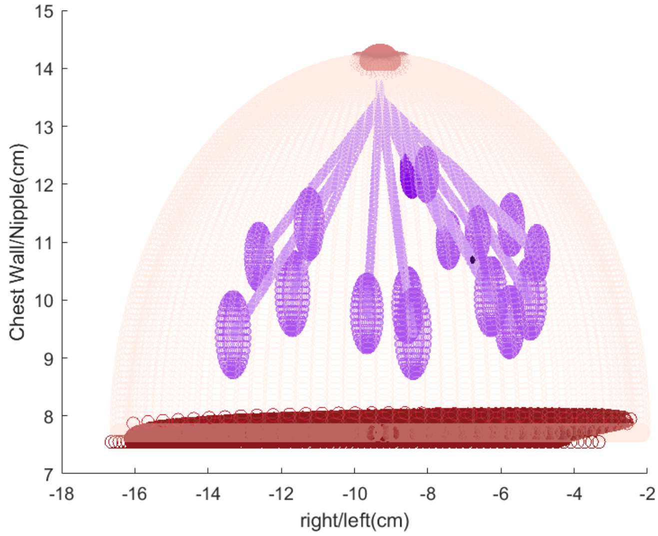

Figure 4.36: Cancionoma Ductal In Situ.

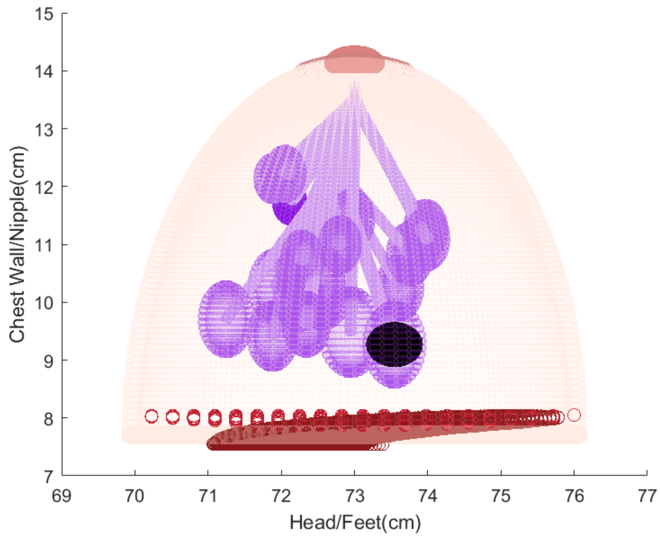

Figure 4.37: Cancionoma Lobular In Situ.

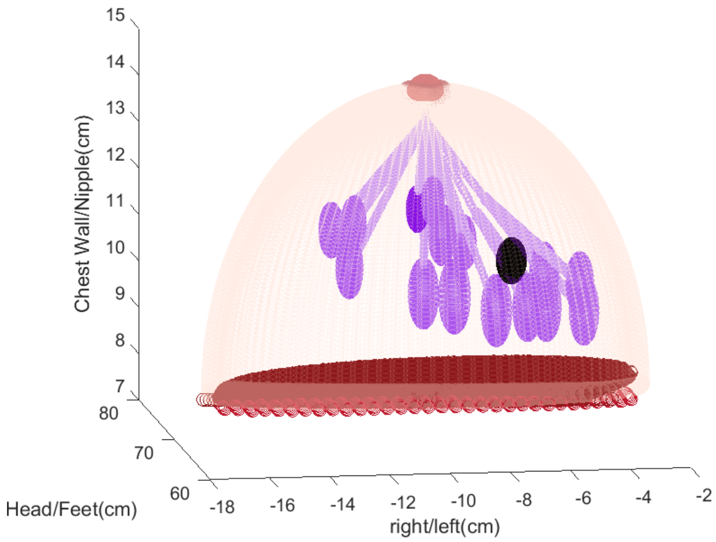

Figure 4.38: Cancionoma Ductal Invasive.

the ductal vessels and in the lobs, since in conjunction with *in situ* are the tumor types that occur more frequently.

Ductal Invasive The method used for ductal invasive is the same as seen for ductal *in situ*. However, the tumor radius is given by the user and the unique restriction is that the radius must be bigger than the duct radius, in order to not lose its nature as invasive characteristic, see Figure 4.38.

Lobular Invasive The invasive lobular methodology is very similar to the lobular *in situ*. The condition of the radius seen in ductal invasive is applicable in this case, since the radius can not be smaller than the host radius in order to not lose its nature, see Figure 4.39.

4.3.1.3 Adipose tissue

Tumor in the adipose tissue is originated in the fat cells and it is the rarest type of breast cancer's tumor. Such as seen for other tumor kinds, this tumor is restricted to a quadrant. The first step is to localize it in the Z axis, between the maximum of the breast and the maximum of the pectoral muscle. A random value between this interval is chosen, to be the tumor Z coordinate.

To find the tumors X coordinate, a search was done to find in the breast the correspondent tumor Z value and so the correspondent breast interval of X values. Depending of the quadrant, the X values is picked randomly, being the tumor's X value between the X value of the nipple and the maximum/minimum of the X interval. Finding the Y value of the tumor, is quite similar to finding the X value. A search is done to find in the breast the tumors Z and X values. To chose randomly the Y value it was necessary to consider in which quadrant the tumor will be hosted.

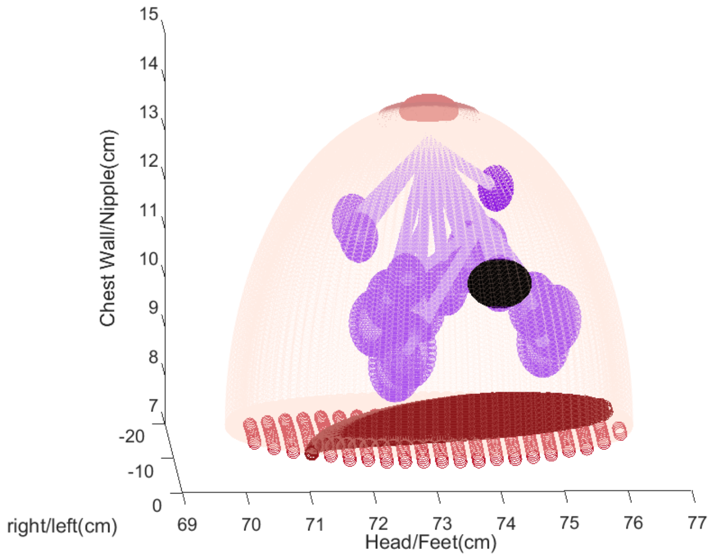

Figure 4.39: Carcionoma Lobular Invasive.

The future value will be between the Y value of the nipple and the maximum/minimum of the Y interval.

To be sure that the tumor does not intersect a breast structure, an euclidean distance was used to calculate the nearest structure by picking the minimum distance to the tumor. If the distance was greater than the tumor radius, it means that the tumor does not intersect the structure else, and, in this case, the whole process were repeated. Figure 4.40 shows the results for an adipose tumor, where the tumor is demonstrated in black colour.

4.3.2 Tumor Shape

Since in real life a tumor is not a perfect sphere, it was decided that the best method was to have two different tumor forms, since the tumor can have several different shapes. Therefore, the two

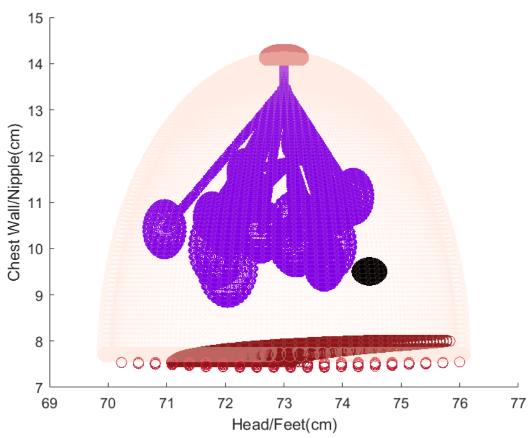

Figure 4.40: Adipose tissue tumor.

tumor forms simulated were the round (elliptic) and the speculated (elliptic with spikes), that is approached in [60]. For both cases, a super-ellipsoid was created with features of parametric equations previously described (Equation 4.7), obtaining an identical rounded form. To move from a roundish form to a speculated form, it was necessary to create speaks. Speaks are recreated by cones, where two cones are generated in opposite sides, see Figure 4.41. The cone equation's parameters, such as radius and height are dependent on the tumor's radius. The cones were created with the base in the tumor's center, considering the axes as referential origin. The speculated form for the different types of tumor are represented in the Figure 4.42.

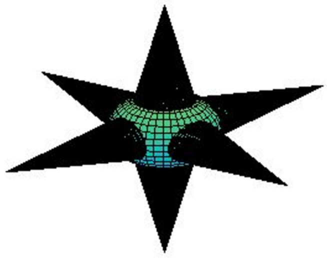

Figure 4.41: Speculated tumor.

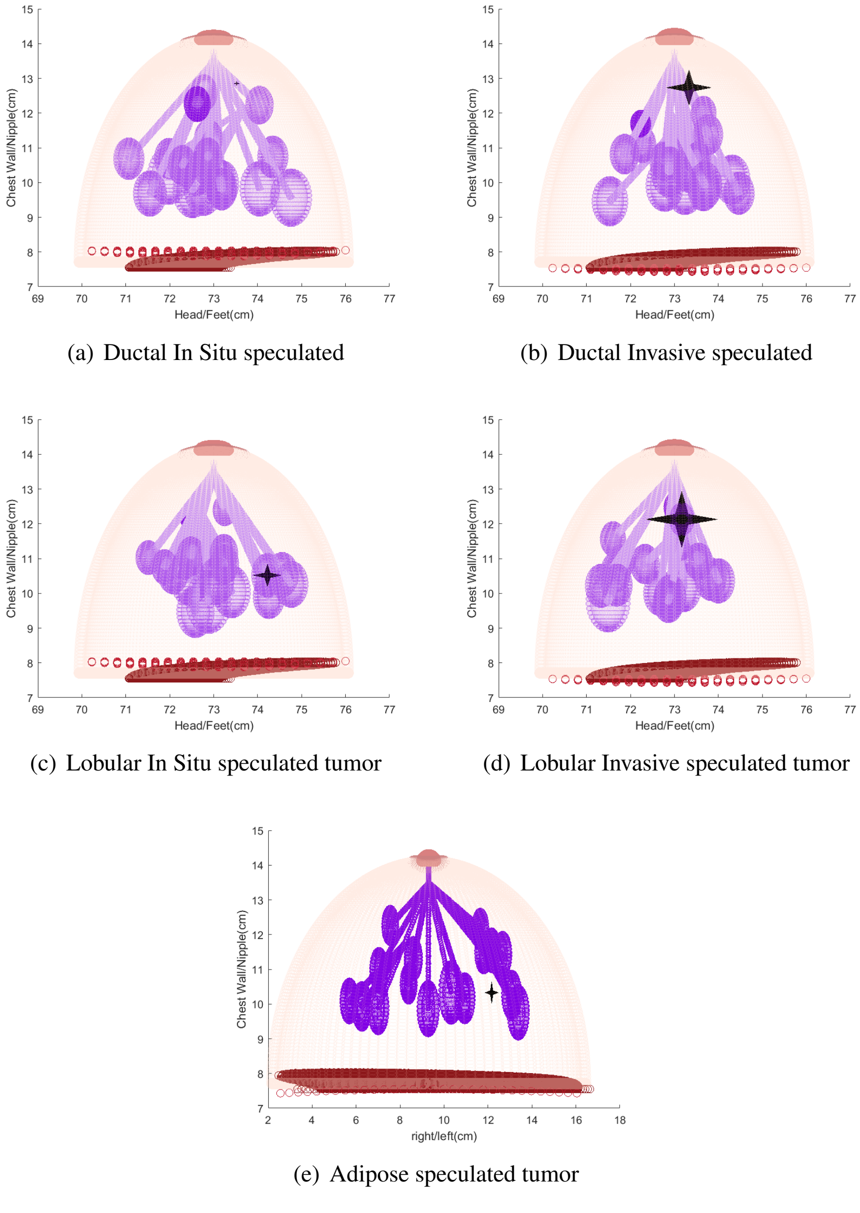

(a) Ductal In Situ speculated

(b) Ductal Invasive speculated

(c) Lobular In Situ speculated tumor

(d) Lobular Invasive speculated tumor

(e) Adipose speculated tumor

Figure 4.42: Several types of tumor with a speculated tumor.

Chapter 5

Interface and Surveys

An interface is a design for the human-computer interaction. This interaction may occur for example to control a machine operation or to program it. Therefore, an interface can make the process description easier and more efficient, helping to reproduce the desired results and to improve the user-friendliness. Typically, interfaces are created when a program depends on information given by the user, or users need to receive feedback information about the process.

For an educational framework, an interface should include all the required fields that allows to join all the information needed to obtain the wished output in only few steps. The interface may also be functional, efficient and user-friendly, that were the main concerns of the interfaces conception in this work. On this wise, the developed interface allows the user to introduce the information requested to accomplish the outcome in only a few steps. Therefore, the interface create for this dissertation will guide the user through the several steps to created the 3D breast. Obtain the requested input from the user in order to simulate the several structures and breast shapes that constituent the 3D breast model, explained in Chapter 4 .

5.1 How to test interfaces

In this dissertation, two different mockups were created, which allow to compare the results between them and to choose the best mockup, according to A/B testing, usability, and simplicity properties. The interface selected between the two was then implemented using Matlab guide (GUI).

5.1.1 Usability testing

The usability testing is focused on measuring the product capacity to its intended purpose. This test is commonly used for: food industry, web applications, computer interfaces, consumer products and devices.

This technique consists on testing the product design by analyzing how easy it is to use for the representative group. This test is practical since it has direct input from real users. Making it possible to define their system usage, since it usually involves the observation of the users to complete tasks.

There are a few different types of usability tests:

- **Comparative usability testing**: are commonly used to compare two designs and to establish which provides the best user experience.
- **Explorative usability testing**: before a new product is released, explorative usability testing can establish which content and functionalities should the new product include in order to meet the users' needs.
- **Usability evaluation**: this usability test introduces users to a new design, aiming to mark if it is intuitive and provides a proper user experience. The usability evaluation intent to ensure any potential issues before the product is launched. As such, usability testing is often conducted on prototypes.

This type of testing provides direct feedback from the target audience. Internal debates can be solved by testing the issue to see how the user reacts to different issues, and potential problems are highlighted, which provides significant product improvements.

5.1.2 A/B testing

A/B testing is also named split testing, is an experimental approach to understand which of the user interface design the user prefers. As the name implies, two versions (A and B) are compared, which are identical except for one variation that might impact the user's behavior. Multivariate testing or multinomial testing is similar to A/B testing, but may test more than two versions at the same time or variation.

The benefits of A/B testing are considered to be performed on almost anything, having the following goals:

- **To analyze user engagement**: elements of a page, app, or emails that can be A/B tested such as the headline or subject line, forms, language, layout, fonts, colour, among others. Testing one change at a time, will show which affected users' behavior and which did not.
- **To improve content**: This testing technique requires a potential improvements list. The very process of creating, considering and evaluating of this list makes the final versions better for users.
- **Quick results**: even a relatively small sample size in an A/B test can provide significant results. This allows a short-order optimization of new sites, new apps, and low-converting pages.
- **Everything is testable**: forms, images and text are typical items for A/B testing and updates. However, any element of a page or app can be tweaked and tested such as headline styles,

button colors, length, etc. All of the changes in the elements mentioned can affect the user engagement in ways that may never be known if they are not tested.

In summary, A/B testing proofs what works and what does not.

5.2 Mockups

In this dissertation, two mockups were created and they were presented to three oncological doctors with the aim of select the best interface through A/B testing.

Both mockups are provided with a menu, back, next and help buttons, a remove panel for the surgeon to remove unnecessary structures. All pages of the mockups are provided with the visualization tools: Zoom In, Zoom Out, Save image and Rotate.

The main difference between the two mockups is the layout of the characteristic. In the mockup A only one image is demonstrated and by changing the characteristic of this image, it will be displayed the image with the selected attribute. In mockup B, it is possible to compare each attribute due to each characteristic has its own image. Both mockups have the same flow, which starts with:

1. Breast Shape;
2. Breast Projection;
3. Breast Symmetry;
4. Breast Ptosis;
5. Breast Density;
6. Tumor;
7. Visualization panel.

In the breast shape page, the user must choose between six types of breast shapes. Where in mockup A, only one breast shape is shown at a time, which corresponds to the type of breast selected. By contrast, in mockup B, all breast shape options are shown simultaneously. The motivation is to analyze the user preference to have all the information available at once or if the user prefers to control access to information.

In this panel the user has a slider to introduce the breast volume, the Figure 5.1 demonstrates the mockup A and mockup B layout.

In the breast projection page, the user must choose between the five attributes: Round, Linear, Ogge, Concave, and Convex. The layout is shown in Figure 5.2.

Symmetry page is the same in mockup A and mockup B, due to the difficulty to simulate all values in the range of 0 to 1 in order to provide comparability like seen in the layout of mockup B (Figure 5.3).

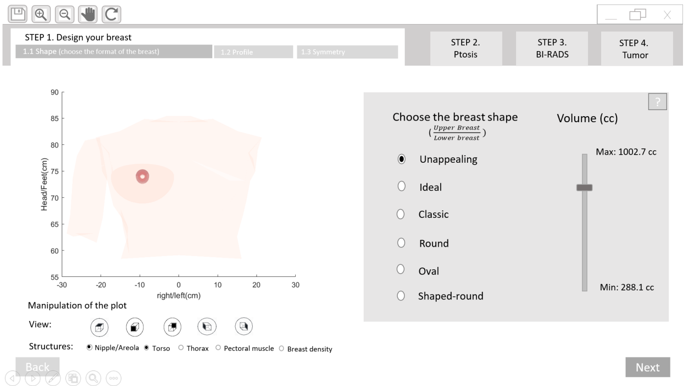

(a) Mockup A

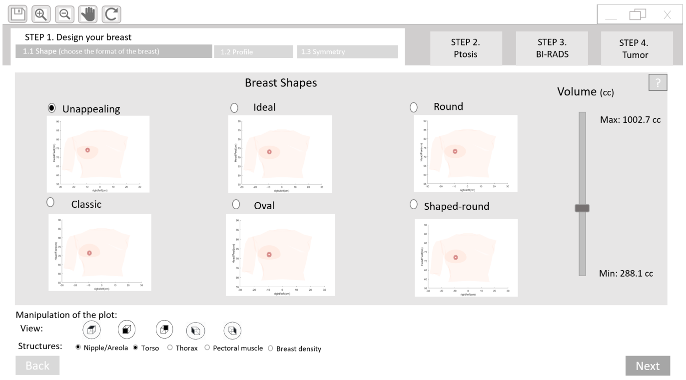

(b) Mockup B

Figure 5.1: Mockups for breast shape.

The next page is the breast ptosis page. In mockup A only one image is shown and the user must choose between the four degrees of ptosis. By updating the attribute, the image will change and show the breast with the selected attribute. In mockup B the different ptosis degrees are presented where each characteristic has its own image (Figure 5.4).

Breast density page are represented by the four types of BI-RADS. Similar to what is done in the steps of selection of breast shape and projection, mockup A will only represent the characteristic that the user wants to see, and in mockup B the four density types will be simulated in order to provide a way of comparison. The two layouts are shown in Figure 5.5.

The tumor page is the same for A and B. The layout consists of nine quadrants (upper inner, upper outer, lower inner, lower outer, upper transition, lower transition, outer transition, inner transition and center) and the tumors' nature, in situ or invasive ductal, lobular in situ or invasive tumor and adipose tissue tumor. As the tumor never has an exactly round shape the user can choose between the round and speculate form. In this panel, the user can change the radius of the tumor, Figure 5.6.

The last page is the visualization panel where all the selected attributes are shown to the user with the complete image of the breast simulation, Figure 5.7.

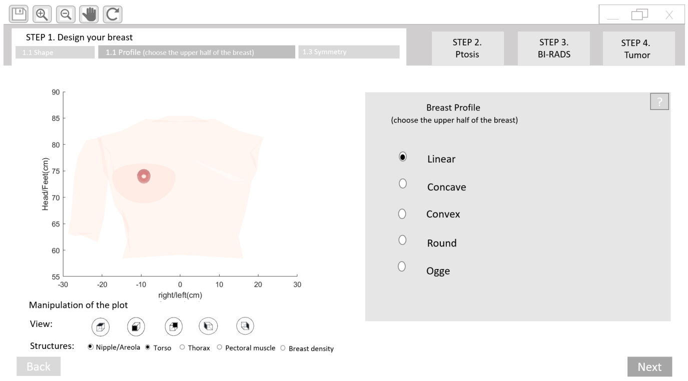

(a) Mockup A

(b) Mockup B

Figure 5.2: Mockups for breast projection.

The two types of mockups were presented to three oncological doctors in order to know which of the mockups they prefer, confirming certain attributes names and to obtain suggestions for possible improvements before the implementing phase of the winning interface. The results are shown in the Table 5.1.

Results for	Mockup A	Mockup B	Winning Interface
Shape	1	2	Mockup B
Projection	1	2	Mockup B
Ptosis	1	2	Mockup B
Density	1	2	Mockup B

Table 5.1: Results from A/B testing.

The other mockup pages, tumor and turn deformation are the same for mockup A and B. These pages were also shown in order to obtain feedback. In the results, it is clear that the questioned doctors prefer the mockup B layout, for the reason that it is possible to compare the several characteristics and so it would be easier to compare it with real patients information. One of the doctors suggested the addition of a button to simulate attributes randomly in order to help the new

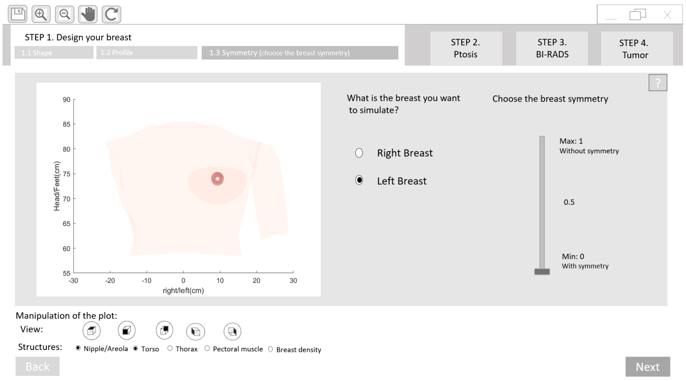

Figure 5.3: Symmetry page for mockup A and mockup B.

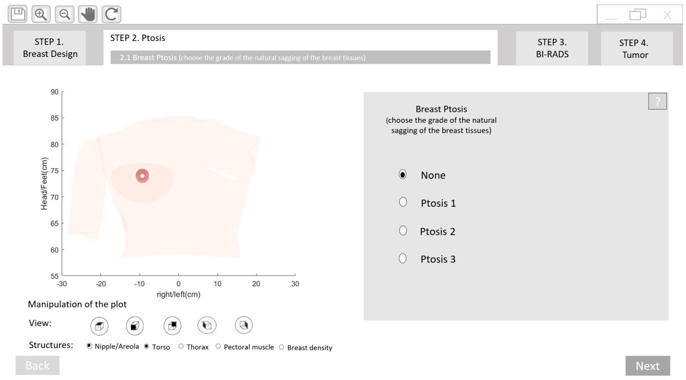

(a) Mockup A

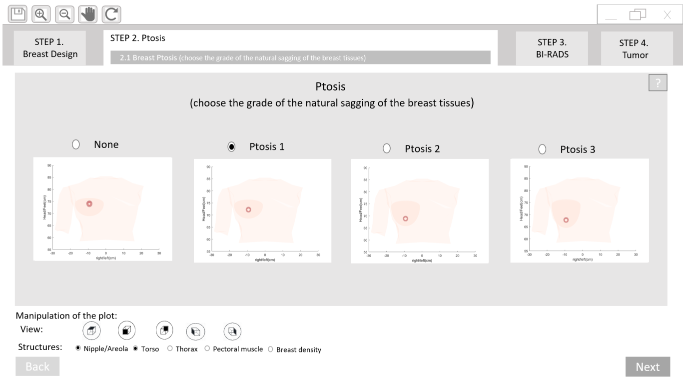

(b) Mockup B

Figure 5.4: Mockups for breast ptosis.

surgeons to study different attributes.

5.2.1 Implementation of the winning interface

The winning interface is designed to be a simple interface with several images, demonstrating the several breast characteristics, trying to be similar to the mockup demonstrated to the doctors.

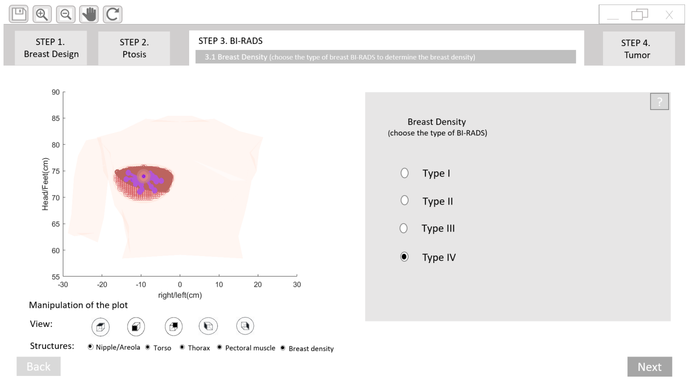

(a) Mockup A

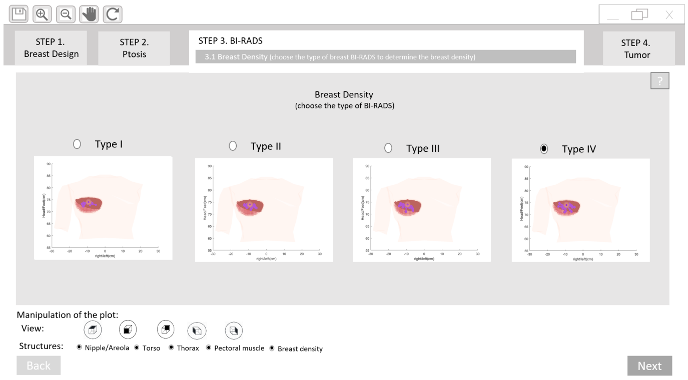

(b) Mockup B

Figure 5.5: Mockups for breast density.

All pages of the interface are provided with the visualization tools: Zoom In, Zoom Out, Save image, Rotate, next, back and help buttons; and a removal panel with the text "remove structures": nipple/aureole, torso, thorax, pectoral muscle and density. This panel removes structures in order to help to better visualize the intended structure. Some of the removable structures will be enabled when they appear in the images such as thorax, pectoral muscle and density. In the first four pages (shape, projection, symmetry and ptosis) it is possible only to remove the nipple/aureole and torso. For the density it is possible to remove thorax and pectoral muscle and in the tumor it is possible to remove density too. So it is observable that the remove panel is always present but with different functionalities.

The pages have above them a menu for the user to navigate through the several pages. In the menu, the text identifies the characteristic of each interface page, in which the actual page stands out from the others through color. Changing one of the characteristics will trigger a loading panel, to inform the user that the program is processing the request. At this time all kinds of buttons are blocked, so it is impossible for the user to change attributes. When the loading panel disappears, the buttons will be enabled so the user can change them again until obtaining the intended result, see Figure 5.8.

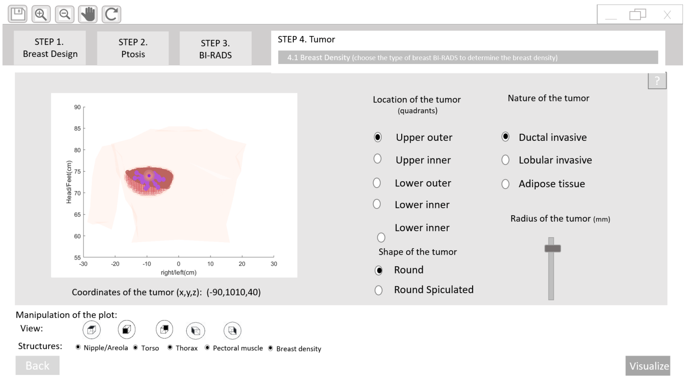

Figure 5.6: Tumor page for mockup A and mockup B.

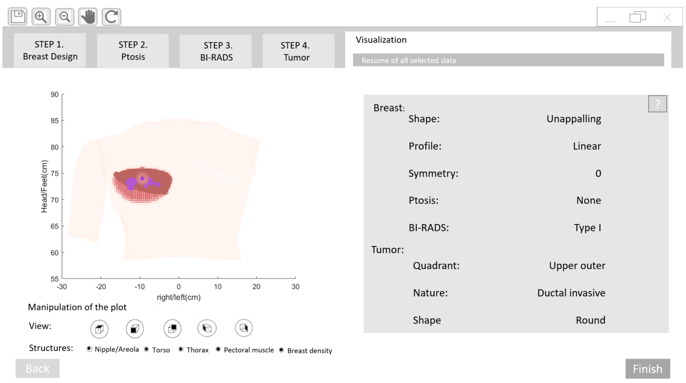

Figure 5.7: Visualization page for mockup A and mockup B.

The interface begins with only two push buttons, where the user chose if the 3D breast model will be simulated with specific values or if the 3D breast model will be created with random values, incorporating so, the suggestion of the doctor. By clicking one of the push buttons, the interface will redirect the user to the breast shape if the user has selected specific values, or the interface will be redirected to the visualization panel, where the several characteristics are chosen randomly by the interface code. If the user picks the button with the text specific, the workflow will be the same presented in the workflow above. All the chosen characteristics will appear in the succeeding images in order to have a continuous process, and so the user can see the evolution of the 3D breast model.

The volume range in the shape panel was fixed between 100 and 600 cubic centimeters, the display will be refreshed according the value of the volume slider.

In the symmetry panel, the user decides which breast the interface will simulate, if it is the left or right breast. This has a big impact in the symmetry because by changing it to the left breast the turn deformity will adapt the simulation to the left breast, in other words, the breast will turn to the left instead to the right, conserving the breast turn value.

In the density page, the same lobs and ducts distribution selected in the density panel, will appear in the tumor and visualization panel.

In the tumor panel, the slider of the tumor radius will change according to the tumor's nature. When the user selects *in situ*, the radius slider will be disabled so the user can not change it, preventing the user to modify the radius to a radius greater than the structure that hosts it. In the case the user selects nature invasive, the minimum value of the slider is the radius of the structure that hosts it, so it is granted that the tumors radius is always bigger than the host's radius. The tumor coordinates will be displayed since the ductal *in situ* tumor may be to small to visualize it soon.

The visualization panel will resume all the characteristics of the simulated breast model, in order to get together all the information and to ensure that the selected attributes are the ones that the user wanted.

All of the pages are associated with a help button where the article and a short description are provided, some of the help buttons have an image too in order to allow a better understanding of the short description.

To navigate through the interface the user should use the next and back button. The back button will reverse the workflow. However, it will display the panel with the default characteristics.

In Figure 5.8 is represented the full interface with help panel and loading bar.

5.3 Surveys and their outcomes

Two surveys were created to obtain professional validation for the 3D breast models and its constituents, and to evaluate the interface in its efficiency and usability. The professional validation were not done at the same time, to not influence the results. All answers were anonymous and treated like that.

(a) Types of simulation (b) Shape (c) Shape Help

(d) Projection (e) Projection Help (f) Symmetry

(g) Symmetry Help (h) Ptosis (i) Ptosis Help

(j) Density (k) Density Help (l) Tumor

(m) Tumor Help (n) Visualization (o) Loading Bar

Figure 5.8: Implemented interface

The first survey (see Attachment A) was created with the purpose of obtaining professional validation of the 3D breast models. On this wise, the main goal was to validate the synthetic 3D breast models and its constituents, in order to verify if they are similar to the real structures. The user classifies several breast shape, profiles, thorax, pectoral muscles from 1 (very artificial) to 5 (very realistic). In some cases, the professionals also chose between different strategies such as ptosis and breast density. In the Table 5.2, the survey outcomes are grouped by characteristic, since the different attributes of each characteristic were always evaluated with the same value, for example, for the characteristic shape, it was given the same evaluation value for each of its attributes such as ideal, round, shaped round, classic, oval or unappeling.

Structures	Doctor 1	Doctor 2	Doctor 3	Average Quote
Breast Shape	1	2	2	1.66
Breast Projections	1	2	3	2
Pectoral Muscle	1	2	3	2
Thorax	1	2	2	1.66

Table 5.2: Survey results.

Approaches	Doctor 1	Doctor 2	Doctor 3	Average Quote
Chen approach	4	3	3	3.33
VCMI approach	4	4	4	4

Table 5.3: Ptosis approaches results.

The second goals of the same survey was to understand which of the several approaches of ptosis and breast density are the most accepted. For the ptosis evaluation, two different ptosis evolution were presented. Between the two ptosis approaches, the Chen approach [49] counted with an average quotation of 3.33 while the other approach with an average quotation of 4 (Table 5.3). When comparing the two approaches with the same ptosis degree, the winning one was always the ptosis degree of the second approach, reinforcing its higher acceptance in relation to the approach made by Chen. With regard to breast density, to understand which one of the three algorithms (previously explained in the Section 4.2.1), is the preferred to be incorporated into the 3D model, three different images, one per algorithm, were exposed to the questioned professionals. Each reporting person should choose which of them is more similar to the reality. With a quote of 0.66, the third algorithm had the best evaluations, and for this reason, it is the algorithm used to simulate the breast density in the 3D breast model in this dissertation.

About the 3D breast model, the question '*In your opinion, do the 3D breast models present at the interfaces look like reality?*' was evaluated with an average of 2.33 on a scale from 1 to 5, were 1 was very artificial and 5 very natural. In Table 5.2 shows the result of each characteristic, where the doctors classified the structures below the average value of the interval. Concluding, that the structures simulated are seen as artificial, which may be due to the fact that all structures are based on non real data.

For the interface survey (see Attachment B), the questions are based on usability and efficiency, so the answers should be simple and the question objective. The questions are in the area of navigation, orientation, intuition, simplicity and if the user understands the concept shown in the interface. One of the most important questions is if the user recognizes the educational potential of this application in the training of new breast cancer surgeons. An opinion space were created to include possible additional comments. Every questioned person evaluated the interface in different aspects by giving it values between 1 to 5, where 1 is bad and 5 is very good, the results are shown in Table 5.4.

Usability	Doctor 1	Doctor 2	Doctor 3	Average Quote
Navigation through interface	3	4	4	3.66
Manipulation of the images	4	4	4	4
Intuitiveness	3	3	4	3.33

Table 5.4: Usability interface survey results.

Question	Yes quote	No quote
Is the concept of an educational tool well represented?	1	0
Do you agree with the steps to creation of the breast?	1	0
Is the Help button ("?") Useful?	1	0
The tool has the expected functionalities and capabilities	$\frac{2}{3}$	$\frac{1}{3}$
Is it easy to navigate and control the interface	$\frac{2}{3}$	$\frac{1}{3}$
You have been able to use the program without further explanation	$\frac{2}{3}$	$\frac{1}{3}$
Would you recommend the tool to new surgeons	$\frac{2}{3}$	$\frac{1}{3}$
Do you recognizes the educational potential of this application	1	0
Would you use the tool	1	0
Has there been any difficulty/problem in executing the Program?	0	1

Table 5.5: Interface survey results.

Table 5.5 includes some of the several questions where the doctors had to respond with 'yes' or 'no'.

The results obtained for the interface usability are mostly positive since the doctors have managed to navigate through the interface, creating several breast models without great explanations, and manipulating the image without major problems. About the interface's intuitiveness and navigation, the results were within the average. However, these results could be explained by the lack of time that the doctors had to explore more deeply the interface. The potential of the educational framework to train and help new surgeons was recognized by the questioned doctors whom agreed with the different steps to achieve the 3D breast model, as intended for this survey.

In summary, the outcomes of these surveys were generally positive, although doctors see the structures still as artificial, an area that must be improved, they managed to navigate and control the interface without problems, recognizing its educational potential to train new surgeons and its usage, in which two thirds of the doctors would recommend the use of this framework to new surgeons.

Chapter 6

Conclusion and Future work

Like seen in chapter 2, breast cancer has a high incidence rate. Many women diagnosed with breast cancer, live in agony due to the deformations that may occur in breast cancer removal surgery. Since it is difficult to predict the surgery outcomes, although it is possible to train new surgeons in order to understand better the surgery procedure and to learn better which kind of situation leave to bad deformities. For these reasons, it is necessary an educational tool for new surgeons to train and learn better the outcomes of the BCS surgery in order to gain practice without practicing it on real patients. In this way, this dissertation had the objective to developed an interface and incorporate 3D breast model with adjustable parameters such as : volume, shape, profile, symmetry, ptosis, breast density, also the location, nature and size of the tumor, for the user to select.

In the end, the user can simulate in the developed framework the left and right breast, different volumes, six types of breast shapes based on Mallucci [56] work, five different breast projection adapted from the breast deformities top-shape of Chen [49] work. Four types of ptosis degree adapted from previous work of the VCMI group, and also adapted from Chen, the turn deformity, with the values comprehended between 0 to 1. Breast density, has a big impact in the healing processes. It is simulated with the BI-RADS regulation, where four types of breast density can be selected. The percentage of the fibroglandular tissue is given by a random function within the parameters of each breast density type, 15 to 20 lobs are distributed all over the breast.

To obtain a more realistic 3D breast model, structures like Nipple and Areola Complex were added in the breast surface, which follows any breast deformations. In the breast interior, a pectoral muscle, which adapts to the breast side, and a thorax were added to the 3D breast model. The breast is localized above of a torso in order to give the surgeons a referential. Only with this data is it possible to simulate 480 different breasts with the same volume and turn value, this value was obtained by multiplying: the 6 breast shapes, 5 breast projection, 4 ptosis degree and the 4 BI-RADS type. As this tool is for cancer removal surgery, it is conceivable to introduce the tumor's localization in nine breast places (quadrants). The user can choose between invasive or *in situ*, originated in ducts, lobs or in the fat tissue. The radius of the tumor can be manipulated, such as the tumors' shape. So it is achievable, in this dissertation, to simulate approximately 43.200 breasts without counting the breast with different volumes and turn deformation. This value was obtained by multiplying the the 6 breast shapes, 5 breast projection, 4 ptosis degree, 4 BI-RADS type, 9 quadrants, 5 types of tumor nature and 2 different tumor shapes.

To evaluate the quality of the educational framework, an inquiry was done to doctors specialized in the field of breast cancer, where the following questions were answered "Do you recognize the educational potential of this application in the training of new breast cancer surgeons?", "Would you use the tool?" and "Is the information presented effectively?". The results of inquiry was very satisfactory, confirming that the questioned surgeons recognize the educational potential and the usability of the framework.

Although the results obtained in the survey of breast naturality, were not as expected. One of the future work is to improve the framework in this manner. In order to make them less artificial, shadows could be added, giving color variations and so depth to the 3D breast model. For the pectoral muscle it would help to simulated it with curve lines like it is observable in anatomy books. Another future work is to incorporate the work of Hooshiar Zolfagharnasab *et. al* [61]. Since the work consists of a regression model to predict aesthetic results after BCS surgery. Incorporating this work, it is possible to complete the educational tool, with all functionalities needed to train new surgeons.

In summary, the new surgeons are able to simulate several 3D breast models. Along the interface, the user will make several choices about the different characteristics, in order to train different breast. Although the questioned doctors see the simulated structures as artificial, they recognize the educational potential and would use the tool.

References

[1] Mama Help. 2. estatistica. Available in: http://www.mamahelp.pt/index.php/temas/item/49-b-estatisticas, last accessed 27 de Novembro de 2017.

[2] Liga Portugues Contra o Cancro. O canncro da mama. Available in: https://www.ligacontracancro.pt/cancro-da-mama/, last accessed 20 de Novembro de 2017.

[3] World Cancer Research Fund International. Breast cancer statistics. Available in: http://www.wcrf.org/int/cancer-facts-figures/data-specific-cancers/breast-cancer-statistics, last accessed em 26 de Dezembro de 2017.

[4] Andrew Russo Cinnamon VanPutte, Jennifer Regan. *Seeley's essentials of Anatomy Physiology*. McGraw-Hill Education, ninth edition edition, 2016.

[5] André Vallejo Gustavo Zucca-Matthes, Cícero Urban. Anatomy of the nipple and breast ducts. *Gland Surgery*, 2016.

[6] Educate Advocate eradicate Michigan breast Cancer Coalition. Types of breast density. Available in: http://www.roche.pt/sites-tematicos/infocancro/index.cfm/tipos/cancro-da-mama/cdm-metodos-de-tratamento/, last accessed December 26, 2017.

[7] Harvey M.D. Viktor Jennifer, A. Quantitative assessment of mammographic breast density: Relationship with breast cancer risk. *Radiology*, 2004.

[8] Thirdlove. Breast shape dictionary. Available in: https://www.thirdlove.com/pages/breast-shape-dictionary, last accessed 27 July, 2018.

[9] E.Swanson. A measurement system and ideal breast shape. *Evidence-Based Cosmetic Breast Surgery,Springer International Publishing*, 2017.

[10] Mark Hanikeri. Breast lift (mastopexy). Available in: https://www.markhanikeri.com/lift.html, last accessed 27 July, 2018.

[11] instituto CUF de Oncologia. Cancro da mama. Available in: https://www.saudecuf.pt/oncologia/o-cancro/cancro-da-mama, last accessed 26 de Dezembro de 2017.

[12] GLOBOCAN. Global cancer statistics 2018: Globocan estimates of incidence and mortality worldwide for 36 cancers in 185 countries. Available in: http://globocan.iarc.fr/old/FactSheets/cancers/breast-new.asp, last accessed 26 de Dezembro de 2018.

[13] National Cancer Institute. Breast cancer treatments. Available in: https://www.cancer.gov/types/breast/hp/breast-treatment-pdq, last accessed 22 de Novembro de 2017.

[14] Merck Manual. Breast disorders: Breast cancer. 2008.

[15] Educate Advocate eradicate Michigan breast Cancer Coalition. Breast cancer stages. Available in: https://www.dreamstime.com/stock-photography-stages-breast-cancer-image253796, last accessed January 10, 2018.

[16] INFO Cancro. Cancro da mama : Tratamentos disponiveis. Available in: https://www.mibcc.org/educate/breast-density-notification-law/, last accessed 26 de Dezembro de 2017.

[17] Physiopedia. Surgery. Available in: https://www.physio-pedia.com/Physiotherapy_and_cancer_treatment, last accessed June 14, 2018.

[18] American Cancer Society. Breast cancer: Facts figures 2017-2018. *American Cancer Society*, 2017.

[19] W G Lewis A N Hopper, M H Jamison. Learning curves in surgical practice. *Postgrad Med J*, 2007.

[20] Samuel Eberhardt, Ana Cristina; Lincoln Bezerra Lins. Qualidade de vida e a cirurgia em cancro da mama. *Universidad CES Medellín, Colombia*, 2017.

[21] Jussara Bôtto Neves Paola Moraes Vasconcelos. The importance of family support to the woman submitted to surgery in the treatment of breast cancer. Available in: https://www.unilestemg.br/enfermagemintegrada/artigo/v3/05-importancia-apoio-familiar-mulher.pdf, last accessed 26 de Dezembro de 2017.

[22] Brian Curless Brett Allen and Zoran Popovi´c. The space of human body shape. *ACM Transactions on Graphics*, 2003.

[23] V. Rajagopal Poul M F Nielsen Angela W C Lee, Julia A. Schnabel and Martyn P. Nash. Breast image registration by combining finite elements and free-form deformations. *Lecture Notes in Computer Science*, 2010.

[24] Gunther Greiner Marc Stamminger Michael Zollhofer, Michael Martinek and Jochen Sußmuth. Automatic reconstruction of personalized avatars from 3d face scans. *Computer Animation And Virtual Worlds*, page 22:195–202, 2011.

[25] David Hirshberg Alexander Weiss and Michael J Black. 3d body scans from noisy image and range data. *In International Conference on Computer Vision*, pages 1951–1958, 2011.

[26] Daphane Koller Sebastian Thurun Jim Rodgers Dragomir Anguelov, Praveen Srinivasan and James Davis. Scape: Shape completion and animation of people. *SIGGRAPH'05 ACM SIGGRAPH 2005 Papers*, pages 408–416, 2005.

[27] Jonathan CK Wells Philip Treleaven. 3d body scanning and healthcare applications. *IEEE Xplore*, 2007.

[28] Xinyi Cui Mingchen Gao Junzhou Huang Dimitris Metaxas Shaoting Zhang, Yiqiang Zhan. 3d anatomical shape atlas construction using mesh quality preserved deformable models. *Computer Vision and Image Understanding*, pages 1061–1071, 2013.

[29] Giovanni Gallo Salvatore Spoto Giuseppe Catanuto Giovanni Maria Farinella, Gaetano Impoco and Maurizio B. Nava. Objective outcome evaluation of breast surgery. *PLab - DMI , University of Catania, Italy and Unit of Plastic and Reconstructive Surgery - INT, Milano, Italy*, 2006.

[30] G. Gallo S. Spoto G. Catanuto G. M. Farinella, G. Impoco. Umambiguous analysis of woman breast shape for plastic surgery outcome evaluation. *Eurographics Italian Chapter Conference*, 2006.

[31] Frederic Cordier Hyewon Seo and Kyunghi Hong. A breast modeler based on analysis of breast scans. *Computer Animation and Virtual Worlds*, 2007.

[32] H. B. Skinner J. H. Keyak, J. M. Meagher and C. D. Mote. Automated three-dimensional finite element modeling of bone: A new method. *J.Biomed. Eng*, pages 389–397, 1990.

[33] T. J. Reiter W. Krach, T. J. Rammerstorfer and P. Zenz. In vivo ct-based 3-d-modeling of human bones with respect to inhomogeneity,. *ASME Bioengineering Conf*, 1995.

[34] K. D. Costa J. M. Guccione and A. D. McCulloch. Finite element stress analysis of left ventricular mechanics in the beating dog heart. *J.Biomed. Eng*, pages 1167–1177, 1995.

[35] S. J. Zinreich S. K. Kyriacou, C. Davatzikos and R. N. Bryan. Nonlinear elastic registration of brain images with tumor pathology using a biomechanical model. *IEEE Trans. Med. Imag*, pages 580–592, 1999.

[36] H. S. Stiehl U. Spetzger A. Hagemann, K. Rohr and J. M. Gilsbach. Biomechanical modeling of the human head for physically based nonrigid image registration. *IEEE Trans. Med. Imag*, pages 875–884, 1999.

[37] Bakic PR. Breast tissue description and modeling in mammography. *PhD Thesis, Lehigh University*, 2000.

[38] J. Herrero J. López M. Doblaré A. Pérez del Palomar, B. Calvo. A finite element model to accurately predict real deformations of the breast. *Medical Engineering Physics*, 2008.

[39] Hill DLG Hawkes DJ Tanner C, Schanabel JA. Factors influencing the accuracy of biomechanical breast models. *Med Phys*, 2006.

[40] Jalil Jalali Alexander Volf Markus Settles Hans Günther Machens Maximilian Eder, Stefan Raith and Laszlo Kovacs. Comparison of different material models to simulate 3- d breast deformations using finite element analysis. *Annals of Biomedical Engineering*, page 42(4):843–857, 2014.

[41] Stotzka R Gemmeke H Reichenbach J Kaiser W. Ruiter N, Muller T. Automatic image matching for breast cancer diagnostics by a 3d deformation of the mamma. *Biomed Tech*, 2002.

[42] Yaffe MJ Plewes DB Samani A, Bishop J. Biomechanical 3-d finite element modelling of the human breast using mri data. *IEEE TRANSACTIONS ON MEDICAL IMAGING, VOL. 20*, 2001.

[43] Menzel E. Reishner R, Balogh B. Two dimensional elastic properties of human skin in temrs of an incremental model at the in vivo configuration. *Med Eng Phys*, 1995.

[44] Maria Francesca Spadea Giovanna Trecate Daniele Vergnaghi Luca Tommaso Mainardi Paolo Patete, Maria Ida Iacono and Guido Baroni. A multi-tissue mass-spring model for computer assisted breast surgery. *Medical engineering physics*, page 47–53, 2013.

[45] Ivan Costa Remis Balaniuk and Jairo Melo. Cosmetic breast surgery simulation. *III Simposium on Virtual Reality*, pages 387–396, 2006.

[46] G M Farinella G Impoco A Pennati A Spano G Catanuto, G Gallo and M B Nava. Breast shape analysis on three dimensional models. *In proceedings of Plastic and Reconstructive Surgery of the Breast: Third European Conference*, 2005.

[47] Alan H Barr. Superquadrics and angle-preserving transformations. *IEEE Computer graphics and Applications*, pages 1(1):11–23, 1981.

[48] Laurent D Cohen Eric Bardinet and Nicholas Ayache. A parametric deformable model to t unstructured 3d data. 1995.

[49] Michael J Miller R Bowen Loftin David T Chen, Ioannis A Kakadiaris and Charles Patrick. *Modeling for plastic and reconstructive breast surgery*. Springer, 2000.

[50] Hélder P. Oliveira Diogo Pernes, Jaime S Cardoso. Fitting of superquadrics for breast modelling by geometric distance minimization. *In Proceedings - 2014 IEEE International Conference on Bioinformatics and Biomedicine, IEEE BIBM 2014,*, pages 293–296, 2014.

[51] Sarah FF Gibson and Brian Mirtich. A survey of deformable modeling in computer graphics. technical report. *Citeseer*, 1997.

[52] Romain Raffin. Free form deformations or deformations non-constrained by geometries or topologies. *In Deformation Models*, pages 49–74, 2013.

[53] Laurent D Cohen Eric Bardinet and Nicholas Ayache. A parametric deformable model to fit unstructured 3d data. *Computer vision and image understanding*, page 71(1):39–54, 1998.

[54] Kunwoo Lee Youngjun Kim and Wontae Kim. 3d virtual simulator for breast plastic surgery. *Computer vision and image understanding*, pages 515–526, 2008.

[55] Walterio Mayol-Cuevas. Nancy h-anim humanoid under matlab. Available in: `https://www.mathworks.com/matlabcentral/fileexchange/236-nancy_body-m`, last accessed October 14, 2018.

[56] O.A.Brandford P.Mallucci. Concepts in aesthetic breast dimensions: Analysis of the ideal breast. *Journal of Plastic, Reconstructive Aesthetic Surgery*, 2012.

[57] James S. Michaelson Frederick C. Koerner Barbara L. Smith Jennifer E. Rusby, Elena F. Brachtel. Breast duct anatomy in the human nipple: three-dimensional patterns and clinical implications. *Breast Cancer Res Treat*, 2008.

[58] Ricki Lewis Dr. David N. Shier Dr., Jackie L. Butler. *Hole's Human Anatomy Physiology*. 14^{th} edition edition, 1996.

[59] BioDigital. Biodigital: 3d human visualization platform for anatomy and disease. Available in: `https://www.biodigital.com/`, last accessed 25 July, 2018.

[60] Spencer Gunn Andy KW Ma and Dimitra G Darambara. Introducing debra: a detailed breast model for radiological studies. *PHYSICS IN MEDICINE AND BIOLOGY*, 2009.

[61] Sara P. Oliveira Pedro Faria João F. Teixeira Jaime S. Cardoso Hooshiar Zolfagharnasab, Silvia Bessa and Helder P. Oliveira. A regression model for predicting shape deformation after breast conserving surgery. *Sensors*, 2018.

Appendix A

Attachments A - Survey about naturality

Semelhança com a realidade das estruturas que constituem a mama

O trabalho no qual estão inseridos os modelos 3D da mama aqui apresentados, tem como objetivo a criação de uma ferramenta educativa. Esta ferramenta, inserida na área do cancro da mama, tem como finalidade uma melhor compreensão, por parte de novos cirurgiões, da intervenção.

Este estudo tem como finalidade o melhoramento dos modelos 3D de forma a que estes sejam o mais semelhantes possíveis as mamas reais.

Todas as respostas serão anónimas e irão ser usadas para o propósito do estudo.

*Obrigatório

1. **Na sua opinião, os modelos 3D da mama, presentes nas interfaces, assemelham-se à realidade? ***
   Marcar apenas uma oval.

	1	2	3	4	5	
nada semelhante	◯	◯	◯	◯	◯	bastante semelhante

Tipos de mama

2. **Na sua opinião, quão natural é o modelo que simula o tipo de mama "unappeling"?** *

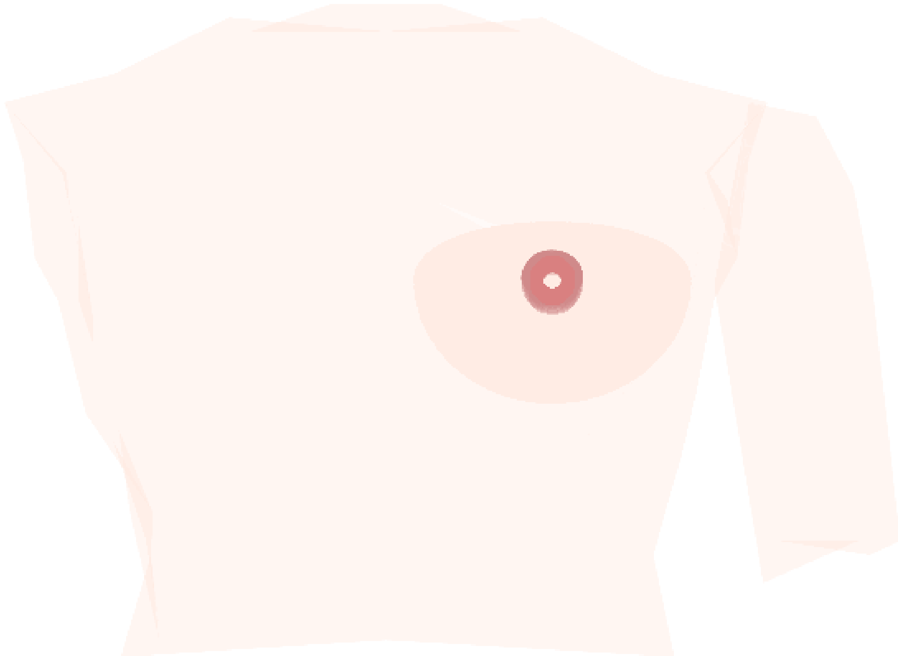

Marcar apenas uma oval.

	1	2	3	4	5	
Muito Artificial	⬭	⬭	⬭	⬭	⬭	Muito Natural

3. **Na sua opinião, quão natural é o modelo que simula o tipo de mama "ideal"?** *

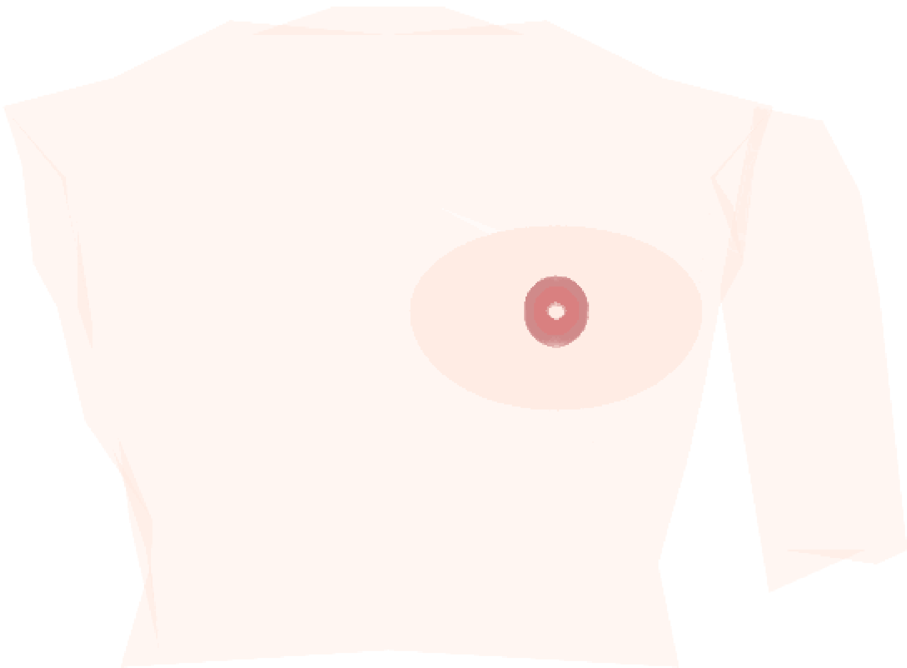

Marcar apenas uma oval.

	1	2	3	4	5	
Muito Artificial	◯	◯	◯	◯	◯	Muito Natural

4. **Na sua opinião, quão natural é o modelo que simula o tipo de mama "shaped-round"?** *

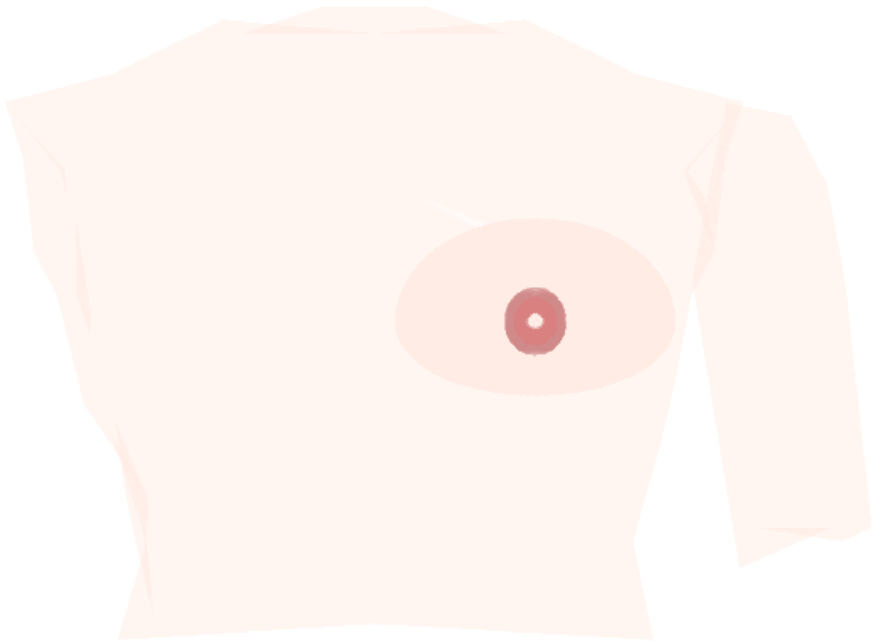

Marcar apenas uma oval.

	1	2	3	4	5	
Muito Artificial	⬭	⬭	⬭	⬭	⬭	Muito Natural

5. **Na sua opinião, quão natural é o modelo que simula o tipo de mama "oval"?** *

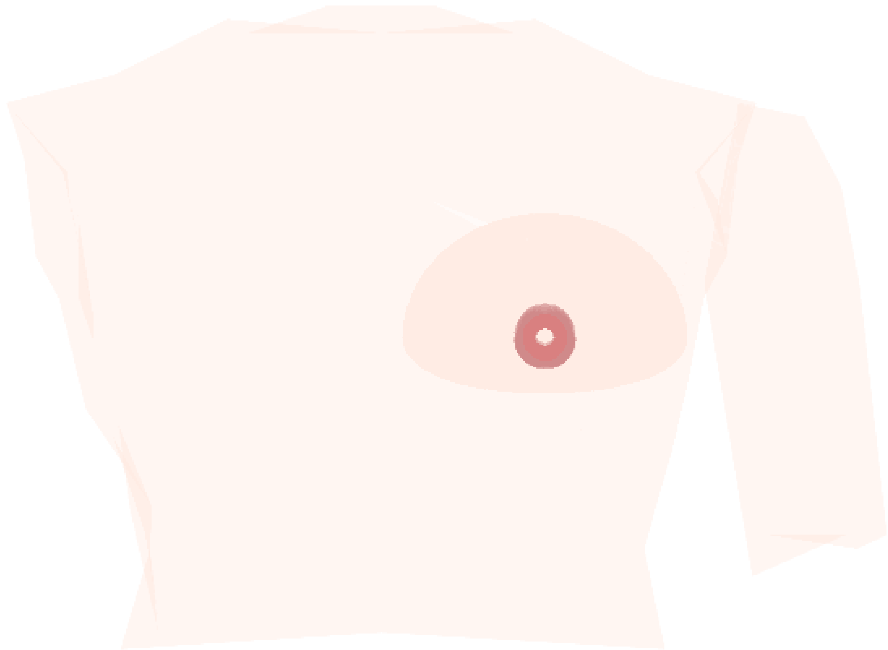

Marcar apenas uma oval.

	1	2	3	4	5	
Muito Artificial	◯	◯	◯	◯	◯	Muito Natural

6. **Na sua opinião, quão natural é o modelo que simula o tipo de mama "classic"?** *

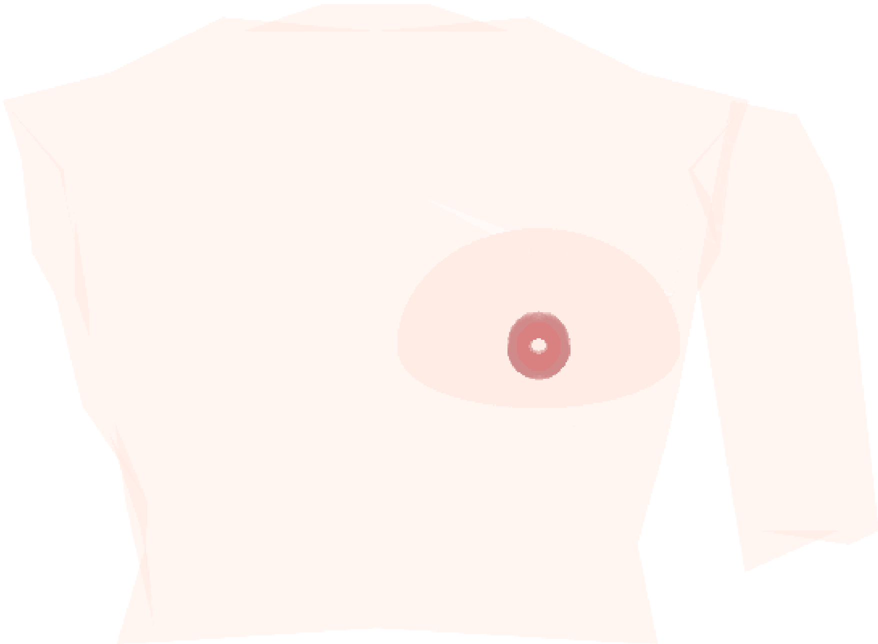

Marcar apenas uma oval.

	1	2	3	4	5	
Muito Artificial	⬭	⬭	⬭	⬭	⬭	Muito Natural

7. **Na sua opinião, quão natural é o modelo que simula o tipo de mama "round"?** *

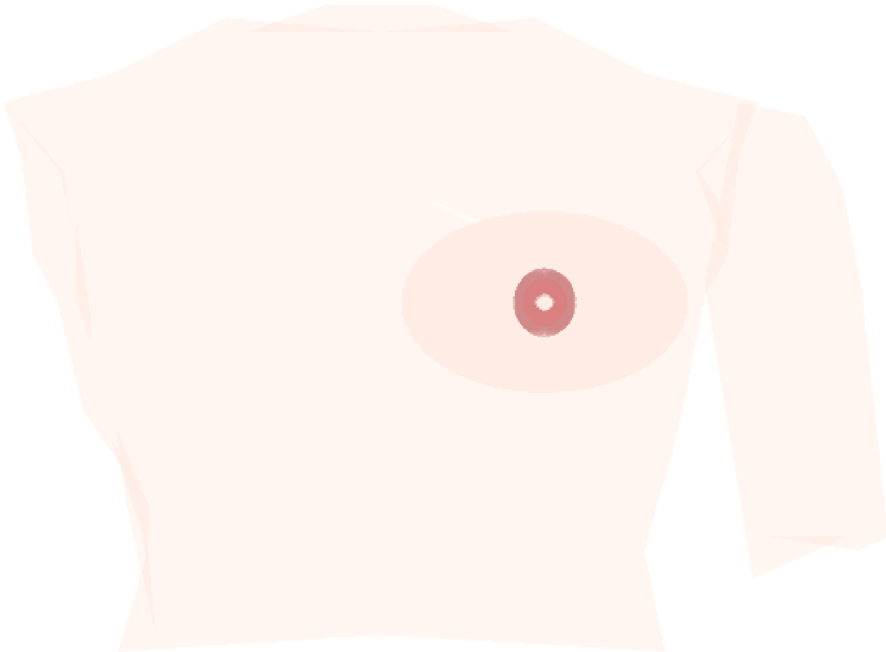

Marcar apenas uma oval.

	1	2	3	4	5	
Muito Artificial	◯	◯	◯	◯	◯	Muito Natural

8. **Comentários adicionais**

Perfil da Mama

Todos os modelos são simulados com CNL (Chest Nipple Length) de 60 mm, e com o tipo de Mama Round

9. **Na sua opinião, quão natural é o modelo que simula a projeção de mama "convex"?** *

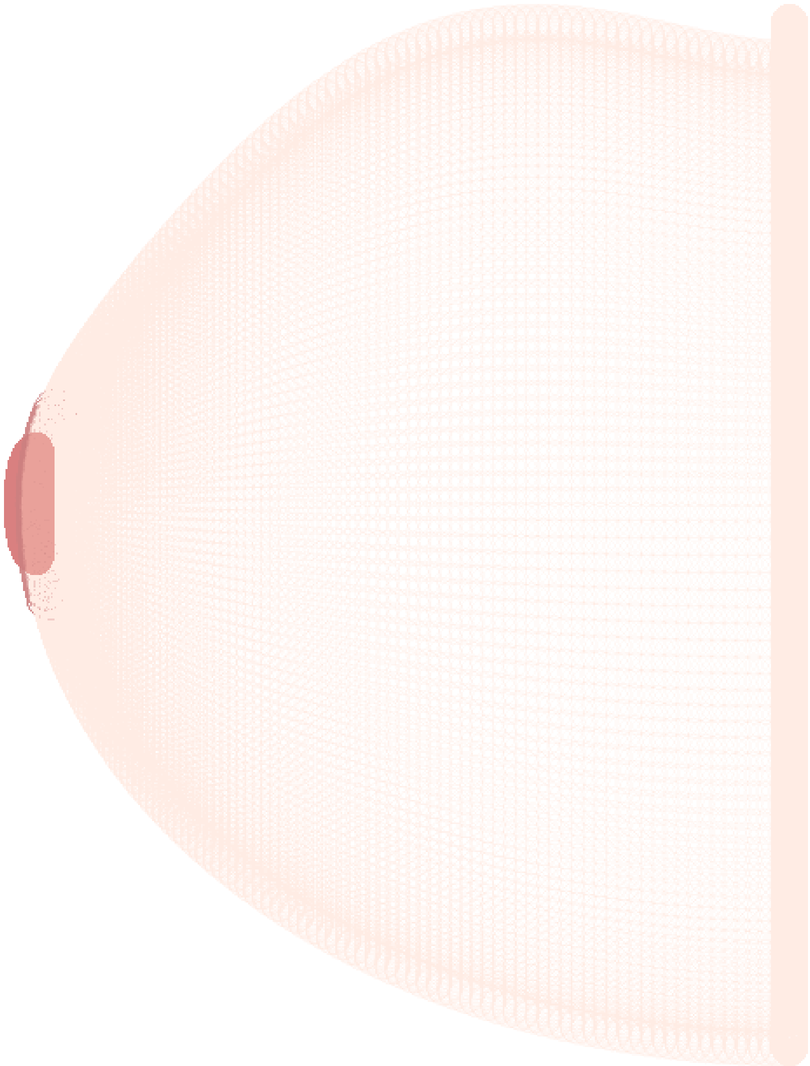

Marcar apenas uma oval.

	1	2	3	4	5	
Muito Artificial	⬭	⬭	⬭	⬭	⬭	Muito Natural

10. **Na sua opinião, quão natural é o modelo que simula a projeção de mama "concave"?** *

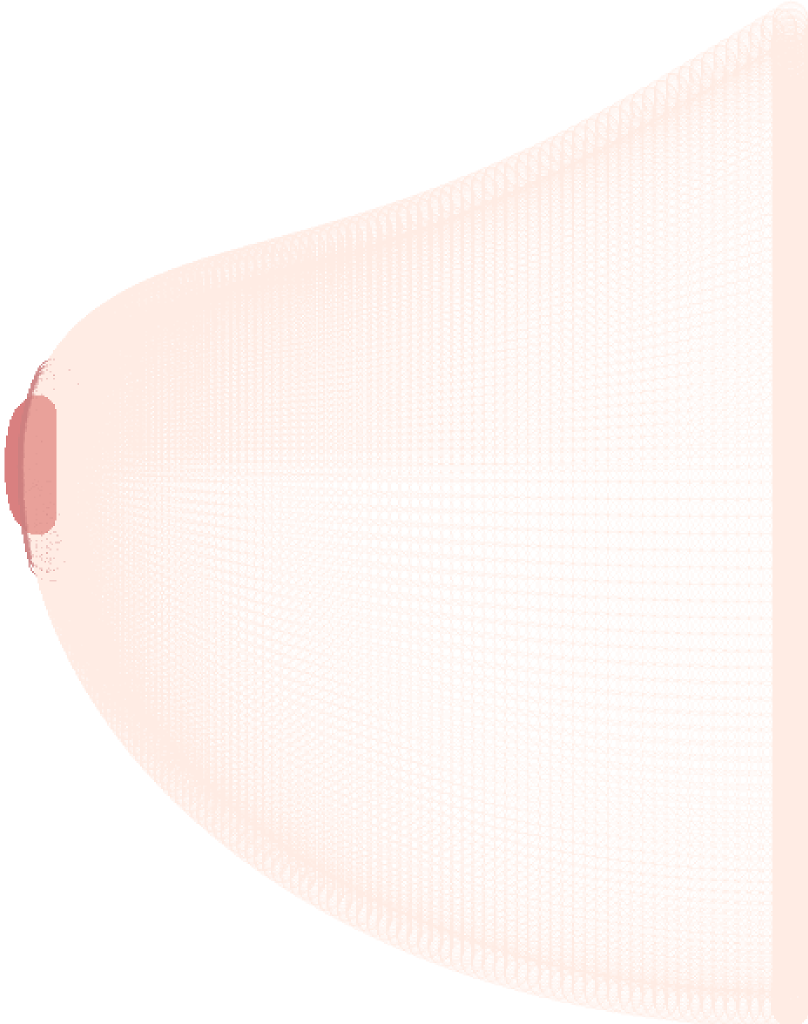

Marcar apenas uma oval.

	1	2	3	4	5	
Muito Artificial	⬭	⬭	⬭	⬭	⬭	Muito Natural

11. **Na sua opinião, quão natural é o modelo que simula a projeção de mama "linear"?** *

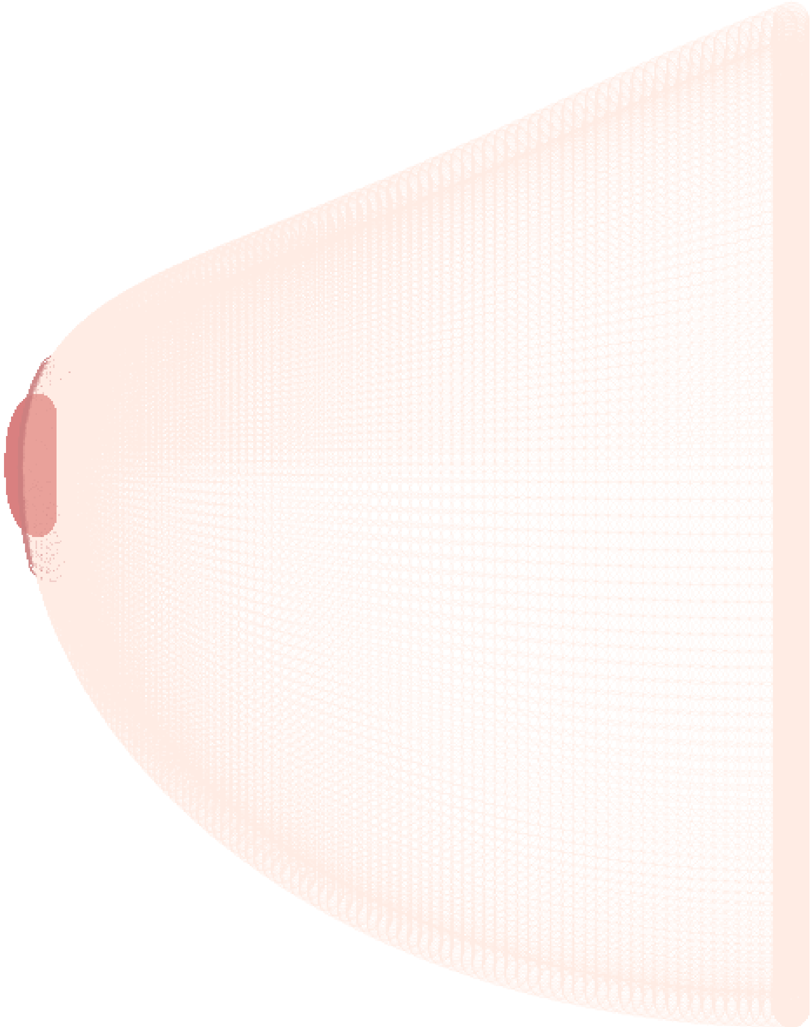

Marcar apenas uma oval.

	1	2	3	4	5	
Muito Natural	⬭	⬭	⬭	⬭	⬭	Muito Artificial

12. **Na sua opinião, quão natural é o modelo que simula a projeção de mama "round"?** *

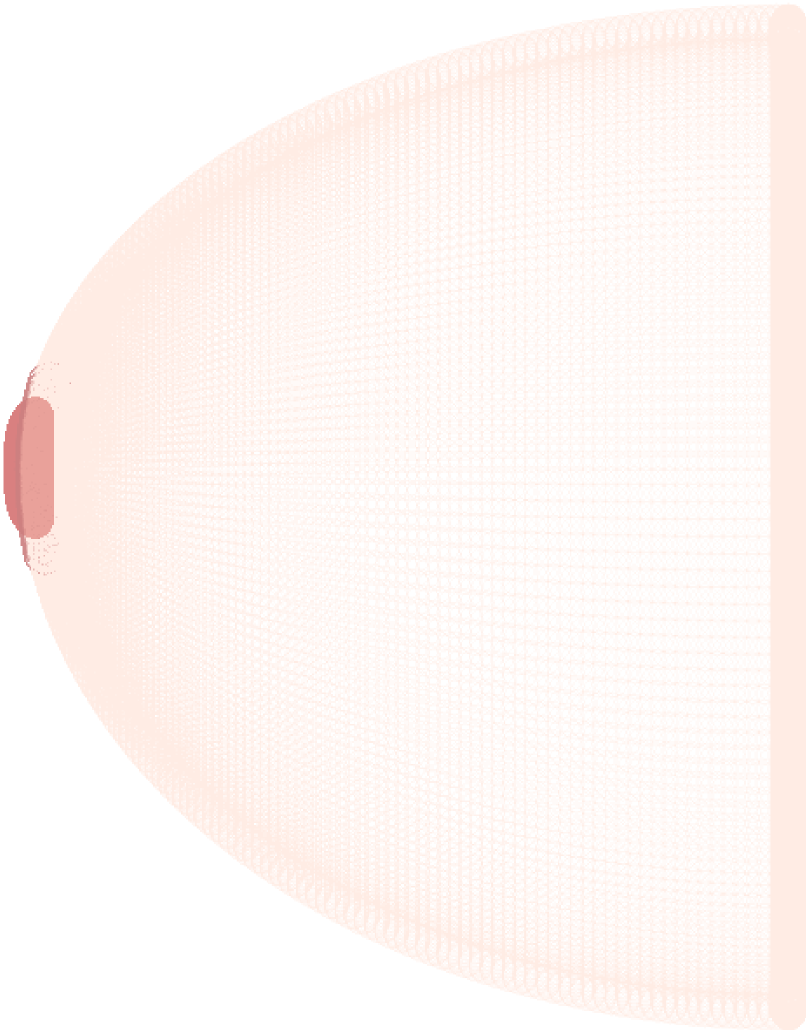

Marcar apenas uma oval.

	1	2	3	4	5	
Muito Artificial	⬭	⬭	⬭	⬭	⬭	Muito Natural

13. **Na sua opinião, quão natural é o modelo que simula a projeção de mama "ogge"?**

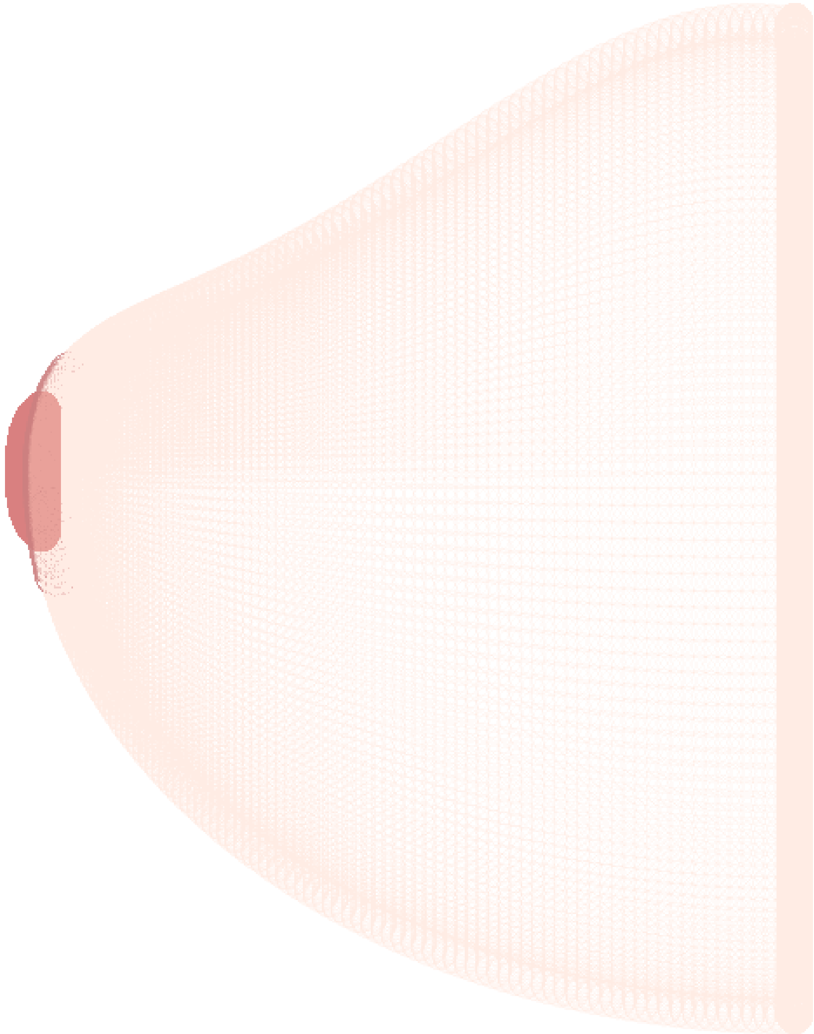

Marcar apenas uma oval.

	1	2	3	4	5	
Muito Artificial	◯	◯	◯	◯	◯	Muito Natural

14. **Comentários adicionais**

Ptosis

15. **Concorda com a "evolução" que a ptosis da mama teve, na figura abaixo?** *

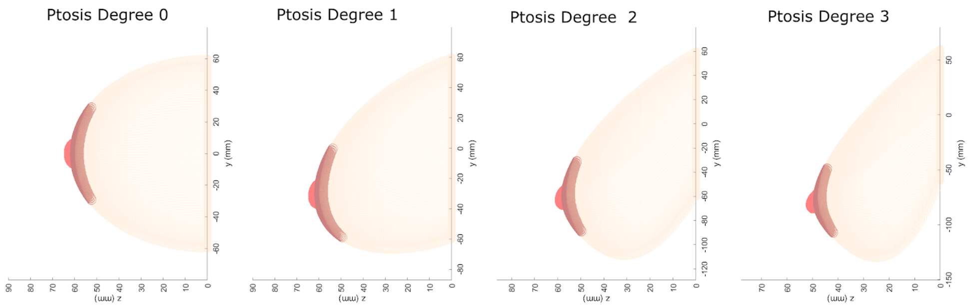

Marcar apenas uma oval.

	1	2	3	4	5	
Não concordo	⬭	⬭	⬭	⬭	⬭	Concordo totalmente

16. **Concorda com a "evolução" que a ptosis da mama teve, na figura abaixo?** *

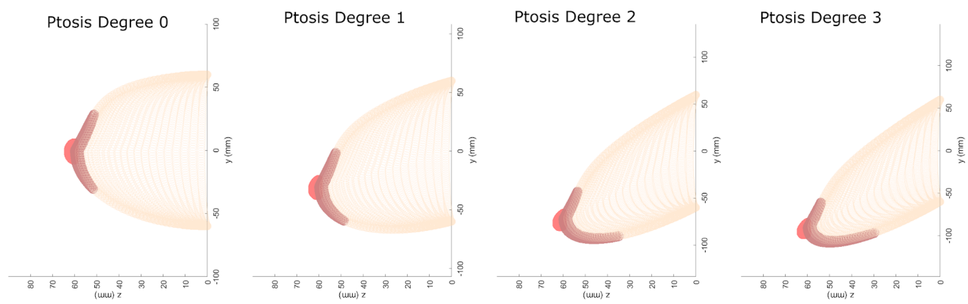

Marcar apenas uma oval.

	1	2	3	4	5	
Não concordo	⬭	⬭	⬭	⬭	⬭	Concordo totalmente

17. **Na sua opinião, o que pode ser melhorado na evolução da ptosis da mama**

18. **Qual das ptosis de grau 1 se assemelha mais à realidade?** *
Marcar apenas uma oval.

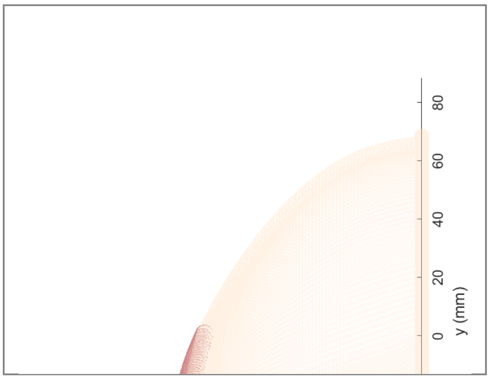

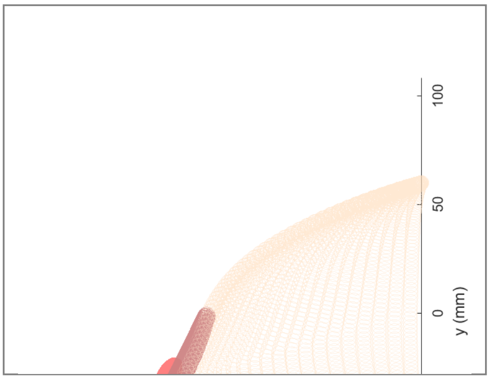

Opção 1 Opção 2

19. **Qual das ptosis de grau 2 se assemelha mais à realidade?** *
Marcar apenas uma oval.

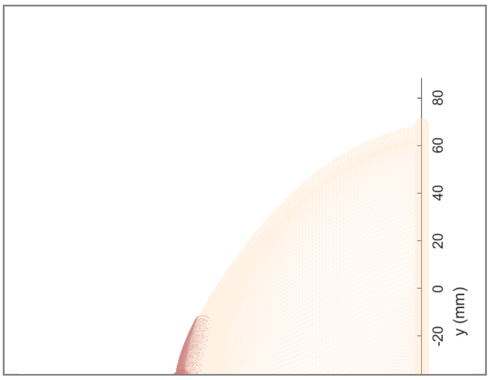

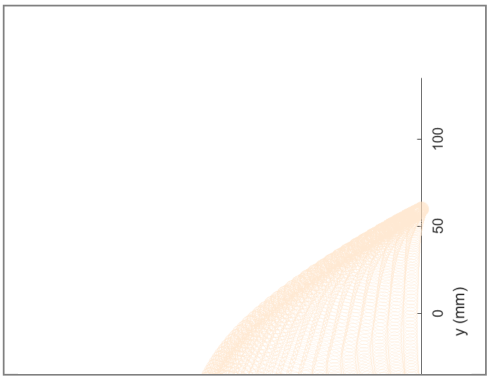

Opção 1 Opção 2

20. **Qual das ptosis de grau 3 se assemelha mais à realidade?** *
Marcar apenas uma oval.

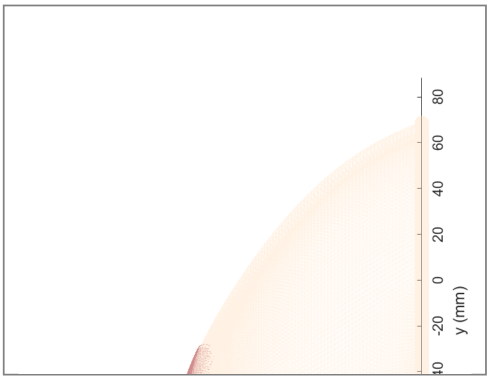

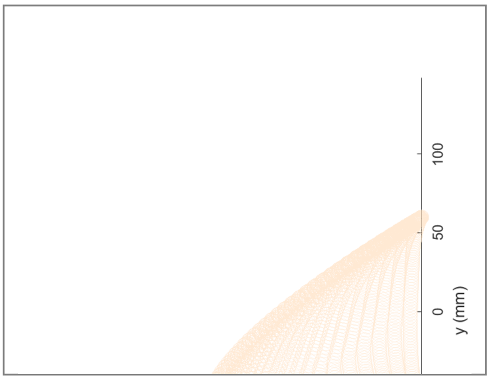

Opção 1 Opção 2

21. **Comentários adicionais**

Densidade

22. **Na sua opinião, qual é a densidade que mais se assemelha com a realidade?** *

Marcar apenas uma oval.

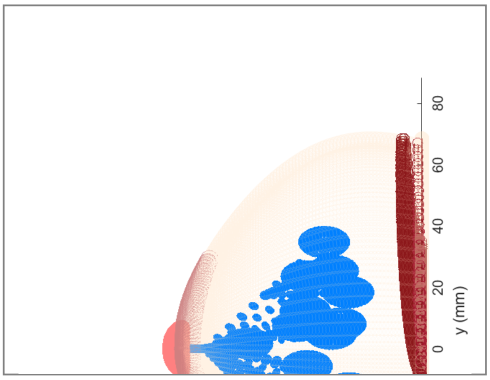

Opção 3

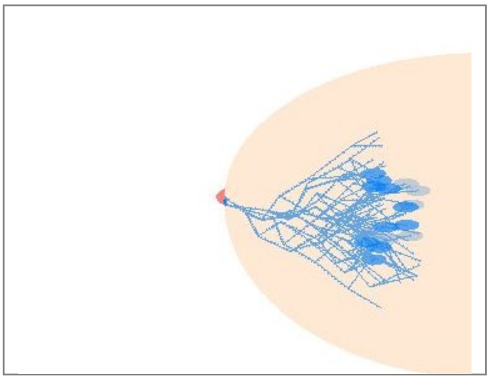

Opção 1

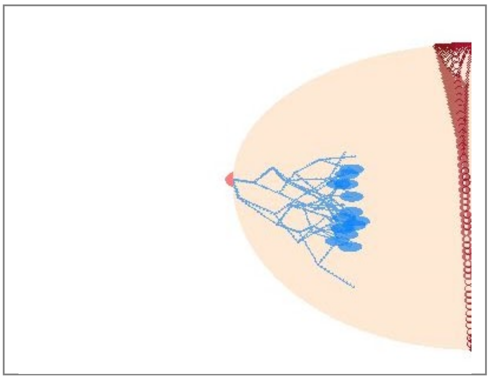

Opção 2

23. **Comentários adicionais**

Tórax/Peitoral

24. **Na sua opinião, quão semelhante é o tórax, simulado nos modelos, à realidade?** *

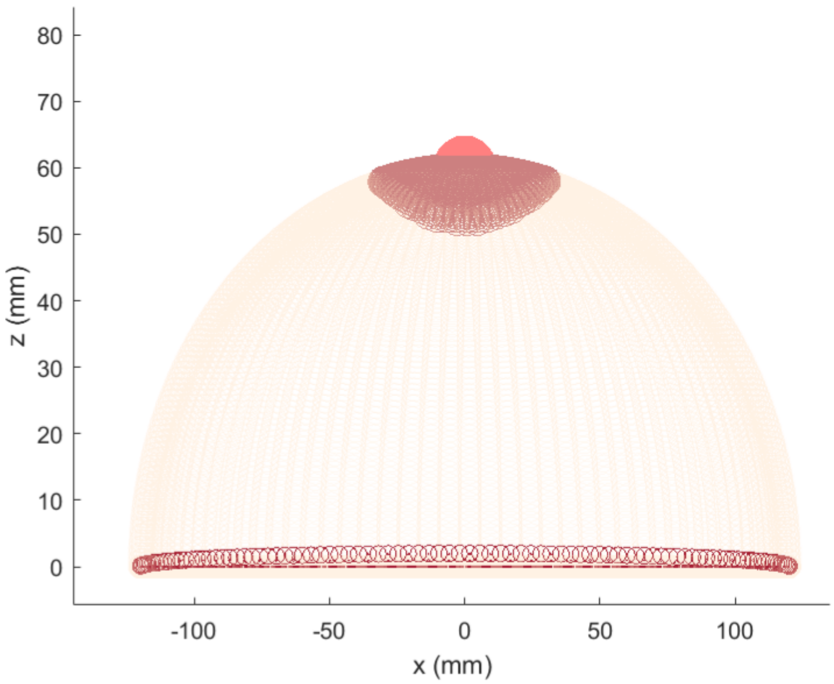

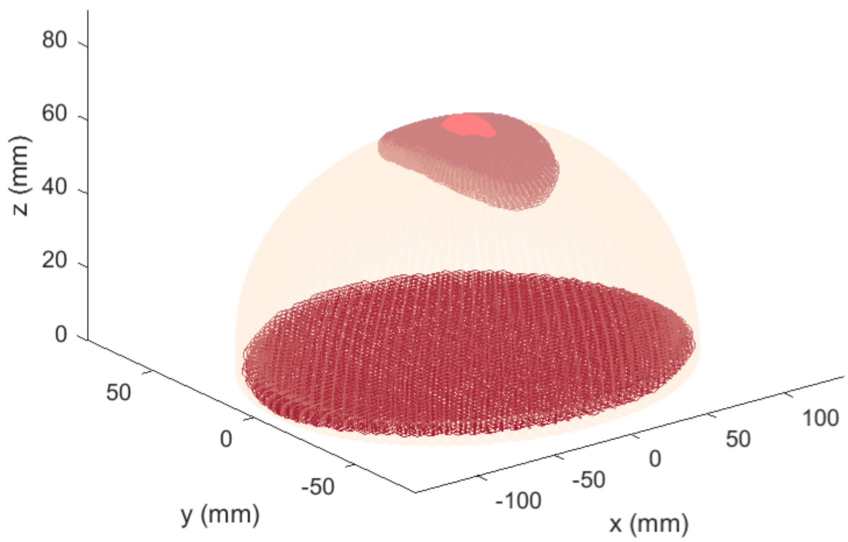

Marcar apenas uma oval.

	1	2	3	4	5	
Muito Artificial	◯	◯	◯	◯	◯	Muito Natural

25. **Na sua opinião, quão semelhante é o peitoral, simulado nos modelos, à realidade?** *

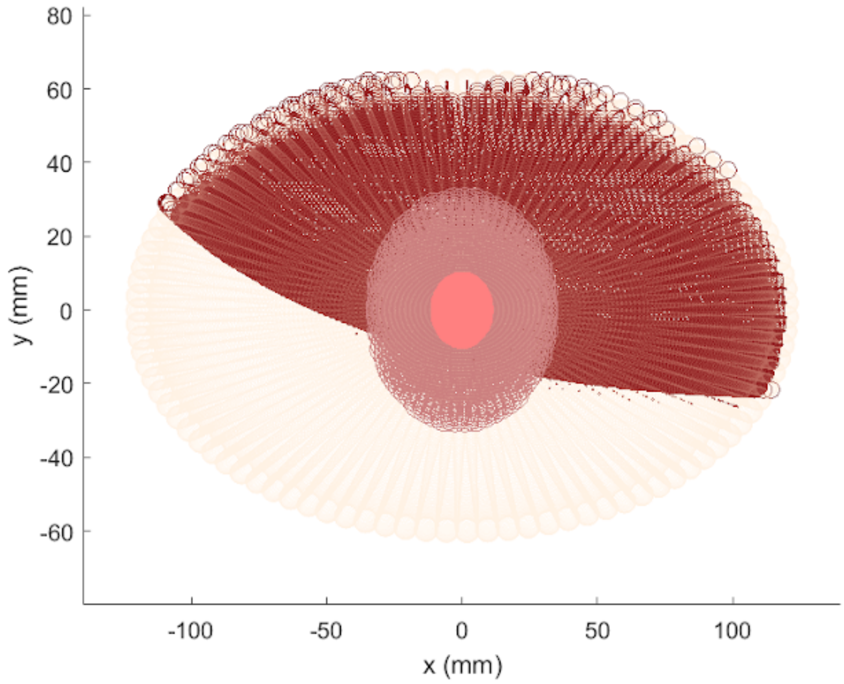

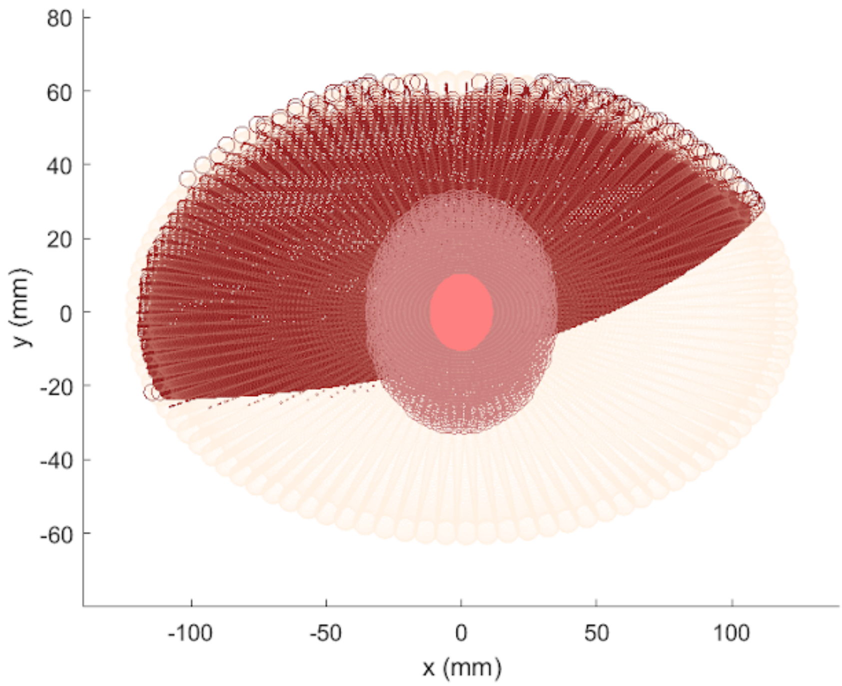

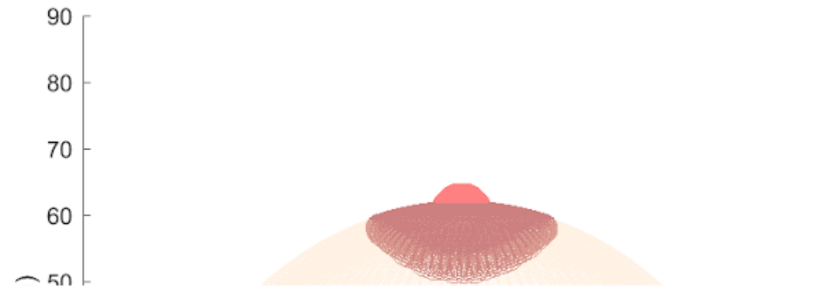

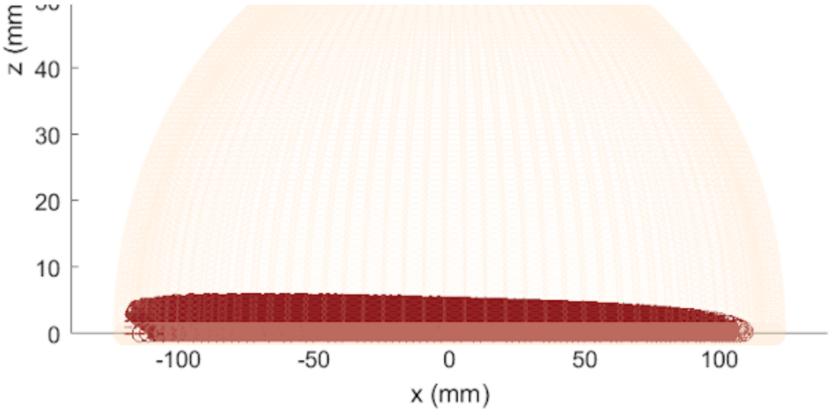

Marcar apenas uma oval.

	1	2	3	4	5	
Muito Artificial	⬭	⬭	⬭	⬭	⬭	Muito Natural

26. **Comentários adicionais**

____

____

____

____

____

Com tecnologia Google Forms

Appendix B

Attachments B - Survey about the interface

Interface

*Obrigatório

1. **A navegação no sistema é fácil? ***

Marcar apenas uma oval.

	1	2	3	4	5	
Dificil	⬭	⬭	⬭	⬭	⬭	Fácil

2. **Conseguiu utilizar o programa sem serem necessárias explicações adicionais? ***

Marcar apenas uma oval.

⬭ Sim
⬭ Não

3. **Surgiu algum dificuldade/problema na execução do Programa? ***

Marcar apenas uma oval.

⬭ Sim (qual? escreva nos comentários adicionais)
⬭ Não

4. **É fácil de navegar e controlar a interface em causa? ***

Marcar apenas uma oval.

⬭ Sim
⬭ Não

5. **É fácil a manipulação das imagens? ***

Marcar apenas uma oval.

	1	2	3	4	5	
difícil de manipular	⬭	⬭	⬭	⬭	⬭	facil de manipular

6. **Quão intuitiva é a interface? ***

Marcar apenas uma oval.

	1	2	3	4	5	
Pouco intuitiva	⬭	⬭	⬭	⬭	⬭	Muito Intuitiva

7. **Acha o conceito de ferramenta educativa bem representado nesta interface? ***

Marcar apenas uma oval.

⬭ Sim
⬭ Não

8. **Concordo com os vários passos usados na interface, que levam à criação da mama?** *
Marcar apenas uma oval.
- Sim
- Não

9. **Considera o botão Help("?") útil?** *
Marcar apenas uma oval.
- Sim
- Não(porquê? escreva nos comentários adicionais)

10. **A informação é apresentada de forma efectiva?** *
Marcar apenas uma oval.
- Sim
- Não

11. **A interface tem as funcionalidades e capacidades esperadas?** *
Marcar apenas uma oval.
- Sim
- Não

12. **Recomendaria a ferramenta a novos cirurgiões?** *
Marcar apenas uma oval.
- Sim
- Não(porquê? escreva nos comentários adicionais)

13. **Reconhece o potencial educativo desta aplicação na formação de novos cirurgiões de cancro da mama?** *
Marcar apenas uma oval.
- Sim
- Não. (porque? escreva no comentário)

14. **Usaria a ferramenta** *
Marcar apenas uma oval.
- Sim
- Não(porquê? escreva nos comentários adicionais)

15. **Que outros tipos de estruturas gostaria de ver?** *

16. **Na sua opinião, seria útil visualizar os modelos nas diferentes posições (Prone, Suprina)?** *
Marcar apenas uma oval.
- Sim
- Não

17. **Comentários adicionais**

Com tecnologia
Google Forms